UNIVERSITÉ DE STRASBOURG

N° d'ordre :

École Doctorale Mathématiques, Sciences de l'Information et de l'Ingénieur

UdS – INSA – ENGEES

THÈSE

présentée pour obtenir le grade de

Docteur de l'Université de Strasbourg
Discipline : MATHEMATIQUES

par

Etienne Will

Constructions tropicales de noeuds algébriques dans $\mathbb{R}P^3$

Soutenue publiquement le 20 Septembre 2012

Membres du jury:

Directeur de thèse : Pr. Ilia Itenberg, Université Pierre et Marie Curie (Paris)
Rapporteur externe : Pr. Hannah Markwig, Université de Saarbrucken
Rapporteur externe : Pr. Grigory Mikhalkin, Université de Genève
Examinateur : Pr. Michèle Audin, Université de Strasbourg
Examinateur : Pr. Viatcheslav Kharlamov, Université de Strasbourg
Examinateur : M. Jeremy Blanc, Université de Bâle

Institut de Recherche Mathématiques Avancées UMR 7501

Remerciements

Je ne pourrai remercier Ilia Itenberg à la hauteur de son influence : de son cours introductif de DEA aux nombreuses conférences auxquelles il m'a permis de me rendre, il a été de toutes les étapes de ce travail. Sa patience, sa disponibilité et la clarté de ses mises au point m'ont influencées au delà de ces pages.

Je remercie sincérement Hannah Markwig et Grigory Mikhalkin pour avoir, en tant que rapporteurs externes, accepté de relire intégralement ma thèse. Je suis bien placé pour savoir que ce n'est pas une tâche évidente !

Michèle Audin et Viatcheslav Kharlamov ont largement participé a mon « éducation mathématique » au cours de mes études à l'Université de Strasbourg. Je les en remercie autant que pour avoir accepté d'être membre de mon jury. Ces remerciements s'adresse également à Jérémy Blanc, qui a accepté d'être membre du jury dans un court délai.

J'adresse globalement des remerciements à tous les membres de l'IRMA et de l'UFR de Mathématiques qui, à un moment ou à un autre, d'une manière ou d'une autre, ont accompagné et encouragé ce travail.

La liste des amis qui ont m'accompagné et soutenu au cours de ces 7 années est trop longue pour être reproduite intégralement. Ils ont tous contribué à sa réussite, en me parlant d'autres choses ou en me forçant à leur expliquer les raisons et motivations (obscures par moment) de mon travail. Qu'ils en soient tous profondément remerciés.

J'adresse des pensées particulières à ceux qui m'ont accompagné, encouragé et aidé de manière plus personnelle au cours de notre cursus commun et malgré que nous ayons pris depuis des chemins différents. Olivier bien sûr, avec qui j'ai partagé mon bureau (et bien plus) pendant 4 ans, et qui n'a jamais renoncé à m'apprendre les rouages de LaTex. Je pense également à Gilles, Nicolas, Manu et Nermin. Qu'ils sachent que, bien que je n'en parle pas souvent, ce travail ne serait pas allé à son terme sans eux.

Pour l'influence qu'elle a eu sur tout ce qui était extérieur à ce travail, l'aboutissement de ce dernier doit sans doute plus à ma famille qu'à moi-même. Je remercie également ma « deuxième famille » pour son constant soutien.

Enfin, “last but not least”, Céline (et Hugo sur la fin) était aux premières loges : elle sait donc mieux que personne ce qu'ont représenté ces 7 années de travail.

Table of contents

Chapter 1

Introduction

1.1 Topologie des variétés algébriques réelles

L'étude de la topologie des variétés algébriques réelles trouve son origine dans l'article [14] publié par A. Harnack en 1876. L'auteur y pose la question suivante.

Problème : *quel est le nombre maximal de composantes connexes que peut avoir la partie réelle d'une courbe algébrique réelle plane projective non singulière de degré donné ?*

Une *hypersurface algébrique réelle dans un espace projectif de dimension* n est un polynôme homogène $P \in \mathbb{R}[X_0, X_1, \ldots, X_n]$, considéré à multiplication par une constante réelle non nulle près. On définit le degré d'une hypersurface comme étant le degré d'un polynôme la définissant. Elle est dite *non singulière* si les dérivées partielles $\partial_i P$, $i = 0, \ldots, n$ ne s'annulent pas simultanément dans $\mathbb{C}^{n+1} \setminus \{0\}$. Si $n = 2$, on parle de *courbes algébriques réelles dans le plan projectif.*

Remarque. Dans tout le texte, l'expression « hypersurface réelle » désignera une hypersurface algébrique réelle projective et non singulière.

La *partie réelle* d'une hypersurface réelle X définie par un polynôme P est le lieu des zéros de P dans l'espace projectif réel $\mathbb{R}P^n$. On la note $\mathbb{R}X$. Comme X est non singulière, sa partie réelle est une sous-variété lisse fermée de codimension 1 dans $\mathbb{R}P^n$. En particulier, les composantes connexes de la partie réelle d'une courbe réelle plane sont des cercles plongés de manière lisse dans $\mathbb{R}P^2$. Le seul invariant topologique de la partie réelle d'une courbe réelle plane est le nombre de composantes connexes.

Théorème 1 (Harnack, [14])**.** *Le nombre de composantes connexes de la partie réelle d'une courbe réelle plane et projective de degré d est compris entre* 0 *(ou* 1 *si d est impair) et* $\frac{1}{2}(d-1)(d-2)+1$.

De plus, en tout degré $d \geq 1$, Harnack a construit une courbe dont la partie réelle possède $\frac{1}{2}(d-1)(d-2)+1$ composantes connexes. Une telle courbe est appelée *M-courbe* ou *courbe maximale*. En particulier, il a construit une M-courbe de degré 6 dont les composantes connexes de la partie réelle sont disposées comme illustré sur la figure 1.1. Elle possède une composante connexe dont l'intérieur en contient une autre, et 9 composantes qui ne sont à l'intérieur d'aucune autre.

Fig. 1.1. *La courbe maximale de degré 6 construite par Harnack.*

Le type topologique d'une courbe réelle plane est défini par la position relative des composantes connexes de sa partie réelle. La classification topologique des courbes réelles planes consiste à déterminer quels types topologiques sont réalisables en degré fixé. Elle a été initiée par D. Hilbert en 1891 dans [17] en perfectionnant la méthode de construction utilisée par Harnack. En 1900, lorsque Hilbert formule sa célèbre liste des 23 problèmes mathématiques pour le XX$^{\text{ième}}$ siècle [16], la classification des courbes planes est seulement connue jusqu'en degré 5. Le passage suivant est extrait de l'énoncé du 16$^{\text{ème}}$ problème.

> *The maximum number of closed and separate branches which a plane algebraic curve of the n-th order can have has been determined by Harnack. There arises the further question as to the relative position of the branches in the plane. As to curves of the 6-th order, I have satisfied myself — by a complicated process, it is true — that of the eleven branches which they can have according to Harnack, by no means all can lie external to one another, but that one branch must exist in whose interior one branch and in whose exterior nine branches lie, or inversely.* A thorough investigation of the relative position of the separate branches when their number is the maximum seems to me to be of very great interest [...].

En particulier, Hilbert affirme qu'il n'existe que deux types topologiques de M-courbes de degré 6 : celui obtenu par Harnack (figure 1.1), et celui construit par Hilbert et illustré sur la figure 1.2. Ce dernier possède une composante dont l'intérieur en contient 9 autres, et une dernière composante qui n'est à l'intérieur d'aucune autre.

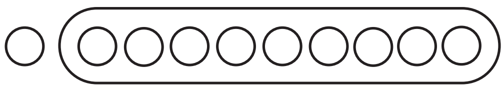

FIG. 1.2. *La courbe maximale de degré 6 construite par Hilbert.*

Durant la première moitié du XX$^{\text{ième}}$ siècle, de nombreux travaux sont menés autour de ce 16$^{\text{ième}}$ problème (voir par exemple [7, 44, 61]). Il faut cependant attendre la fin des années 1960, et le tournant initié par les contributions de « l'école russe » , pour que D. A. Gudkov [10] achève en 1969 la classification des courbes de degré 6. En particulier, il a démontré qu'il n'existe, en plus de ceux obtenus par Harnack et Hilbert, qu'un seul type topologique supplémentaire de M-courbes de degré 6 . La courbe qu'il a construit est illustrée sur la figure 1.3. Elle possède une composante connexe dont l'intérieur en contient 5 autres, et 5 composantes qui ne sont à l'intérieur d'aucune autre.

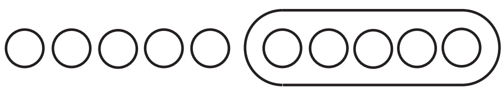

FIG. 1.3. *La courbe maximale de degré 6 construite par Gudkov.*

Les recherches effectuées depuis plus d'un siècle autour du 16$^{\text{ième}}$ problème de Hilbert ont menées à deux types de résultats. Les restrictions, d'une part, donnent des conditions nécessaires pour qu'une topologie donnée puisse être celle d'une variété algébrique réelle appartenant à une famille choisie de variétés algébriques complexes. D'autre part, les constructions, dont les principes sont, avant 1979, inspirés des méthodes développées par Harnack, Hilbert et Gudkov.

1.2 La méthode du patchwork de Viro

Une étape importante dans l'étude des problèmes de la topologie des variétés algébriques réelles est la découverte, à la fin des années 1970 par O. Ya. Viro, d'une nouvelle méthode de construction de variétés algébriques réelles appelée *méthode du patchwork*. Elle peut être vue comme une version algébrique de "copier-coller" et permet de construire des hypersurfaces algébriques réelles dans $\mathbb{R}P^n$ en contrôlant leur topologie. Son cas particulier le plus élémentaire, la méthode du patchwork combinatoire dans le plan, peut être présenté de la manière suivante.

Méthode du patchwork combinatoire dans le plan. Considérons un entier naturel d. On note T_d le triangle, contenu dans le quadrant positif de $\mathbb{R}^2$, dont les sommets de T_d sont les points de coordonnées $(0,0)$, $(0,d)$ et $(d,0)$. On note $T_d^\star$ le carré obtenu en symétrisant T_d dans les autres quadrants. Une *triangulation convexe* τ de T_d est une subdivision de T_d composée d'un nombre fini de triangles dont les sommets ont des coordonnées entières, qui peut être obtenue en projetant sur le plan $\{z=0\}$ le graphe d'une fonction convexe affine par morceaux $T_d \to \mathbb{R}$. On étend une telle triangulation à $T_d^\star$ par symétrie, et on note $\tau^\star$ la triangulation obtenue. Si chaque sommet (i,j) de τ est muni d'un signe $\sigma_{i,j} \in \{-,+\}$, l'image $(\varepsilon_1 i, \varepsilon_2 j)$ de ce sommet dans le quadrant de signe $(\varepsilon_1, \varepsilon_2)$ est muni d'un signe selon la règle suivante :

$$\sigma_{\varepsilon_1 i, \varepsilon_2 j} = \varepsilon_1^i \varepsilon_2^j \sigma_{i,j}.$$

Enfin, dans chaque triangle de $\tau^\star$, on sépare les sommets de signes contraires par un segment reliant les milieux des deux côtés, voir figure 1.4. La ligne brisée obtenue par recollement de ces segments est notée L. L'espace obtenu en identifiant les points antipodaux du bord de $T_d^\star$ est noté $\tilde{T}_d^\star$. Il est homéomorphe à $\mathbb{R}P^2$. L'image de L dans $\tilde{T}_d^\star$ est notée $\tilde{L}$.

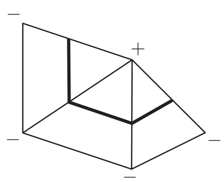

Fig. 1.4. *Construction de L.*

Théorème 2 (O. Viro, [59]). *Pour toute triangulation convexe de T_d et tout choix de signes aux sommets de celle-ci, il existe une courbe réelle plane projective non singulière X de degré d telle que $(\mathbb{R}P^2, \mathbb{R}X) \simeq (\tilde{T}_d^\star, \tilde{L})$.*

Ce résultat a permis à O. Ya. Viro d'obtenir dans [59] la classification des courbes algébriques réelles de degré 7 dans $\mathbb{R}P^2$ en 1980, et à I. Itenberg de construire, en 1993, des contres-exemples réfutant la conjecture de Ragsdale, vieille de près d'un siècle [18, 45]. En se basant sur la méthode du patchwork, ces contre-exemples ont ensuite été améliorés successivement par B. Haas [12], Itenberg [19] et enfin E. Brugallé [6]. Le patchwork combinatoire a été modifié par B. Sturmfels [49] afin de permettre la construction de variétés algébriques réelles qui sont des intersections complètes dans $\mathbb{R}P^n$.

1.3 Courbes tropicales

Les origines de la géométrie tropicale remontent au moins aux années 70 [2, 3]. Elle a maintenant des applications et connexions avec plusieurs branches des mathématiques comme, par exemple, la géométrie algébrique, la géométrie symplectique, la géométrie énumérative, les systèmes dynamiques, la théorie des nombres, la combinatoire. Plongées dans un espace euclidien, des variétés tropicales apparaissent dans plusieurs champs de la recherche mathématique : en géométrie non-archimédienne [22, 21], en géométrie complexe [37, 47], ou en physique statistique [25, 26]. Suggérée en 2000 par M. Kontsevich, une relation entre courbes algébriques complexes et courbe tropicales a été confirmée et précisée par le théorème de correspondance de G. Mikhalkin [34].

Définition. *Une courbe tropicale abstraite est un graphe fini $\overline{\Gamma}$ n'ayant pas de sommet isolé, et dont le complémentaire Γ des sommets de valence 1 est muni d'une métrique telle que :*

- *une arête adjacente à un sommet de valence 1 est isométrique à une demi-droite, et est dite non-bornée ;*
- *une arête qui n'est adjacente à aucun sommet de valence 1 est isométrique à un intervalle ouvert borné, et est dite bornée.*

Le *genre* d'une courbe tropicale abstraite est le premier nombre de Betti du graphe sous-jacent. Une courbe tropicale abstraite de genre 1 est présentée sur la figure 1.5. Les sommets de valence 1 ou 2 sont représentés par des points.

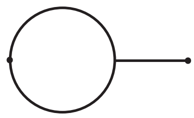

Fig. 1.5. *Courbe tropicale abstraite de genre 1.*

Définition. *Une courbe tropicale paramétrée est une paire $(\overline{\Gamma}, h)$ constituée d'une courbe tropicale abstraite $\overline{\Gamma}$ et d'une application continue $h : \Gamma \to \mathbb{R}^n$, dont la restriction a toute arête de Γ est une application affine vérifiant les conditions suivantes :*

– *pour toute arête e de Γ, le vecteur $dh_P(u_e)$ (où P est un point intérieur de e, et u_e est un vecteur tangent unitaire à e en P) est à coordonnées entières ;*
– *pour tout sommet V de Γ, on a*

$$\sum_{e \ni V} dh_P(u_e) = 0,$$

où la somme est faite sur toutes les arêtes adjacentes à V, un point P est choisi à l'intérieur de e, et u_e est le vecteur tangent unitaire à e en P tel que u_e ne soit pas dirigé vers V.

Comme $dh_P(u_e)$ est un vecteur à coordonnées entières, il existe un vecteur primitif entier $u_{e,h} \in \mathbb{Z}^n$ et un entier $w_{e,h} \in \mathbb{Z}_{\geq 0}$ tels que $dh_P(u_e) = w_{e,h} u_{e,h}$. On les appelle respectivement le *vecteur primitif entier* et le *poids* de e. Comme en géométrie algébrique complexe, certaines courbes tropicales peuvent être munies de structures réelles.

Définition. *Une courbe tropicale paramétrée réelle est une courbe tropicale paramétrée $(\overline{\Gamma}, h)$ munie d'une involution isométrique $c : \Gamma \to \Gamma$ telle que $h \circ c = h$.*

Les résultats de ce texte sont obtenus à partir de courbes tropicales dont tous les poids sont impairs. Pour une courbe tropicale de ce type, la structure réelle peut être décrite sur l'image $h(\Gamma)$ du graphe sous-jacent.

Définition. *Une courbe tropicale impaire $T \subset \mathbb{R}^n$ est un complexe polyédral de dimension 1 dans $\mathbb{R}^n$ dont chaque arête est de pente rationnelle, est munie d'un poids entier strictement positif, et tel que*

– *le poids d'une arête non bornée est 1 ;*
– *le poids d'une arête bornée est un nombre impair ;*
– *tout sommet de T est de valence 3 si $n \geq 3$, et de valence 3 ou 4 si $n = 2$; dans le cas d'un sommet de valence 4, les 4 arêtes adjacentes sont alors contenues dans la réunion de 2 droites sécantes ;*
– *la condition d'équilibre suivante soit satisfaite à chaque sommet V de T :*

> *si $v_1, \ldots, v_r$ sont les vecteurs primitifs entiers (issus de V) des arêtes adjacentes à V et $w_1, \ldots, w_r$ leurs poids respectifs, alors $w_1 v_1 + \cdots + w_r v_r = 0$.*

Le genre de T est celui du graphe obtenu en « explosant » chaque sommet de valence 4 comme illustré sur le figure 1.6.

Une structure réelle sur une courbe tropicale impaire T peut être définie combinatoirement de la manière suivante. Soit e une arête de T, de poids $w \in \mathbb{Z}_{>0}$ et de vecteur primitif entier $v \in \mathbb{Z}^n$. Un $n-$uplet de signes $\varepsilon \in \{-, +\}^n$ est identifié au vecteur ϵ à coordonnées dans $\mathbb{Z}/2\mathbb{Z}$ obtenu en remplaçant $+$ par 0 et $-$ par 1. Alors, $\varepsilon, \varepsilon' \in \{-, +\}^n$ sont équivalents relativement à e si

$$\epsilon + (wv \bmod 2) = \epsilon'.$$

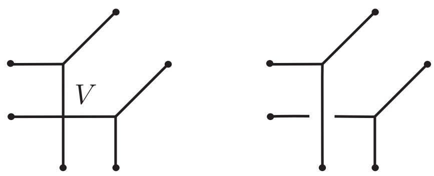

FIG. 1.6. *Graphe obtenu en explosant le sommet* 4*-valent* V*.*

On munit chaque arête de T d'une *phase*, c'est-à-dire d'une classe d'équivalence pour la relation ainsi définie.

Définition. *Une courbe tropicale impaire réelle dans* $\mathbb{R}^n$ *est la donnée d'une courbe tropicale impaire* $T \subset \mathbb{R}^n$*, dont chaque arête* e *est munie d'une phase* s_e*, et vérifiant la condition de compatibilité suivante à chacun de ses sommets trivalents :*

> *Si* s_1, s_2, s_3 *sont les phases des* 3 *arêtes adjacentes à un sommet trivalent* V*, alors chaque* n*-uplet de signes appartenant à l'un des* s_i *appartient à exactement l'un des deux autres.*

La partie réelle de T *est alors la réunion* $\mathbb{R}T \subset \mathbb{R}^n \times \{-,+\}^n$ *des ensembles de la forme*

$$\tilde{e} = \big\{\big(x, (\varepsilon_1, \dots, \varepsilon_n)\big),\ x \in e,\ (\varepsilon_1, \dots, \varepsilon_n) \in s_e\big\}$$

où e *parcourt l'ensemble des arêtes de* T*.*

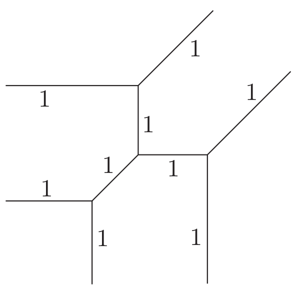

1.7 (a) Une courbe tropicale impaire plane.

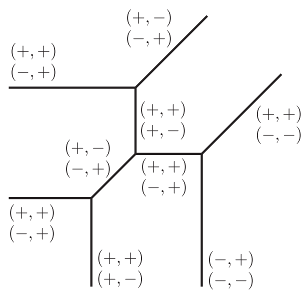

1.7 (b) Une courbe tropicale plane réelle.

FIG. 1.7. *Une courbe tropicale impaire dans* $\mathbb{R}^2$*.*

La figure 1.7 (a) montre une courbe tropicale impaire plane dont tous les poids sont égaux à 1. Cette courbe est munie d'une structure réelle sur la figure 1.7 (b). Dans ce cas, chaque phase est une paire de couples de signes.

1.4 Courbes tropicales en géométrie réelle

Le théorème du patchwork combinatoire dans le plan peut être présenté dans le language de la géométrie tropicale de la manière suivante. Une courbe tropicale $T \subset \mathbb{R}^n$ est dite *projective de degré* d si elle possède d arêtes non bornées dans chacune des directions $(-1, 0, \ldots, 0)$, $(0, -1, 0, \ldots, 0)$, ..., $(0, \ldots, 0, -1)$ et $(1, \ldots, 1)$, chaque arête étant comptée avec une multiplicité égale à son poids. Si T est en outre impaire et réelle, l'adhérence dans $\mathbb{R}P^n$ de l'image de $\mathbb{R}T$ par l'application $\mu : \mathbb{R}^n \times \{-, +\}^n \longrightarrow (\mathbb{R}^*)^n$ définie par :

$$\mu(x_1, \ldots, x_n, \varepsilon_1, \ldots, \varepsilon_n) = (\varepsilon_1 \exp x_1, \ldots, \varepsilon_n \exp x_n)$$

est une sous-variété topologique fermée de dimension 1 de $\mathbb{R}P^n$. On l'appelle *projectivisation* de T, et on la note $\mathbb{P}T$. Dans ce cadre, le résultat suivant est un corollaire du théorème 2 du patchwork combinatoire.

Théorème 3. *Pour toute courbe tropicale trivalente impaire, réelle et projective $T \subset \mathbb{R}^2$, il existe une courbe algébrique réelle non singulière $X \subset \mathbb{C}P^2$, de même genre et degré que T, dont la partie réelle est isotope à $\mathbb{P}T$.*

Remarque. Mikhalkin [34] a démontré une généralisation du théorème du patchwork combinatoire dans le plan permettant, en élargissant la classe de courbes tropicales considérée, d'obtenir des courbes réelles avec un certain type de singularités.

Une courbe algébrique réelle dans $\mathbb{R}P^3$, même non singulière, n'est pas toujours une intersection complète. Le patchwork combinatoire standard et sa généralisation obtenue par Sturmfels ne permettent de construire que des intersections complètes. Le résultat suivant est une généralisation du patchwork combinatoire permettant de construire des courbes algébriques réelles non singulières dans $\mathbb{R}P^3$ qui ne sont pas nécessairement des intersections complètes. Il ne s'applique qu'aux courbes tropicales vérifiant une certaine condition de *régularité* décrite dans la section 3.3.

Théorème 4 (Mikhalkin, [33])**.** *Pour toute courbe tropicale trivalente régulière, réelle et projective $T \subset \mathbb{R}^3$, il existe une courbe algébrique réelle non singulière $X \subset \mathbb{C}P^3$, de même genre et degré que T, dont la partie réelle est isotope à $\mathbb{P}T$.*

La partie réelle d'une courbe algébrique réelle non singulière dans $\mathbb{R}P^3$ est une sous-variété topologique fermée de dimension 1 dans $\mathbb{R}P^3$. C'est un exemple d'entrelacs projectif.

Définition. *Une sous-variété topologique fermée de dimension* 1 *dans* $\mathbb{R}P^3$ *est un entrelacs projectif. Si il ne possède qu'une seule composante connexe, on dit que c'est un noeud projectif.*

Un entrelacs dans $\mathbb{R}^3$ est une collection de cercles disjoints plongés dans $\mathbb{R}^3$ de manière continue. Il est possible de le voir comme un entrelacs projectif en utilisant l'application

$$\iota : (x, y, z) \in \mathbb{R}^3 \mapsto [x : y : z : 1] \in \mathbb{R}P^3,$$

un système de coordonnées homogènes de $\mathbb{R}P^3$ étant fixé. Cette application est un plongement qui identifie $\mathbb{R}^3$ avec la carte affine $x_3 \neq 0$ de $\mathbb{R}P^3$.

1.5 Un analogue du $16^{\text{ième}}$ problème de Hilbert en dimension 3

Le $16^{\text{ième}}$ problème de Hilbert s'interroge sur la topologie (de la partie réelle) d'une courbe réelle plane non singulière dont le degré est fixé. Dans $\mathbb{R}P^3$, le type topologique (de la partie réelle) d'une courbe réelle est déterminé par le type d'entrelacs qu'elle réalise. Une modification possible du $16^{\text{ième}}$ problème au cas des courbes dans un espace de dimension 3 peut être énoncée comme suit :

> *En quels genre et degré est-il possible de réaliser un noeud donné comme partie réelle d'une courbe algébrique réelle non singulière dans $\mathbb{R}P^3$?*

1.5.1 Résultats antérieurs

L'intérêt pour cet analogue du $16^{\text{ième}}$ problème de Hilbert est relativement récent. Un des premiers résultats le concernant est le suivant, dû à Mikhalkin. Sa démonstration fait appel au théorème 3.10.

Théorème 5 ([36])**.** *Soit $L \subset \mathbb{R}^3$ un entrelacs à $g+1$ composantes. Il existe une courbe algébrique réelle non singulière X de genre g dont la partie réelle est isotope à ιL.*

Le nombre de composantes connexes de la partie réelle d'une courbe algébrique réelle non singulière dans $\mathbb{C}P^3$ est majoré par $g+1$, où g est le genre de la courbe (voir [27]). Une courbe dont la partie réelle possède le nombre maximal de composantes connexes est appelée *M-courbe* ou *courbe maximale.* Autrement dit, une telle courbe est de genre minimal parmi toutes celles dont la partie réelle possède $g+1$ composantes. Ainsi le théorème précédent affirme que tout entrelacs dans $\mathbb{R}^3$ est isotope à la partie réelle d'une M-courbe réelle non singulière. Par contre, il ne donne aucune information sur le degré de cette courbe. Tenant compte de cet invariant algébrique, et en utilisant également le théorème 3.10, Mikhalkin et S. Orevkov ont obtenu dans [39] la classification topologique des courbes réelles non singulières de degré au plus 5 et de genre 1 dans $\mathbb{R}P^3$ (voir aussi [36]).

En considérant les courbes à isotopie rigide près, J. Björklund a classifié dans [5] les courbes réelles non singulières de degré au plus 5 et de genre 0 dans $\mathbb{R}P^3$.

V. A. Vassiliev a démontré que tout noeud peut être représenté par un plongement polynômial $\mathbb{R} \hookrightarrow \mathbb{R}^3 \subset \mathbb{S}^3$ [56]. Observant (théorème 3 de [29]) que tout noeud dans $\mathbb{R}^3$ peut, à isotopie près, être projeté sur une courbe plane de la forme $\{(x = T_a(t), y = T_b(t)),\ t \in \mathbb{R}\}$, où

- a et b sont des entiers premiers entre eux,

– T_a et T_b sont les polynômes de Tchebyshev définis par $T_n(\cos t) = \cos(nt)$ pour tout $n \in \mathbb{N}$,

P.-V. Koseleff et D. Pecker se sont intéressés dans [28, 29, 30, 31] aux plongements polynomiaux de la forme $(T_a(t), T_b(t), C(t))$. En particulier, ils ont obtenu les résultats suivants.

Théorème ([29]). *Le plongement polynomial* $(T_3(t), T_{3n+2}(t), T_{3n+1}(t))$ *représente le noeud torique* $K(2, 2n+1)$.

Théorème ([30]). *Tout noeud à* 2 *ponts, dont on note* N *le nombre de croisements, peut être représenté par un plongement polynomial* $(T_3(t), T_b(t), C(t))$, *où* $\deg C = 3N - b$.

En particulier, tout noeud rationnel de nombre de croisements N admet une paramétrisation polynomiale de degrés $(3, b, c)$ avec $b + c = 3N$ et $N < b < c < 2N$.

1.5.2 Résultats obtenus

La méthode utilisée dans ce texte peut être décrite de la manière suivante. Un noeud $K \subset \mathbb{R}^3$ étant donné, on note σ une tresse dont la cloture est K, et on note N (respectivement, k) le nombre de croisements (respectivement, le nombre de brins) de σ.

Proposition. *Il existe une courbe tropicale réelle trivalente, impaire et régulière* T_σ, *de genre* 1 *et de degré* $N + 3k$, *telle que l'ensemble des arêtes de* T_σ *dont la phase contient* $(+,+,+)$, *noté* T_σ^+, *est isotope à* K.

Autrement dit, il existe un homéomorphisme φ de $\mathbb{R}^3 \times \{(+,+,+)\}$ tel que $\varphi(\mathbb{R}T_\sigma^+) = K \times \{(+,+,+)\}$. Comme la restriction de μ à $\mathbb{R}^n \times \{(+,+,+)\}$ est un homéomorphisme sur $(\mathbb{R}_+^*)^3$, la projectivisation de T_σ contient une sous-variété fermée $\mathcal{K}$ isotope à ιK. Le résultat suivant est alors un corollaire de la régularité de T_σ et du théorème 3.10.

Théorème. *Il existe une courbe algébrique réelle non singulière* $X_\sigma \subset \mathbb{C}P^3$, *de genre* 1 *et de degré* $N+3k$, *dont la partie réelle est isotope à* $\mathbb{P}T_\sigma$. *En particulier,* $\mathbb{R}X_\sigma$ *possède deux composantes connexes, dont l'une est isotope à* $\mathcal{K}$ *et donc à* ιK.

Cependant la seconde composante est, en général, un noeud projectif non trivial. Pour certains noeuds toriques, il est possible de modifier la courbe T_σ de telle manière que sa projectivisation ne possède qu'une seule composante connexe isotope à ιK.

Théorème. *Si* $p = 2$ *et* $q > 0$ *est impair, ou si* p *est impair et* $q = p + 2$, *il existe une courbe tropicale réelle trivalente, impaire et régulière* $T_{p,q}$, *de genre* 1 *et de degré* $2p + q - 1$, *dont la projectivisation est isotope à* $\iota K(p, q)$.

Le théorème de Mikhalkin assure alors qu'il existe une courbe algébrique réelle non singulière, de genre 1 et de degré $2p + q - 1$, dont la partie réelle est isotope à $\iota K(p, q)$.

Chapter 2

Braids and links

2.1 Braids and diagrams

In this section (widely inspired by [23]), we recall — and, sometimes, slightly modify for our purposes — some fundamental notions of braid theory.

Definition 2.1. *Consider a collection of $n \geq 1$ piecewise-smooth embeddings $f_1, \ldots, f_n : [0,1] \to \{(x,y,z) \in \mathbb{R}^3,\ x \in [0,1]\}$ satisfying the following properties.*

1. *The points $f_1(0), \ldots, f_n(0)$ are on the line $\{x = 0, z = 0\}$.*
2. *The points $f_1(1), \ldots, f_n(1)$ are on the line $\{x = 1, z = 0\}$.*
3. *For every $t \in \,]0,1[$ and $1 \leq i \leq n$, the image of f_i intersects the plane $\{x = t\}$ either in exactly one point or along a segment. For every $1 \leq i \leq n$, the image of each f_i intersects the planes $\{x = 0\}$ and $\{x = 1\}$ orthogonally.*
4. *The images of any two of the maps f_1, …, f_n do not intersect:*
$$\forall i \neq j \in \{1, \ldots, n\} \quad \forall t, s \in [0,1] \ : \quad f_i(t) \neq f_j(s).$$
5. *If p (resp. q) is the point having the smallest y-coordinate (resp. the largest y-coordinate) among $f_i(0), f_i(1)$, $i = 1, \ldots, n$, then the image of f_i is contained in the cylinder over the open disk D^2 contained in the yz plane and having diameter $[pq]$.*

A geometric braid with n strings (or an n-braid) in $\mathbb{R}^3$ is the image b of a map
$$\coprod_{i=1}^{n} f_i : \coprod_{i=1}^{n} [0,1] \to [0,1] \times \mathbb{R}^2,$$
with f_i's as above. From now on we put $\mathcal{I}_n = \coprod_{i=1}^{n} [0,1]$.

The points $f_i(0)$ (respectively, $f_i(1)$) are called the *origins* (respectively, the *ends*) of the strings. Two geometric braids b, b' are *isotopic* if there exists a continuous map $h : \mathcal{I}_n \times [0,1] \to \mathbb{R}^3$ such that:

- for any $t \in [0,1]$, the map $h(\cdot, t) : \mathcal{I}_n \to \mathbb{R}^3$ defines a geometric n-braid,
- the image of $h(\cdot, 0)$ is b,
- the image of $h(\cdot, 1)$ is b'.

Such a map h is called an isotopy of b on b'. It connects b to b' by a continuous family of geometric n-braids. For every $n \geq 1$, the relation of being isotopic is an equivalence relation on the set of geometric n-braids. The class of a geometric braid b will be denoted by $\overline{b}$ and is called a topological n-braid in $\mathbb{R}^3$. The set of topological n-braids is denoted by $\mathcal{B}_n$.

Definition 2.2. *A braid diagram with n strings is a collection of n piecewise smooth topological intervals $D \subset [0,1]^2$, called the strings of the diagram, such that:*

1. *the projection* $[0,1]^2 \to [0,1]$ *on the first factor realizes a homeomorphism of each string and* $[0,1]$,

2. *the set* $D \cap (\{0\} \times [0,1])$ *coincides with* $\{(0,0), (0, \frac{1}{n-1}), \ldots, (0, \frac{n-2}{n-1}), (0,1)\}$,

3. *the set* $D \cap (\{1\} \times [0,1])$ *coincides with* $\{(1,0), (1, \frac{1}{n-1}), \ldots, (1, \frac{n-2}{n-1}), (1,1)\}$,

4. *each point of* $[0,1]^2$ *belongs to at most* 2 *strings. Each intersection (or crossing) is transverse and involves a smooth point of each string. One of the* 2 *strings is distinguished: it is called the lower string. The other one is the upper string. The lower arc of a crossing is graphically represented by a line with a hole.*

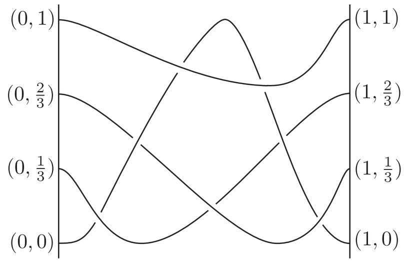

Figure 2.1. *A braid diagram with* 4 *strings.*

A braid diagram D with n strings defines a topological n-braid $\overline{b}_D$ in an obvious way. Reciprocally, any n-braid $\overline{b}$ can be represented by a braid diagram. For this, consider a generic projection $\pi : \mathbb{R}^3 \to \mathbb{R}^2$ such that the possible multiple points of $\pi(b)$ are transversal double points, where b is any representative of $\overline{b}$. The preimage of each double point P of $\pi(b)$ consists of two distinct points P_1, P_2 of b. If we assume that P_1 has a larger third coordinate than P_2, we define the upper string at P as the projection of the arc of b containing P_1, see figure 2.2. The result is a collection D' of n topological intervals in $\mathbb{R}^2$. Definition 2.1 implies that D' can be homeomorphically mapped in $[0,1]^2$ onto a braid diagram D such that $\overline{b}_D = \overline{b}$.

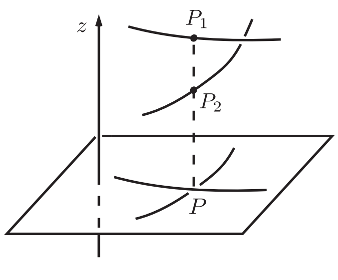

Figure 2.2.

Given two geometric n-braids b and b', we denote by $(1, y_i, 0)$ the ends of b and $(0, y'_i, 0)$ the origins of b'. Without modifying the isotopy class of b, we can assume that $y_i = y'_i$ for every $i = 1, 2, \dots, n$. The set of points $(x, y, z) \in [0, 1] \times \mathbb{R}^2$ such that

$$\begin{cases} (2x, y, z) \in b & \text{if } 0 \leq x \leq 1/2, \\ (2x-1, y, z) \in b' & \text{if } 1/2 \leq x \leq 1. \end{cases}$$

is a (geometric) n-braid, see figure 2.3. Its isotopy class depends only on the isotopy classes of b and b'. In other words, the multiplication

$$(\overline{b}, \overline{b}') \in \mathcal{B}_n \times \mathcal{B}_n \longmapsto \overline{bb}' \in \mathcal{B}_n$$

is well defined. Moreover, it is associative and has a neutral element: the topological n-braid $\mathbb{1}_n$ represented by the geometric n-braid $[0, 1] \times \{0, 1, \dots, n\} \times \{0\}$. The following result is then a direct consequence of lemma 1.10 in [23].

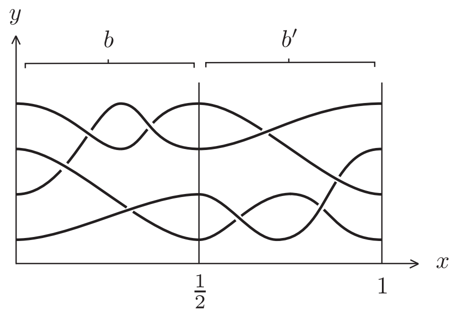

Figure 2.3. *Diagram of the product of two 4-braids b, b'.*

Theorem 2.1. *The set $\mathcal{B}_n$ of topological n-braids with the multiplication defined as above is a group.*

The ends of the first geometric braid b do not necessarily coincide with the origins of the second. Thus the multiplication defined above does not make the set of geometric braids into a group. For each $i = 1, \dots, n-1$, we define the topological n-braid σ_i represented by the braid diagram with one crossing of figure 2.4. The following result is well known (for example [23], theorem 1.12).

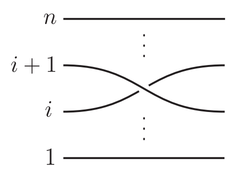

Figure 2.4. *The braid σ_i.*

Theorem 2.2. *The group $\mathcal{B}_n$ is generated by the topological braids $\sigma_1, \dots, \sigma_{n-1}$. In other words, any topological n-braid b can be written as a word in $\sigma_1, \dots, \sigma_{n-1}$ and their inverses.*

2.2 Links and knots in $\mathbb{R}^3$

We denote by $\mathcal{L}_n$ the disjoint union of n copies of the 1-dimensional sphere S^1.

Definition 2.3. *A geometric link with n components in $\mathbb{R}^3$ (or simply a n-link) is the image of a smooth embedding $\mathcal{L}_n \to \mathbb{R}^3$. It is a smooth closed (i.e., compact without boundary) 1-dimensional submanifold of $\mathbb{R}^3$.*

Equivalently, a n-link is the union of n pairwise disjoint smoothly embedded circles in $\mathbb{R}^3$. Two geometric links $L, L' \subset \mathbb{R}^3$ are *isotopic* (or equivalent) if their exists a continuous map $h : \mathcal{L}_n \times [0,1] \to \mathbb{R}^3$ such that:

- for any $t \in [0,1]$, the map $h(\cdot, t) : \mathcal{L}_n \to \mathbb{R}^3$ is a smooth embedding,
- the image of $h(\cdot, 0)$ is L,
- the image of $h(\cdot, 1)$ is L'.

In particular, two isotopic geometric links have the same number of components. Such a map h is called an *isotopy* between L and L'. It connects L to L' by a continuous family of geometric links in $\mathbb{R}^3$. The relation of being isotopic is an equivalence relation on the set of geometric links in $\mathbb{R}^3$.

Definition 2.4. *The isotopy class of a geometric link L in $\mathbb{R}^3$ is called a topological link, and is denoted by $\overline{L}$. A topological (resp. geometric) link with 1 component is called a topological (resp. geometric) knot.*

A trivial geometric n-link is the union of n pairwise disjoint unknotted circles. As in the case of braids, the way how a geometric link lies in the 3-dimensional space is well described by diagrams.

Definition 2.5. *A link diagram D is a piecewise smooth closed plane curve having a finite number of transversal double points and no other singularities. Moreover, at each double point, one of the two local branches is distinguished. The latter is called the lower branch, while the other one is the upper branch. The lower branch is graphically represented by a line with a hole.*

A link diagram D defines a topological link in the following way. The plane curve D is embedded in $\mathbb{R}^3$ by the map $(x, y) \longmapsto (x, y, 0)$. Then, at each (planar) transversal double point, is performed the following smooth deformation: the upper branch is locally pull up inside the hyperplane $\{z > 0\}$ and the lower one is locally pull down inside the hyperplane $\{z < 0\}$ such that there intersection point disappears. These deformations should be done without “breaking” the curve, see figure 2.5. The result is an isotopy class of links denoted by $\overline{L}_D$.

Definition 2.6. *Let L be a geometric link in $\mathbb{R}^3$. A diagram of L is a link diagram D such that $\overline{L}_D = \overline{L}$.*

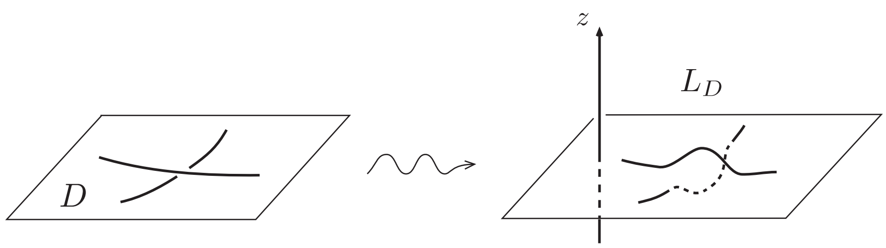

Figure 2.5.

Any (geometric) link L has a link diagram. Consider a generic projection $\pi : \mathbb{R}^3 \to \mathbb{R}^2$ such that the projection of L has only a finite number of transversal double points as only possible multiple points. The preimage of each double point P of $\pi(L)$ consists of two distincts points P_1, P_2 of L. If we assume that P_1 has a larger third coordinate than P_2, we define the upper branch at P as the projection of the arc of L containing P_1. The resulting object is a link diagram D of L.

Definition 2.7. *The mirror image of a geometric link L is represented by the link diagram obtained by reversing all the crossings in a diagram of L. A link is achiral (or amphicheiral) if it is isotopic to its mirror image.*

A link L has many different link diagrams. Without modifying the rest of a diagram D, any arc can be twisted as shown on figure 2.6. This transformation (or move) of a diagram is denoted by Ω_1, and called the first Reidemeister move. It does not modify the corresponding topological link. In other words, a geometric link corresponding to the diagram after Ω_1 is isotopic to the original geometric link. Similarly, the inverse transformation is a diagram move, denoted by Ω_1^{-1}, which does not modify the corresponding topological link.

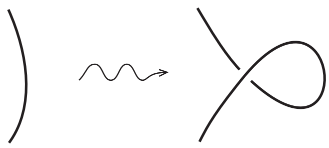

Figure 2.6. *The Reidemeister move Ω_1.*

There are infinitely many diagram transformations which do not modify the corresponding topological link. Figure 2.7 describes two of them, called the second and third Reidemeister moves and denoted by Ω_2 and Ω_3. It is a fundamental result of link theory that the moves Ω_1, Ω_2 and Ω_3 (and their inverses) can diagrammaticaly describe any link isotopy. This is the content of the next theorem, due independently to J.W. Alexander and K. Reidemeister (see [40] for example). We say that two diagrams are equivalent if one can be transformed into the other by a finite sequence of Reidemeister moves (or their inverses) and diagram isotopies.

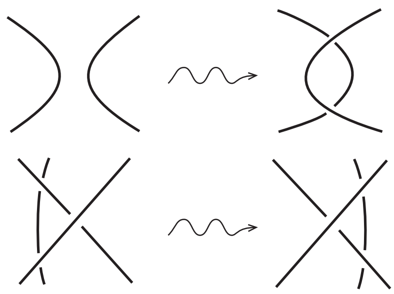

Figure 2.7. *The Reidemeister moves Ω_2 and Ω_3.*

Theorem 2.3. *Two geometric links are isotopic if and only if they admit equivalent diagrams.*

2.3 Long and RPL-knots in $\mathbb{R}^3$

We adapt definitions 2.1 and 2.3 to include long and piecewise-linear knots used in the constructions of chapters 4 and 5.

Definition 2.8. *Consider a collection of $n \geq 1$ piecewise-linear embeddings $f_1, \ldots, f_n : [0,1] \to \{(x,y,z) \in \mathbb{R}^3,\ x \in [0,1]\}$ satisfying the following properties.*

1. *The points $f_1(0), \ldots, f_n(0)$ belongs to the plane $\{x = 0\}$.*
2. *The points $f_1(1), \ldots, f_n(1)$ belongs to the plane $\{x = 1\}$.*
3. *For every $t \in \,]0,1[$ and $1 \leq i \leq n$, the image of f_i intersects the plane $\{x = t\}$ either in exactly one point or along a segment. For every $1 \leq i \leq n$, the image of f_i intersects the planes $\{x = 0\}$ and $\{x = 1\}$ orthogonally.*
4. *The images of any two of the maps f_1, …, f_n do not intersect:*

$$\forall i \neq j \in \{1, \ldots, n\} \quad \forall t, s \in [0,1] \ : \quad f_i(t) \neq f_j(s).$$

5. *If p (resp. q) is the point having the smallest y-coordinate (resp. the largest y-coordinate) among $f_i(0), f_i(1)$, $i = 1, \ldots, n$, then the image of f_i is contained in the cylinder over the open disk D^2 contained in the yz plane and having diameter $[pq]$.*

A PL-braid with n strings (or a PL n-braid) in $\mathbb{R}^3$ is the image b of a map

$$\coprod_{i=1}^{n} f_i : \mathcal{I}_n = \coprod_{i=1}^{n} [0,1] \to [0,1] \times \mathbb{R}^2,$$

with f_i's as above.

In particular, a PL-braid is a geometric braid. Two PL-braids are isotopic if they are isotopic as geometric braids. Given a geometric braid σ (respectively, a topological braid σ), a *PL-realization* of σ is a PL-braid isotopic to σ (respectively, to any geometric braid representing σ) in the class of geometric braids.

Definition 2.9. *A PL-knot is the image of a piecewise-linear embedding $f : S^1 \to \mathbb{R}^3$. A RPL-knot is a PL-knot whose edges have rational slopes.*

Thus a PL-knot is a piecewise-linear closed 1-dimensional submanifold of $\mathbb{R}^3$. In particular, a PL-knot is a geometric knot. Two PL-knots are isotopic if they are isotopic as geometric knots. Given a geometric knot K (respectively, a topological knot K), a *PL-realization* or a *RPL-realization* of K is a PL-knot or a RPL-knot isotopic to K (respectively, to any geometric knot representing K) in the class of geometric knots.

Remark 2.1. The existence of a RPL-realization of an arbitrary knot in $\mathbb{R}^3$ is an immediate corollary of lemma 4.1 of section 4.1.

A *RPL-graph* in $\mathbb{R}^3$ is a piecewise-linear graph whose edges have rational slopes. Recall that a geometric link is the image of a smooth embedding $S^1 \to \mathbb{R}^3$.

Definition 2.10. *A geometric long knot is the image of a smooth embedding $f : \mathbb{R} \to \mathbb{R}^3$.*

The notions of isotopic and topological long knots can be defined similarly to the case of knots as above, except that we restrict to the class of (geometric) long knots. A *long knot diagram* is a knot diagram, as in definition 2.5, which is homeomorphic to a line in $\mathbb{R}^2$. A long knot is a PL-long knot if the embedding of definition 2.10 is piecewise-linear. A RPL-long knot is a PL-long knot such that the edges of the image of the embedding have rational slopes.

2.4 From braids to links

Remark : from now until the end of the current chapter, braids and links are topological unless specified.

Braids are useful in the study of knots and links as every link can be obtained as the closure of a braid in the following way. Given a geometric braid with n strings, denote by $P_1, \dots, P_n$ the origins of the strings, by $Q_1, \dots, Q_n$ their ends and by C a cylinder containing the braid as in definition 2.1. Let us connect, by parallel smooth arcs lying outside C, the points $Q_1, \dots, Q_n$ to the points $P_1, \dots, P_n$. Moreover, these arcs should intersect orthogonally the plane $\{x = 0\}$ and $\{x = 1\}$, see figure 2.8. The result is a geometric link having at most n connected components, called the canonical closure of the given braid. Two isotopic geometric braids have isotopic canonical closures.

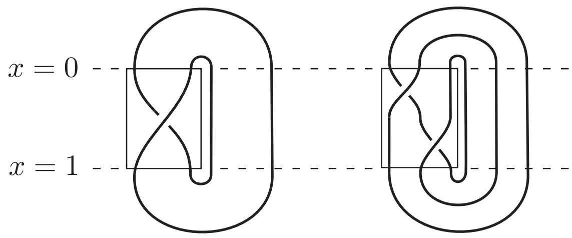

Figure 2.8. *Canonical closures of the braids σ_1 and $\sigma_1\sigma_2$.*

Definition 2.11. *Given a braid b, the isotopy class of the canonical closure of any geometric braid representing b is the canonical closure of b, and is denoted by $l(b)$.*

The canonical closure of the braids σ_1 and $\sigma_1\sigma_2$ are shown on figure 2.8. This closing procedure induces a surjective map from the set of braids onto the set of links. This is the content of the following theorem, due to J.W. Alexander ([40], theorem 10.3.1).

Theorem 2.4 (Alexander's theorem)**.** *Any link is the canonical closure of a braid.*

A braid whose canonical closure is a link l is called a braid representative of l. As we said above, isotopic geometric braids have isotopic canonical closures. Reciprocally, non-isotopic geometric braids can have isotopic canonical closures. In other words, a given link can has different braid representatives. For instance, the canonical closures of the braids σ_1 and $\sigma_1\sigma_2$ are both equal to the unknot, see figure 2.8. Thus the canonical closing procedure does not induce a bijective correspondence between braids and links. Denote by B_∞ the union of the braid groups B_k for $k \geq 1$.

Definition 2.12. *Given an element $b \in B_n$, we consider the following Markov transformations (or moves) of b, shown on figure 2.9:*

1. *The move M_1 transforms b into the n-braid $\alpha b \alpha^{-1}$, where α is any element of B_n. The element $\alpha b \alpha^{-1}$ is called a conjugate of b, and M_1 is the operation of conjugation.*
2. *The move M_2 transforms b into the $(n+1)$-braid $b\sigma_n$ or $b\sigma_n^{-1}$, where σ_n is the generator of B_{n+1}. The element $b\sigma_n^{\pm 1}$ is called a stabilization of b, and M_2 is the operation of stabilization.*

Consider two elements b, b' of B_∞. If b can be transformed into b' by a finite sequence of Markov moves and their inverses, we say that b and b' are Markov equivalent, and denote it by $b \sim_M b'$.

The terminology introduced in the definition is not ambiguous: one can easily checks that $\sim_M$ is an equivalence relation.

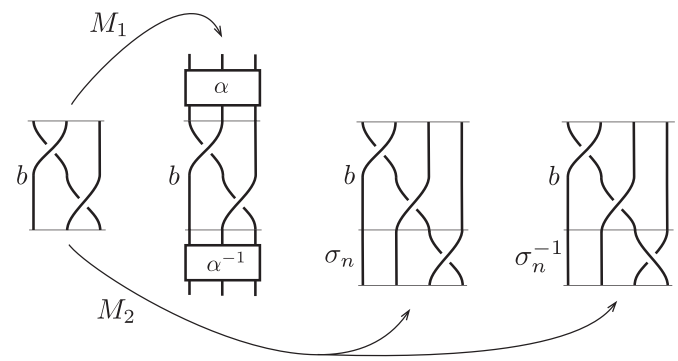

Figure 2.9. *Markov transformations of a braid.*

Example 2.1. The canonical closures of the braid σ_1 and of its stabilization $\sigma_1\sigma_2$ are both isotopic to the unknot (figure 2.8).

The following result describes the fundamental role played by Markov's moves in the correspondence between braids and links.

Theorem 2.5 (Markov's theorem, [1])**.** *Two braids have the same canonical closure if and only if they are Markov equivalent.*

Therefore a link has infinitely many braid representatives. Another classical closing procedure is the following. Given a braid having an even number of strings, say $2m$, we close it with $2m$ simple arcs as described on figure 2.10.

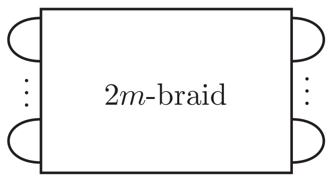

Figure 2.10. *The $2m$-plat closure of a braid with $2m$ strings.*

The resulting topological link is called the *plat closure* of the given braid. A link which can be represented as the plat closure of a $2m$-braid is called a $2m$-plat. According to theorem 2.6 of the next section, every link is the plat closure of a braid.

2.5 Classical knot invariants

The notion of knot or link invariant is fundamental to distinguish non-isotopic knots or links.

Definition 2.13. *Given a positive integer n, a link invariant is a map defined on the set of geometric n-links which is constant on each isotopy classes.*

Therefore one can define the invariant of a topological link as the invariant of any geometric link representing it. The number of crossing points of a diagram of a geometric link is not a link invariant. For example, every link diagram with one crossing represents the trivial link. Instead, denote by $\mathrm{cr}(L)$ the minimum number of crossings among diagrams of a geometric link L. Then $\mathrm{cr}(L)$ is a numerical link invariant, called the *crossing number of* L.

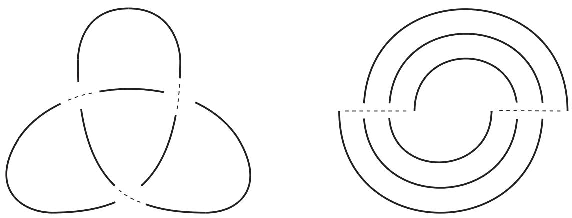

2.11 (a) 2.11 (b)

Figure 2.11. *Diagrams of the same knot with bridge numbers* 3 *and* 2*.*

A bridge is a sub-arc of a link diagram D containing only upper branches of crossings. The number of bridges of D is the minimal number of disjoint bridges necessary to pass over all crossings of D. The bridge numbers of the diagrams shown on figure 2.11 are 3 and 2. Those diagrams both represent the isotopy class of the trefoil. Thus the bridge number of a diagram is not an invariant of the corresponding topological link. We shall consider the minimal bridge number $\mathrm{br}(L)$ among diagrams of a given geometric link L. Then $\mathrm{br}(L)$ is a numerical link invariant, called the *bridge number of* L. Links having a given bridge number can be characterized using the notions of plats introduced at the end of the preceding section.

Theorem 2.6 ([1], theorem 5.2)**.** *A link has bridge number m if and only if it is a $2m$-plat.*

By convention, the bridge number of the trivial knot is 1. It is the only knot with bridge number 1. With respect to the invariant br, the simplest non-trivial knots have bridge number equal to 2. They are called 2-bridge knots.

Proposition 2.1 ([8], proposition 12.13)**.** *A* 2*-bridge knot is the plat closure of the* 4*-braid defined by*

$$b(a_1, \ldots, a_m) = \sigma_2^{a_1} \sigma_1^{-a_2} \sigma_2^{a_3} \cdots \sigma_1^{-a_{m-1}} \sigma_2^{a_m},$$

where m is odd and a_i are positive integers. We denote by $K(a_1, \ldots, a_m)$ the resulting knot. Two sequences $a_1, \ldots, a_m$ and $b_1, \ldots, b_n$ define the same knot if and only if $m = n$ and $a_i = b_i$ or $a_i = b_{m-i+1}$ for all i.

Remark 2.2. No general method for determining the bridge number of an arbitrary link is known. However, some partial results are known. For example, the bridge number of the connected sum of two knots is the sum of the bridge numbers of the knots diminished by one. In particular, there exist knots with arbitrary large bridge number.

Given a geometric link L, the minimum number of strings among braids whose canonical closure is isotopic to L is denoted by $\mathrm{b}(L)$. It is a numerical link invariant, called the *braid index of L*. The braid index of a topological link is the braid index of any geometric link representing it. Alternatively, it is the minimum number of strings among all its braid representatives. The only link with braid index 1 is the trivial knot. It is known that the links with braid index 2 are the torus knots of type $(2, q)$ defined in section 2.6. The classification of links with braid index 3 has been achieved quite recently [4]. The following result can be proved easily.

Proposition 2.2 ([40], proposition 10.4.1)**.** *If L is a link, then* $\mathrm{br}(L) \leq \mathrm{b}(L)$.

No method is known for computing the braid index of an arbitrary link. For example, the braid index of 2−bridge knots is not known in general. They can be determined for some class of knots, for example, for torus knots.

2.6 Torus knots

Denote by C the cylinder in $\mathbb{R}^3$ of height 1 whose base D_1 is the unit disk in the (xy)-plane. The top unit disk of C is denoted by D_2. We obtain the trivial torus if we glue together D_1 and D_2 in $\mathbb{R}^3$ such that the central axis of C becomes the trivial knot, as described on figure 2.12 (b).

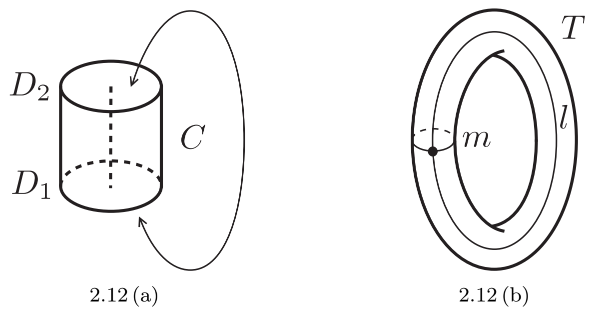

Figure 2.12. *The cylinder C and the torus T.*

The meridian m of T is the image of the unit circle ∂D_1 in T, and its longitude l is the image of the vertical segment lying above the point $(1, 0, 0)$ of C, see figure 2.12 (b).

Definition 2.14. *A link lying on a trivial torus is called a torus link.*

The meaning of the word "trivial" is the following: D_1 and D_2 can be glued together such that the image of the central axis of C is a non-trivial knot, as shown on figure 2.13 where the central axis of the cylinder is a trefoil knot.

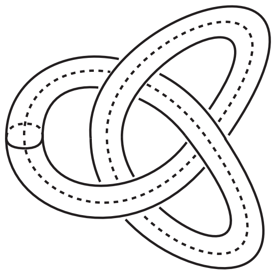

Figure 2.13. *A non-trivial torus.*

Given two integers $p \geq 1$ and $q \in \mathbb{Z}^*$, we denote by $A_0, \ldots, A_{p-1}$ and $B_0, \ldots, B_{p-1}$ the following points, lying respectively on D_1 and D_2:

$$A_k = (\cos \tfrac{2k\pi}{p}, \sin \tfrac{2k\pi}{p}, 0),$$
$$B_k = (\cos \tfrac{2k\pi}{p}, \sin \tfrac{2k\pi}{p}, 1).$$

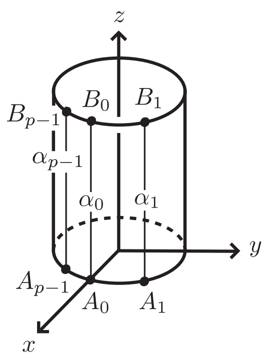

Figure 2.14.

We connect A_k to B_k by a vertical segment α_k lying on the surface of the cylinder, as shown on figure 2.6. Keeping the base D_1 fixed, we twist the cylinder by rotating the top D_2 by an angle of $2q\pi/p$ around the z-axis. We finally glue together D_1 and D_2 as described above. The result is a trivial torus $T \subset \mathbb{R}^3$, together with a collection $[\alpha]$ of non-intersecting closed curves lying on T, coming from the original segments $\alpha_0, \ldots, \alpha_{p-1}$. The number of curves occurring in $[\alpha]$ lies between 1 and p.

Definition 2.15. *Given two integers p, q with p positive, the link $[\alpha]$ obtained by the above construction is called a torus link (or knot) of type (p, q) and is denoted by $K(p, q)$.*

We also denote by $K(0, 0)$ the closed curve on T consisting of a single contractible circle, and by $K(0, 1)$ the closed curve isotopic (on T) to m.

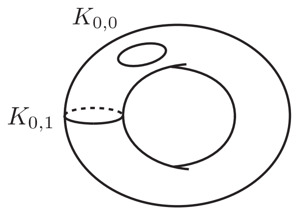

Figure 2.15.

These trivial knots are by definition the torus knots of type $(0,0)$ and $(0,1)$, respectively. If q is not zero, it is clear that $K(p,q)$ is a torus link intersecting p times the meridian and $|q|$ times the longitude.

Proposition 2.3. *Let L be a link lying on a trivial torus T. If none of the components of L is a torus link of type $(0,0)$ or $(0,1)$, then L is isotopic to some torus link $K(p,q)$.*

Proof. The torus T can be seen as a square $[0,1]^2$ in which opposite sides are identified. In this setting, the link L is a collection $\Omega \subset [0,1]^2$ of disjoint smooth curves intersecting the left side (resp., the bottom side) of the square as many times as the right side (resp., the top side). If a curve intersects twice the same side of the square, there is an isotopy of $L \subset T$ such that this curve does no longer intersects the boundary of the square, see figure 2.16.

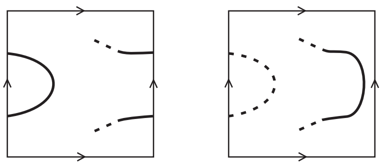

Figure 2.16. *Isotopy of L.*

If a curve connects the two vertical sides horizontally or does not intersect the boundary of the square, then it corresponds to a component of L isotopic to $K(0,1)$ or $K(0,0)$ respectively. These cases are excluded by assumption. Up to isotopy, one can assume that the following conditions are satisfied:

– if p is the number of intersection points of Ω with the bottom side, then the first coordinates of these points are $\frac{k}{p+1}$, $k = 1, \ldots, p$;
– a curve connecting two boundary points is a straight segment;
– all segments have the same slope.

Then, for all except a finite number of values of t, the number of intersection points of Ω with a vertical segment $\{t\} \times [0,1]$ does not depend on $t \in [0,1]$. If we denote this number by q, then L is isotopic to $K(p,q)$ (resp., to $K(p,-q)$) if the sommon slope of the segments is positive (resp., negative). $\square$

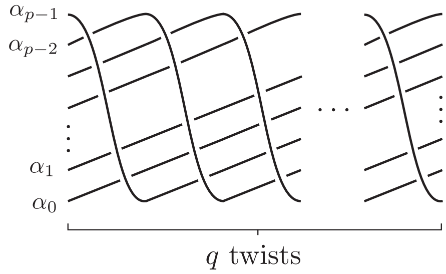

Figure 2.17. *A braid representative of $K(p,q)$ if $p,q>0$.*

If p and q are positive, we obtain a link diagram of the (non-oriented) torus link $K(p,q)$ by studying the behavior of the points B_k during the twist of the torus T. The $2q\pi/p$-rotation applied to the top circle D_2 is the composition of q successive $2\pi/p$-rotations.

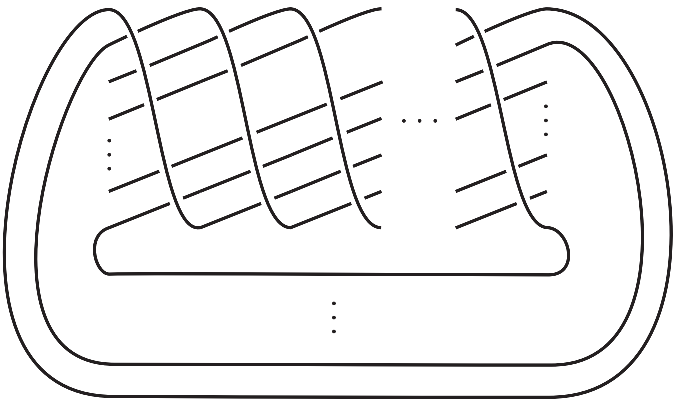

Figure 2.18. *A link diagram of $K(p,q)$ if $p,q>0$.*

Before the first $2\pi/p$-rotation, the image of B_k under the projection along the z-axis is A_k. In other words, we say that B_k is above A_k. Each $2\pi/p$-rotation brings B_k above the next A_j on the base disk D_1. Thus B_k is successively above $A_k, A_{k+1}, \ldots, A_p, A_0, \ldots$ until A_r, where r is the residue of $q+k$ modulo p. Figure 2.17 shows the segments $\alpha_0, \ldots, \alpha_{p-1}$ during the q consecutive $2\pi/p$-rotation of the torus. In particular, $B(p,q) = (\sigma_1 \cdots \sigma_{p-1})^q$ is a braid representative of $K(p,q)$. The corresponding link diagram of $K(p,q)$ is shown on figure 2.18.

Lemma 2.1. *If $p,q>0$, the canonical closure of $B(p,q)$ is isotopic to the torus link $K(p,q)$.*

Starting with $B(p,q)$, we slightly modifiy the canonical closure procedure in the following way. The top origin and end of the braid representative of $K(p,q)$ (depicted on figure 2.17) are left free, then extend to infinity in the directions $(-1,0,0)$ and $(1,0,0)$ respectively. The result is a geometric long knot denoted by $K^0(p,q)$, and called *long torus knot of type* (p,q). For positive integers p,q, the braid $B(p,q)$ is called the *torus braid* of type (p,q). If the segments α_k are oriented from A_k to B_k, it induces an orientation on the torus link $K(p,q)$. We will refer to as the oriented torus link of type (p,q), and will be still denoted $K(p,q)$. The torus link obtained by reversing the orientation of each α_k is denoted by $K(-p,-q)$.

Proposition 2.4 ([40], proposition 7.2.1)**.** *If $p \neq \pm 1$ and $q \neq 0, \pm 1$, then $K(p,-q)$ is the mirror image of $K(p,q)$.*

The classical link invariants introduced in section 2.5 has been entirely determined for torus links.

Proposition 2.5 ([40, 41])**.** *Given two distinct integers $p,q \in \mathbb{Z} \setminus \{0,1,-1\}$, the crossing and bridge numbers of $K(p,q)$ are*

$$\begin{aligned} \mathrm{cr}(K(p,q)) &= \min\{|q|(|p|-1),\, |p|(|q|-1)\}, \\ \mathrm{br}(K(p,q)) &= \min\{|p|,\, |q|\}. \end{aligned}$$

Moreover, the braid index and the bridge numbers of $K(p,q)$ are equal:

$$\mathrm{b}(K(p,q)) = \mathrm{br}(K(p,q)).$$

The classification of torus links is well known.

Theorem 2.7 ([40], theorem 7.4.3)**.** *Consider integers p,q,p',q' not equal to 0 or ± 1. Then the torus link $K(p,q)$ is equivalent to $K(p',q')$ if and only if $\{p,q\} = \{p',q'\}$ or $\{p,q\} = \{-p',-q'\}$.*

In this text, we focus on torus knots. Among torus links, they are characterized by their type.

Proposition 2.6. *Given integers p,q distinct from 0 and ± 1, the torus link $K(p,q)$ has $\gcd(p,q)$ components. In particular, $K(p,q)$ is a knot if and only if p and q are coprime.*

Proof. The number of connected components of a link is the number of cycles appearing in the cycle decomposition of the braid permutation of a braid representative of the link. Assume that p,q have the same sign, say positive. By theorem 2.7, the links $K(p,q)$ and $K(q,p)$ are equivalent. Without loss of generality, we can thus assume that $q \geq p$. As $K(p,q)$ is obtained by taking the canonical closure of $B(p,q)$, its number of components is the number of cycles occuring in the cycle decomposition of the braid permutation of $B(p,q)$. Consider the Euclidean division $q = ps + r$ of q by p. Since p and q have the same sign, the quotient s is positive. The braid permutation of $\sigma_1 \cdots \sigma_{p-1}$ is

$(1,2,\ldots,p-1,p)$, thus those of $(\sigma_1\cdots\sigma_{p-1})^p$ is the identity. Consequently the braid permutation of $B(p,q)$ is the same as $(\sigma_1\cdots\sigma_{p-1})^r$, that is:

$$\begin{aligned}&1\longmapsto r,\ 2\longmapsto r+1,\ \ldots,\ p-r\longmapsto p,\\&p-r+1\longmapsto 1,\ \ldots,\ p\longmapsto r-1,\end{aligned}$$

denoted by c. Given $k\in\{1,\ldots,p\}$, the length n of the cycle of the cycle decomposition of c containing k is the smallest positive integer such that $k+nr\equiv k\ [p]$. The integer $p'=p/\gcd(p,r)$ is convenient:

$$k+p'r=k+\frac{pr}{\gcd(p,r)}=k+\operatorname{lcm}(p,r)\equiv k\ [p].$$

It proves that the cycle decomposition of c contains $\gcd(p,r)$ cycles (of length p'), and therefore $K(p,q)$ has $\gcd(p,r)=\gcd(p,q)$ components.

If p and q does not have the same sign, we can assume that p is positive by theorem 2.7, and then apply the above arguments to the torus link $K(p,-q)$. Therefore it has $\gcd(p,q)$ connected components, and its mirror image also. But the latter is $K(p,q)$ by proposition 2.4. $\square$

2.7 Projective links and diagrams

Recall that a geometric n-component link in $\mathbb{R}^3$ is the image of a smooth embedding $\mathcal{L}_n\to\mathbb{R}^3$ (see section 2.2).

Definition 2.16. *A projective geometric n-component link in $\mathbb{R}P^3$ (or a projective n-link) is the image of a smooth embedding $\mathcal{L}_n\to\mathbb{R}P^3$. A connected (geometric) projective link is called a (geometric) projective knot.*

Two projective geometric links $L,L'\subset\mathbb{R}P^3$ are *isotopic* if there exists a continuous map $H:\mathcal{L}_n\times[0,1]\to\mathbb{R}P^3$ such that

- for any $t\in[0,1]$, the map $H(\cdot,t):\mathcal{L}_n\to\mathbb{R}P^3$ is a smooth embedding,
- the image of $H(\cdot,0)$ is L,
- the image of $H(\cdot,1)$ is L'.

Such a map is called an *isotopy* between L and L'. It deforms L onto L' via a continuous family of projective geometric links in $\mathbb{R}P^3$. The isotopy relation is an equivalence relation on the set of projective geometric links in $\mathbb{R}P^3$.

Definition 2.17. *A topological projective n-component link is an isotopy class of geometric projective n-links in $\mathbb{R}P^3$. A connected topological projective link is called a topological projective knot.*

Real algebraic curves provide a large family of projective geometric links.

Definition 2.18. *A real algebraic link in $\mathbb{R}P^3$ is the real part of a smooth real algebraic curve in $\mathbb{C}P^3$. It is irreducible (respectively, reducible) if the curve is irreducible (respectively, reducible).*

Taking into account the algebraic nature of the objects, it is natural to consider real algebraic links up to continous isotopies consisting of real algebraic links. Such an isotopy is called a *rigid isotopy*, following the terminology established by V.A. Rokhlin for real plane projective curves. In a series of papers [53, 54, 55], Yu. V. Drobotukhina explored some properties of projective knots. A projective link can be represented by diagrams that differ from usuals diagrams of links in $\mathbb{R}^3$.

Definition 2.19. *A projective link diagram is a collection D of topological intervals, the strings of the diagram, in a closed 2-disk Δ such that:*

1. *there is a finite number of crossing points, and each of these points is a transversal double point; at each crossing, one of the arcs is distinguished: it is called the lower arc; the other is the upper arc;*
2. *each string intersect transversally the boundary $\partial\Delta$*
3. *the set $D \cap \partial\Delta$ is divided into pairs of diametrically opposite points.*

Note that a crossing can be a self-intersection of a string of D. At a crossing of a projective link diagram, the lower arc is graphically represented by a line with a hole (see figure 2.19).

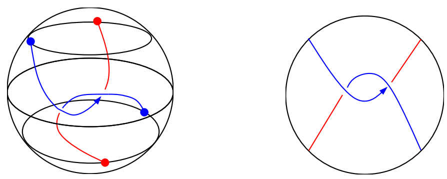

Figure 2.19. *A projective knot in D^3 and its projective diagram.*

Every projective link diagram D represents a projective (topological) link L_D in the following way. As for diagrams of affine links, D is embedded in the 3-dimensional closed ball $B^3 \subset \mathbb{R}^3$ by identifying Δ with equatorial disk of B^3. At each crossing, the upper arc is locally pull up (and the lower one is pull down) in order to obtain a non-intersecting curve $\tilde{D}$ lying inside B^3. This curve is neither connected nor closed. The identification of antipodal points of $\tilde{D}$ lying on the boundary sphere ∂B^3 defines a projective link L_D.

Definition 2.20. *Given a projective (topological) link $L \subset \mathbb{R}P^3$, a projective diagram of L is a projective link diagram D such that $L = L_D$.*

Lemma 2.2. *Every projective link has a projective diagram.*

Proof. Recall that $\mathbb{R}P^3$ can be obtained from a closed 3-ball B^3 by identifying pairs of antipodal points on the boundary sphere. Up to isotopy, we can assume that the images of the poles by the map $B^3 \to \mathbb{R}P^3$ do not belong to L. If L' denotes the inverse image of L under this map, let $\pi : L' \to \Delta$ be the projection onto the equatorial disk $\Delta \subset B^3$ defined by

$$\pi(x) = C_x \cap \Delta,$$

where $C_x \subset B^3$ is the circle passing through x and the poles of the ball. Up to a small isotopy, we can assume that L satisfies the following general position properties:

1. the image $\pi(L')$ does not contain any cusp, tangency point or triple point,
2. L' is a smooth submanifold of B^3 intersecting transversally the boundary sphere ∂B^3,
3. there do not exist 2 points of $L' \cap \partial B^3$ projecting to the same point under π; in other words, there do not exist 2 points of L' lying on the same half of a great circle joining the poles of the ball in the boundary sphere ∂B^3.

If an orientation of the arcs along which L' is projected is choosen (from north to south or vice-versa), this determines an order on each pair of arcs of L' projecting to a double point in $\pi(L')$. Therefore, at each double point of $\pi(L')$, an overpassing and an underpassing arc are emphasized, so that the image $\pi(L') \subset \Delta$ is a projective link diagram D such that $L_D = L$. $\square$

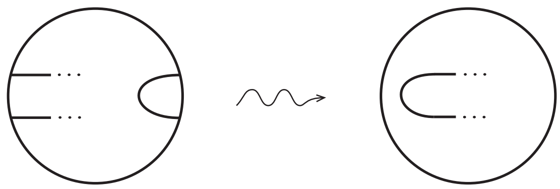

Figure 2.20. *The Ω-move Ω_4.*

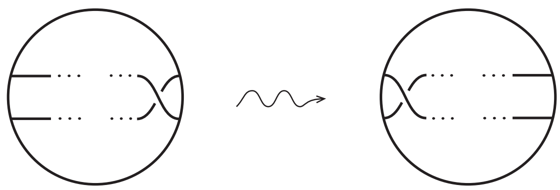

Figure 2.21. *The Ω-move Ω_5.*

Denote by Ω_4 and Ω_5 the transformations of projective diagrams depicted on figures 2.20 and 2.21, and by Ω_1, Ω_2 and Ω_3 the classical Reidemeister moves introduced in section 2.2. These diagram transformations are called Ω-moves. They do not modify the corresponding (topological) projective link. In other words, two geometric projective links having diagrams that can be connected by $\Omega-$moves are isotopic. The first three moves only modify the diagram in a small disk which does not intersect the boundary of Δ, and Ω_4 and Ω_5 affects the intersections of the diagram with the boundary of Δ. The following theorem in the projective analog of theorem 2.3. It can be found in [53], section 2.4.

Theorem 2.8. *Two projective link diagrams represent the same projective link if and only if one can be transformed into the other by a finite sequence of Ω-moves, their inverses and diagram isotopies.*

Chapter 3

Tropical curves

Notation : in this chapter, n is a positive integer and we use the multi-variable notation for polynomial rings. If K is any field, the polynomial ring in n variables $K[z_1, \ldots, z_n]$ is denoted by $K[z]$, and the notation

$$\sum_{\omega \in \Omega} a_\omega z^\omega$$

refers to a polynomial in n variables, whose support is contained in Ω, and whose coefficients are denoted by a_ω.

3.1 Non-archimedean amoebas

Non-archimedean amoebas are piecewise-linear objects contained in $\mathbb{R}^n$. In some cases (for example in the hypersurface case, see theorem 3.2 and section 3.1), they can be described in a purely combinatorial way. We recall the definition of a non-archimedean valued field.

Definition 3.1. *A non-archimedean valued field* (K, ν) *is a field* K *equipped with a non-archimedean valuation* $\nu : K \to \mathbb{R} \cup \{+\infty\}$*, that is, a map satisfying the following conditions:*

- $\nu(z) \in \mathbb{R}$ *for any* $z \in K^*$*;*
- $\nu(1) = 0$ *and* $\nu(0) = +\infty$*;*
- $\nu(zz') = \nu(z) + \nu(z')$ *for any* z *and* z' *in* K*;*
- $\nu(z + z') \geq min(\nu(z), \nu(z'))$ *for any* z *and* z' *in* K.

The divisible group $\nu(K^*)$ *is the valuation group of* (K, ν)*. The ring* $R = \{z \in K \mid \nu(z) \geq 0\}$ *is the valuation ring of* (K, ν)*. It is a local ring of unique maximal ideal* $M = \{z \in K \mid \nu(z) > 0\}$*. The residual field of* (K, ν) *is the quotient field* $k = K/M$.

Example 3.1. (a) Given a prime integer p, the field $\mathbb{Q}$ endowed with the valuation ν_p sending an integer $z \in \mathbb{Z}$ to the largest integer m such that p^m divides z, is a non-archimedean valued field. Its residual field is the finite field $\mathbb{F}_p$.

(b) Let k be any field. The field $K = k((t))$ of formal Laurent series $a(t) = \sum_{j=m}^{\infty} a_j t^j$, where $a_j \in k$ and $m \in \mathbb{Z}$, has a discrete valuation ord defined by

$$\mathrm{ord}(a(t)) = \min\{j \mid a_j \neq 0\} \in \mathbb{Z}.$$

If k is algebraically closed and $\mathrm{char}(k) = 0$, then the field of Puiseux series

$$\bigcup_{l \geq 1} k((t^{1/l}))$$

is algebraically closed [9]. It has a $\mathbb{Q}$-valued valuation ord defined as above. Note that the assumption $\mathrm{char}(k) = 0$ is necessary. If $\mathrm{char}(k) = p$, then the equation $z^p - z = t^{-1}$ has no roots in $k((t^{1/n}))$.

(c) Let k be an algebraically closed field and $G \subset \mathbb{R}$ a divisible subgroup. A transfinite (or generalized) Puiseux series over k with exponents in G is a formal sum $a(t) = \sum_{i \in G} a_i t^i$, where $a_i \in k$ are such that $\mathrm{Supp}(a) = \{i \mid a_i \neq 0\}$ is well-ordered (i.e. every subset has a minimal element). Such series form a field $k((t^G))$ that is always algebraically closed [24, 46]. For example, the equation $z^p - z = t^{-1}$ considered in example (b) has the root

$$z(t) = t^{-1} + t^{-1/p} + t^{-1/p^2} + \dots .$$

We define a non-archimedean valuation on $k((t^G))$ by $\mathrm{val}(a) = \min\{\mathrm{Supp}(a)\}$. In these notes we are mainly concerned with the field of generalized Puiseux series over $\mathbb{C}$ with real exponents. We denote it by $\mathbb{K} = \mathbb{C}((t^{\mathbb{R}}))$.

If (K, ν) is a non-archimedean valued field, the map Val : $(K^*)^n \to \mathbb{R}^n$ defined by

$$\mathrm{Val}(z_1, \dots, z_n) = (-\nu(z_1), \dots, -\nu(z_n))$$

is called the *valuation map* on $(K^*)^n$.

Definition 3.2. *If $V \subset K^n$ is an algebraic variety, the non-archimedean amoeba $\mathcal{A}_K(V)$ of V is the image of $V \cap (K^*)^n$ under the map Val. The non-archimedean amoeba of a hypersurface defined by a polynomial f is also denoted by $\mathcal{A}_K(f)$.*

Recall that a polyhedron in $\mathbb{R}^n$ is a set that can be defined by a finite number of inequalities of the form

$$a_0 + a_1x_1 + \ldots + a_nx_n \leq 0 \text{ or } \geq 0,$$

where the coefficients a_i are real numbers. A polyhedron is rational if it can be defined by inequalities where all coefficients are rational numbers, except possibly a_0. A face of a polyhedron P is a subset of P defined by the same inequalities as P except some of them (possibly all or none) for which the inequality is replaced by an equality. A (rational) polyhedral complex $\mathcal{P}$ in $\mathbb{R}^n$ is the union of a finite set of (rational) polyhedra P_i such that the intersection of any two of them is either empty, or a common face of both.

If the field K is algebraically closed and of characteristic 0, the following result holds true.

Theorem 3.1 ([22], Theorem 2.2.5.)**.** *Assume that $\mathbb{Q} \subset \nu(K^*)$, and let $V \subset K^n$ be an irreducible algebraic variety of dimension d. Then the closure of $\mathcal{A}_K(V)$ is a rational polyhedral complex of pure dimension d.*

In general, if $V_1, \dots, V_m$ are the irreducible components of V, we have $\mathcal{A}_K(V) = \mathcal{A}_K(V_1) \cup \dots \cup \mathcal{A}_K(V_m)$ ([3], §2.2) and thus $\mathcal{A}_K(V)$ is a rational polyhedral complex of the same dimension as V. The hypersurface case is particularly simple due to the following result.

Theorem 3.2 (Kapranov's theorem, [21])**.** *Let (K, ν) be a algebraically closed non-archimedean valued field, with $\mathbb{Q} \subset \nu(K^*)$, and $f(z) = \sum_{\omega \in \Omega} c_\omega z^\omega$ a polynomial in $K[z]$. Then the closure of the amoeba $\mathcal{A}_K(f)$ is the corner locus of the convex piecewise-linear map*

$$\hat{\nu}(x) = \max_{\omega \in \Omega} \{-\nu(c_\omega) + \langle \omega, x \rangle\},$$

that is the set of points where the maximum is attained (at least) twice. In other words, it is the set of $x \in \mathbb{R}^n$ where the piecewise-linear map $\hat{\nu}$ is not smooth.

Remark 3.1. The piecewise-linear map $\hat{\nu}$ occurring in Kapranov's theorem is the Legendre transform of the map $\omega \in \Omega \mapsto \nu(c_\omega)$.

In particular, the valuation of the zeros of a polynomial $f \in K[z]$ depends only on the valuation of its coefficients: a rational point $x \in \mathbb{Q}^n$ is the image under Val of a zero of f if and only if the maximum in $\hat{\nu}(x)$ is attained at least twice. Kapranov's theorem is therefore a generalization of Newton's lemma to the case of hypersurfaces of arbitrary dimension. It extracts an algebraic information about f from a geometric one, namely, valuations of the roots of f from the corner locus of a convex piecewise-linear map.

Example 3.2. Consider the non-archimedean valued field $(\mathbb{K}, \mathrm{val})$ of complex transfinite Puiseux series with real exponents introduced in example 3.1, c). If we consider the polynomial

$$f(z_1, z_2) = t^2 z_1 + t^{-1} z_2 + 1,$$

then the non-archimedean amoeba of $X = \{f = 0\} \subset \mathbb{K}^2$ is the corner locus of the piecewise-linear map $\hat{\nu} : (x, y) \in \mathbb{R}^2 \mapsto \hat{\nu}(x, y) \in \mathbb{R}$ defined by

$$\hat{\nu}(x, y) = \max\{x - 2, y + 1, 0\}.$$

The maximum is attained three times if and only if $x - 2 = y + 1 = 0$, that is, at the point $(2, -1)$. It is attained twice on the half-lines $\{x = 2,\, y \leq -1\}$, $\{y = -1,\, x \leq 2\}$ and $\{x = y + 3,\, x \geq 2\}$. Figure 3.1 shows the resulting non-archimedean amoeba.

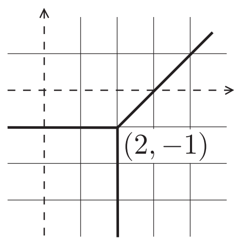

Figure 3.1. *The non-archimedean amoeba of the line* $t^2 z_1 + t^{-1} z_2 + 1 = 0$.

In the case of the valued field $(\mathbb{K}, \mathrm{val})$ of complex transfinite series with real exponents introduced in example 3.1, Theorem 3.2 has the following generalization. An element $z \in (\mathbb{K}^*)^n$ such that $\mathrm{Val}(z) = x$ can be written

$$z = (\alpha_1 t^{-x_1} + \text{h.o.t.}, \ldots, \alpha_n t^{-x_n} + \text{h.o.t.}),$$

where $\alpha_i \in \mathbb{C}^*$ and "h.o.t." contains terms of strictly greater valuation. The n-tuple $(\alpha_1, \ldots, \alpha_n) \in (\mathbb{C}^*)^n$ is called the principal coefficient of z.

Definition 3.3. *Let* $x \in \mathbb{R}^n$ *and* $f(z) = \sum_{\omega \in \Omega} c_\omega x^\omega$ *be a polynomial in* $\mathbb{K}[z]$. *We denote by* $in_w f \in \mathbb{C}[z]$ *the initial form of* f *defined by*

$$in_w f(z) = \sum c_\omega^0 z^\omega$$

where c_ω^0 *is the first non-zero coefficient of the complex transfinite Puiseux series* c_ω, *and the sum is over* $\omega \in \Omega$ *for which* $-\nu(c_\omega) + \langle x, \omega \rangle$ *is maximal.*

In this setting, L. Tabera proved in [52] the following generalization of Kapranov's theorem.

Theorem 3.3 ([52], Theorem 2.4)**.** *Let $f \in \mathbb{K}[z]$ and $(x, \alpha) \in \mathbb{Q}^n \times (\mathbb{C}^*)^n$. Then, there exists a zero z of f such that Val$(z) = x$ and whose principal coefficient is α if and only if the maximum is attained at least twice in $\hat{\nu}(x)$ and $(in_x f)(\alpha) = 0$.*

This result has been independently generalized to the case of non-archimedean amoebas of arbitrary algebraic varieties by S. Payne in [42] (theorem 4.1) and H. Markwig, T. Markwig and A. Jensen in [32] (theorem 2.13).

3.2 Tropical hypersurfaces in $\mathbb{R}^n$

3.2.1 Tropical polynomials and duality

Let (K, ν) be a non-archimedean valued field and

$$f(z) = \sum_{\omega \in \Omega} c_\omega \, z^\omega$$

a polynomial in $K[z]$. We denote by trop$f : \mathbb{R}^n \to \mathbb{R}$ the convex piecewise-linear map appearing in theorem 3.2:

$$(\text{trop}f)(x) = \max_{\omega \in \Omega} \{-\nu(c_\omega) + \langle \omega, x \rangle\}.$$

It can be seen as the *tropical* interpretation of the polynomial f in the following sense. We denote by $\oplus$ and $\otimes$ the tropical addition and multiplication defined by

$$\begin{aligned} a \oplus b &= \max\{a, b\} \\ a \odot b &= a + b, \end{aligned}$$

for every real numbers a and b. In the definition of f, we replace any coefficient c_ω by $-\nu(c_\omega)$, and every addition or multiplication by their tropical analogs. The resulting map, denoted by

$$\bigoplus_{\omega \in \Omega} -\nu(c_\omega) \odot x^{\odot \omega},$$

is equal to trop$f$. For a detailed introduction to tropical mathematics, see [50, 51] and references therein. This interpretation motivates the following definition.

Definition 3.4. *A tropical polynomial in n variables is a function of the form trop$f : \mathbb{R}^n \to \mathbb{R}$ with $f \in K[z]$. We denote by Trop(f) the corner locus of the piecewise-linear map trop$f$:*

$$Trop(f) = \{x \in \mathbb{R}^n \mid \text{the maximum in } (\text{trop}f)(x) \text{ is attained at least twice}\}.$$

Remark 3.2. The map trop$f$ coincides with the map $\hat{\nu}$ of theorem 3.2. Thus, if (K, ν) is an algebraically closed non-archimedean field such that $\mathbb{Q} \subset \nu(K^*)$, a set of the form $\mathrm{Trop}(f)$ is the closure of the non-archimedean amoeba $\mathcal{A}_K(f)$.

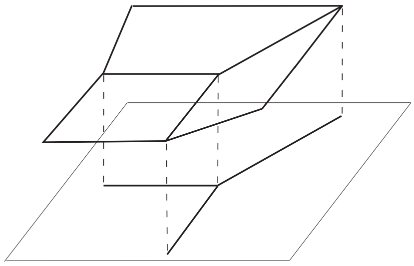

Figure 3.2. *The graph of* $\max\{x-2, y+1, 0\}$ *in* $\mathbb{R}^3$ *and its corner locus in* $\mathbb{R}^2$.

Example 3.3. Consider the polynomial $f(z_1, z_2) = t^2 z_1 + t^{-1} z_2 + 1$ introduced in example 3.2. Figure 3.2 displays the shapes of the 3-dimensional graph of the convex piecewise-linear map $(\mathrm{trop}f)(x, y) = \max\{x - 2, y + 1, 0\}$ and its 1-dimensional corner locus $\mathrm{Trop}(f) \subset \mathbb{R}^2$.

Recall that the Newton polyhedron $\Delta(f) \subset \mathbb{R}^n$ of f is the convex hull of the set of exponent vectors $\omega \in \Omega$ such that $c_\omega \neq 0$. The lattice polyhedron

$$\tilde{\Delta}(f) = \mathrm{ConvexHull}\{(t, \omega) \in \mathbb{R} \times \Omega \mid t \geq \nu(c_\omega)\}$$

is the overgraph of the map $\omega \in \Omega \mapsto \nu(c_\omega) \in \mathbb{R}$. Recall that the latter is a subset of $\mathbb{R} \times \mathbb{R}^n$, consisting of points of the form (t, ω), where $\omega \in \Omega$ and $t \geq \nu(c_\omega)$. The natural projection $p : \tilde{\Delta}(f) \to \Delta(f)$ defines a lattice polyhedral subdivision S_f of $\Delta(f)$ in the following sense: the projections of non-vertical faces $\tilde{\Delta}(f)$ give rise to the faces of S_f (see figure 3.3).

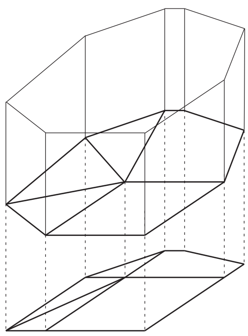

Figure 3.3. *The projection of the lower faces of* $\tilde{\Delta}(f)$ *on* $\Delta(f)$.

Remark 3.3. Subdivisions Δ_ν of a lattice polyhedron $\Delta \subset \mathbb{R}^n$ which are the projection of the overgraph of a function $\nu : A \to \mathbb{R}$, with $\mathrm{Vert}(\Delta) \subset A \subset \mathbb{Z}^n$, are called *coherent* or *convex lattice subdivisions* of $\Delta(f)$. The map ν is called a *height function* of the subdivision. If ν is generic among the maps $A \to \mathbb{R}$ with $\mathrm{Vert}(\Delta) \subset A \subset \mathbb{Z}^n$, the subdivision Δ_ν is a triangulation. Figure 3.4 shows a non-convex lattice subdivision (see [57]).

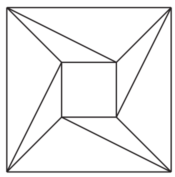

Figure 3.4. *A non-convex lattice subdivision.*

On the other hand, f determines a polyhedral subdivision $\hat{S}_f$ of $\mathbb{R}^n$ in the following way. For $i \in \{0, \ldots, n-1\}$, the faces of dimension i of $\hat{S}_f$ are the faces of dimension i of the polyhedral complex $\mathrm{Trop}(f)$, and the facets of $\hat{S}_f$ are the connected components of the complement $\mathbb{R}^n \setminus \mathrm{Trop}(f)$. The subdivisions S_f and $\hat{S}_f$ are combinatorially dual in the following sense.

Lemma 3.1 ([34], §3.4)**.** *There exists a bijection $\sigma \in S_f \mapsto \sigma^* \in \hat{S}_f$ reversing incidence relations and such that, for every $\sigma \in S_f$, one has:*

1. *$\dim \sigma^* = n - \dim \sigma$;*
2. *σ is a vertex of S_f lying in the interior of $\Delta(f)$ if and only if σ^* is a bounded facet of $\hat{S}_f$ (i.e., a bounded connected component of $\mathbb{R}^n \setminus \mathrm{Trop}(f)$);*
3. *σ is a vertex of S_f lying on $\partial\Delta(f)$ if and only if σ^* is an unbounded facet of $\hat{S}_f$ (i.e., an unbounded connected component of $\mathbb{R}^n \setminus \mathrm{Trop}(f)$);*
4. *the directions of σ and σ^* are orthogonal.*

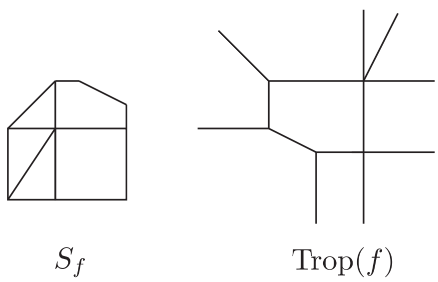

Figure 3.5. *Duality in the planar case.*

When Trop(f) is a rational piecewise-linear graph in $\mathbb{R}^2$, the above mentioned duality has the following description (see figure 3.5). Every edge e of the subdivision S_f corresponds to an orthogonal e^* edge of Trop(f), and e^* is unbounded if and only if $e \subset \partial\Delta(f)$. Every vertex V of S_f corresponds to a connected component F_V of $\mathbb{R}^2 - \text{Trop}(f)$, and F_V is unbounded if and only if $V \in \partial\Delta(f)$. Finally, every 2-dimensional l-gon of S_f corresponds to a vertex of valence l of Trop(f).

3.2.2 Weight structure and tropical hypersurfaces

Lemma 3.1 allows us to put an additional structure on the non-archimedean amoeba $\mathcal{A}_K(f)$ of a hypersurface, or on its closure Trop(f). If τ is a face of dimension $n-1$ of the rational polyhedral complex Trop(f), τ^* is an edge of the dual subdivision S_f of $\Delta(f)$. We assign a weight to τ by

$$w(\tau) = |\tau^*| \in \mathbb{Z}_{>0},$$

where $|\tau^*|$ is the integer length of τ^*, that is, the number of lattice points contained in τ^* diminished by 1.

Definition 3.5. *A tropical hypersurface is the corner locus Trop(f) of a tropical polynomial tropf equipped with the weights defined above. We denote it by (Trop(f), w), or simply Trop(f).*

Remark 3.4. Thus, a tropical hypersurface is a rational polyhedral complex of codimension 1. Moreover, if (K, ν) is an algebraically closed non-archimedean field such that $\mathbb{Q} \subset \nu(K^*)$, it coincides with the closure in $\mathbb{R}^n$ of the non-archimedean amoeba of a hypersurface by Kapranov's theorem 3.2.

Consider a face σ of dimension $n-2$ of a tropical hypersurface, and denote by $\tau_1, \dots, \tau_r$ the facets (faces of dimension $n-1$) adjacent to σ. The affine space containing σ defines a linear projection $\pi : \mathbb{R}^n \to \mathbb{R}^2$. Then $s = \pi(\sigma)$ is a vertex whose adjacent edges are the $\pi(\tau_i)$. Let u_i be the primitive integer vector of $\pi(\tau_i)$ pointing away from s.

Proposition 3.1. *The rational weighted $(n-1)-$polyhedral complex (Trop(f), w) satisfies the following balancing condition at every $(n-2)-$face σ of Trop(f):*

$$\sum_{i=1}^{r} w(\tau_i) \cdot u_i = 0.$$

Proof. Straightforward by duality. □

The balancing condition characterizes the corner loci of tropical polynomials among rational weighted polyhedral complexes of dimension $n-1$.

Proposition 3.2 ([34, theorem 3.15.]). *A rational weighted polyhedral complex of dimension $n-1$ in $\mathbb{R}^n$ is the corner locus of a tropical polynomial if and only if it satisfies the above balancing condition.*

Thus the set of tropical hypersurfaces coincides with the set of balanced rational weighted polyhedral complexes of dimension $n-1$. Following remark 3.4, if (K,ν) is an algebraically closed field of characteristic zero such that $\mathbb{Q} \subset \nu(K^*)$, the set of closures of non-archimedean amoebas $\mathcal{A}_K(f)$ coincides with the set of balanced rational weighted polyhedral complexes of dimension $n-1$. Therefore we can altenatively define a tropical hypersurface either as a balanced rational weighted polyhedral complex of codimension 1, or as the non-archimedean amoeba of an algebraic hypersurface.

tropical hypersurfaces	$\longleftrightarrow$	non-archimedean amoebas of algebraic hypersurfaces	$\longleftrightarrow$	balanced rational weighted polyhedral complexes of dimension $n-1$

We will see in section 3.3 that it is no longer the case in higher codimensions: there exist balanced rational weighted polyhedral complexes of codimension greater than 1 which are not (the closure of) non-archimedean amoebas of algebraic varieties.

Definition 3.6. *A tropical hypersurface Trop(f) is projective if the Newton polygon of f is of the form $\Delta_d = \{(x_1,\ldots,x_n) \in (\mathbb{R}_+)^n \mid x_1+\cdots+x_n \leq d\}$. The degree of the projective tropical hypersurface Trop(f) is the degree of f.*

The tropical hypersurface associated to a polynomial f is also denoted by Trop(X) with $X = V(f)$. The algebraic and tropical projective hypersurfaces defined by f have the same degree, namely $\deg f$. As in classical algebraic geometry, a tropical plane curve of degree 2 (resp., 3, 4, etc.) is called a tropical plane conic (resp., cubic, quartic, etc.). A tropical hyperplane is a tropical hypersurface of degree 1. As a set, it is the corner locus of a piecewise-linear map of the form

$$(x_1,\ldots,x_n) \longmapsto \max\{a_0, x_1+a_1,\ldots,x_n+a_n\}.$$

3.3 Tropical curves in $\mathbb{R}^n$

We denote by $e_1, e_2, \ldots, e_n$ the standard basis vectors of $\mathbb{R}^n$. If $\overline{\Gamma}$ is a finite graph without vertex of valency 0 or 2, we denote by Γ the complement of the set of 1-valent vertices. An edge of Γ is *unbounded* (resp., *bounded*) if it is adjacent to a (resp., if it is not adjacent to any) 1-valent vertex. An unbounded edge is also called an *end* of $\overline{\Gamma}$. The genus of $\overline{\Gamma}$ is $b_1(\overline{\Gamma}) - b_0(\overline{\Gamma}) + 1$, where $b_i(\overline{\Gamma})$ are the Betti numbers of $\overline{\Gamma}$. The following definitions introduce abstract and parameterized tropical curves.

Definition 3.7. *A finite graph as above is an abstract tropical curve if Γ is equipped with a metric such that every bounded edge is isometric to an open bounded interval of $\mathbb{R}$, and every unbounded edge is isometric to a half-line. The genus of an abstract tropical curve is the genus of the underlying graph.*

In particular, the genus of an abstract connected tropical curve is the first Betti number of the underlying graph.

Example 3.4. Some abstract tropical curves are depicted on figure 3.4. The 1-valent vertices are represented by bold points.

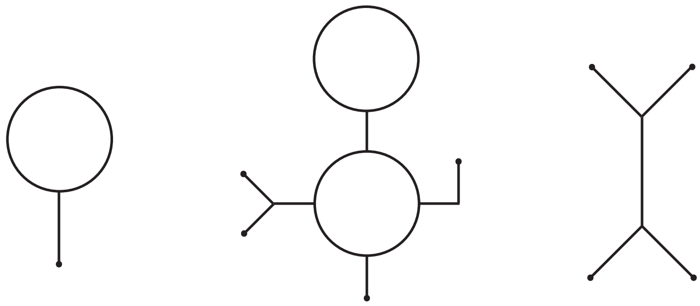

Figure 3.6. *Examples of abstract tropical curves.*

Definition 3.8. *A parameterized tropical curve in $\mathbb{R}^n$ is a pair $(\overline{\Gamma}, h)$ consisting of an abstract tropical curve $\overline{\Gamma}$ and a continuous map $h : \Gamma \to \mathbb{R}^n$ satisfying the following conditions.*

1. *Given any edge e of $\overline{\Gamma}$, the restriction $h_{|e}$ is an affine map.*
2. *For any edge e of $\overline{\Gamma}$, we denote by u_e a tangent unit vector to $\overline{\Gamma}$ at some interior point P of e. Then, $dh_P(u_e)$ is an integer vector. Therefore, if $dh_P(u_e)$ is non-zero, there exist a primitive integer vector $u_{e,h} \in \mathbb{R}^n$ and a positive integer $w_{e,h}$, called the weight of e, such that $dh_P(u_e) = w_{e,h} \cdot u_{e,h}$.*
3. *Given any vertex V of $\overline{\Gamma}$, denote its adjacent edges by $e_1, \ldots, e_r$, and assume that each vector u_e points away from V. Then,*

$$\sum_{i=1}^{r} w_{e_i,h} \cdot u_{e_i,h} = 0.$$

The genus of a parameterized tropical curve is the genus of the underlying abstract tropical curve. Two parameterized tropical curves $(\overline{\Gamma}_1, h_1)$ and $(\overline{\Gamma}_2, h_2)$ in $\mathbb{R}^n$ are equivalent if there exists an isometry $\phi : \overline{\Gamma}_1 \to \overline{\Gamma}_2$ such that $h_1 = h_2 \circ \phi$.

Remark 3.5. In particular, the image under h of a bounded edge is an open segment, and the image of an unbounded edge is either an open half-line or a line if the edge is adjacent to two 1-valent vertices.

A parameterized tropical curve $(\overline{\Gamma}, h)$ in $\mathbb{R}^n$ is *generic* if the following assumptions are satisfied:

– the underlying graph has only vertices of valency 1 or 3;

- if $n \geq 3$, then h is injective;
- if $n = 2$, then each point of $h(\Gamma)$ has at most two inverse images under h, and any point of $h(\Gamma)$ having two inverse images is not the image of a vertex of Γ.

The image of a parameterized tropical curve $(\overline{\Gamma}, h)$ in $\mathbb{R}^n$ is a rational polyhedral complex of dimension 1. If we assign to each edge $\tilde{e}$ of $T = h(\Gamma)$ the sum of the weights of the edges e of Γ such that $\tilde{e} \subset h(e)$, then the following balancing condition is satisfied at each vertex V of T:

> *if we denote by $w_1, \dots, w_r$ the weights of the edges incident to V, and by $u_1, \dots, u_r$ their primitive integer vectors (pointing away from V) then*
> $$\sum_{i=1}^{r} w_i u_i = 0.$$

Therefore, T is a balanced rational weighted polyhedral complex of dimension 1. Reciprocally, a balanced rational weighted polyhedral complex of dimension 1 in $\mathbb{R}^n$ can be parameterized by a tropical curve.

Definition 3.9. *1. A tropical curve T in $\mathbb{R}^n$ (with $n \geq 2$) is a balanced rational weighted polyhedral complex of dimension 1. It is generic if the following conditions are satisfied:*

- *if $n \geq 3$: the vertices of T are of valency 3;*
- *if $n = 2$: the vertices of T are of valency 3 or 4, and the edges adjacent to any 4-valent vertex are contained in two intersecting straight lines.*

2. The genus of T is the minimal genus among all parameterizations of T.

3. If e is an unbounded edge of T, denote by $w_e \in \mathbb{Z}_{>0}$ its weight and by $u_e \in \mathbb{Z}^n$ its primitive integer vector pointing away from the vertex. The degree of T is the list deg(T) composed with the vectors u_e, where each u_e is repeated w_e times.

4. T is projective of degree d if deg$T$ consists of the vectors $-e_1$, $-e_2$, ..., $-e_n, e_1 + \cdots + e_n$, each of them occurring d times.

In particular, a generic tropical curve in $\mathbb{R}^n$ can be parameterized by a generic parameterized tropical curve. A generic plane tropical curve is also called a *nodal* tropical curve.

Example 3.5. Every connected trivalent tropical curve $T \subset \mathbb{R}^n$ admits a natural generic parametrization $(\overline{\Gamma}_T, h)$ where Γ_T is connected and trivalent and h is an embedding. In particular, an edge of T is the image of a unique edge of Γ_T. The genus of this parametrization is minimal and equal to the genus of T. Thus, the genus of a connected trivalent tropical curve in $\mathbb{R}^n$ is equal to the first Betti number of the underlying graph.

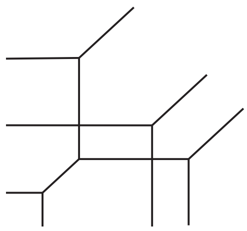

3.7 (a) A projective generic tropical plane cubic.

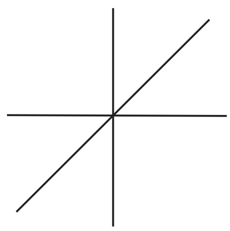

3.7 (b) A non-projective and non-generic tropical plane curve.

Figure 3.7. *Projective and non-projective tropical plane curves.*

Definition 3.10. *Two parametrized tropical curves $(\overline{\Gamma}, h)$ and $(\overline{\Gamma}, h')$ have the same combinatorial type if, given any edge e of Γ, the vectors $u_{e,h}$ and $u_{e,h'}$ are collinear and the weights $w_{e,h}$ and $w_{e,h'}$ are equal.*

Notice that curves of the same combinatorial type are parametrized by the same graph. The lengths of (the image of) its bounded edges determines the image of the graph under h up to translations. These lengths together with the 3 parameters of translations are thus natural parameters for the space of tropical curves of the same combinatorial type. As a length is positive, this space is the relative interior of the intersection of several half-spaces in an affine space.

Theorem 3.4 ([34], proposition 2.14.)**.** *The space of equivalence classes (with respect to the equivalence relation of definition 3.8) of parametrized tropical curves $(\overline{\Gamma}, h)$ of the same combinatorial type is the relative interior of a convex polyhedral complex in a real affine space of dimension*

$$k \geq a_\infty + (n-3)(1-g) - \sum_{V\,vertex\ of\ \Gamma} (\mathrm{Val}(V) - 3),$$

where a_∞ is the number of unbounded edges of Γ. The right-hand side of the inequality is called the expected dimension of the combinatorial type, and k is its actual dimension.

Example 3.6. Results of this text (exposed in chapter 4 and 5) concern a wide class of tropical curves in $\mathbb{R}^3$, namely those which are projective, trivalent and whose unbounded edges have weight 1. If its degree is denoted by d, such a curve has $4d$ unbounded edges. Therefore the expected dimension of its combinatorial type is $4d$. Notice that $4d$ is also the dimension of the space of irreducible non-planar algebraic curves of degree d in $\mathbb{C}P^3$ (see [15]).

Definition 3.11. *A parametrized tropical curve $(\overline{\Gamma}, h)$ is called regular if the inequality of theorem 3.4 is an equality. Otherwise, the curve is called superabundant. A tropical curve in $\mathbb{R}^n$ is said to be regular if it admits a regular parametrization.*

If a non-archimedean valued field of characteristic zero is fixed, recall that a tropical projective curve in $\mathbb{R}^2$ is the non-archimedean amoeba of an algebraic plane curve of the same degree by definition 3.6. This definition coincides with definition 3.9 if $n = 2$. If $n \geq 3$, the fact that the non-archimedean amoeba of an algebraic curve of degree d is a projective tropical curves of degree d as defined in definition 3.9 is a consequence of theorem 3.1 of [48]. Reciprocally, a projective tropical curve of degree d is not always the non-archimedean amoeba of an algebraic curve of the same degree. The complete answer to this question for curves of genus 0 or 1 has been given in [48]. The following result is a particular case of theorems 3.2 and 3.3 of [48].

Theorem 3.5. *Let (K, ν) be a non-archimedean valued field of characteristic zero and $T \subset \mathbb{R}^n$ a parametrized tropical curve of genus g and degree d. If $g = 0$, there exists an nonsingular algebraic curve $X \subset KP^n$ of genus 0 and degree d such that $\mathrm{Val}(X \cap (K^*)^n) = T$. If $g = 1$, assume that the edges of the cycle of T span $\mathbb{R}^n$. Then there exists a nonsingular algebraic curve $X \subset KP^n$ of genus 1 and degree d such that $\mathrm{Val}(X \cap (K^*)^n) = T$.*

We should also mention the following similar result. It is a particular case of a result due to Mikhalkin concerning the question of approximating curves of arbitrary genus by complex algebraic curves of the same degree and genus. The edges of a tropical curve are equipped with phases that can be schematically described as follows (see [35, 38] for details). If a tropical curve $(\overline{\Gamma}, h)$ is approximated by a family of complex algebraic curves C_t, then, for sufficiently large $t >> 1$, any open edge of Γ corresponds to a "piece" of C_t, precisely a smooth cylinder, and a small neighborhood of a k-valent vertex of Γ corresponds to a sphere with k punctures. A compatible system of phases is a collection of data responsible for the gluing of these "pieces".

Theorem 3.6 ([33]). *A regular parametrized tropical curve $(\overline{\Gamma}, h)$ in $\mathbb{R}^n$, equipped with any compatible system of phases, is the limit of a family of complex algebraic curves of the same degree and genus under a suitable renormalization.*

A nodal tropical plane curve is always regular (proposition 2.23 in [34]), but their exist trivalent tropical curves in $\mathbb{R}^3$ which are not regular.

Example 3.7. This example is due to G. Mikhalkin ([35], ex. 5.12). The tropical curve shown on figure 3.8, naturally parametrized by itself as explained in example 3.5, has degree 3, genus 1 and 12 unbounded edges. Thus the expected dimension of its combinatorial type is 12. Parameters for the polyhedral complex parametrizing this combinatorial type are the position of a root vertex, the length of four edges of the cycle (instead of 5 as the cycle is planar) and the position of the six vertices which does not belong to the loop (with the restriction that each of these vertices must stay on a fixed line). The actual dimension of the combinatorial type is $3 + 4 + 6 = 13$, therefore the curve is superabundant.

The following result shows that the previous example is a particular case of a general statement.

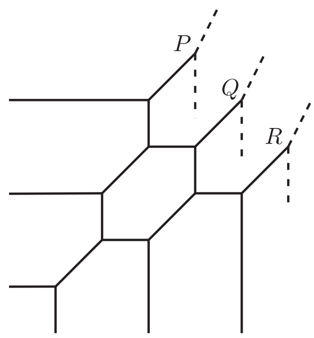

Figure 3.8. *A superaboundant tropical curve in* $\mathbb{R}^3$.

Lemma 3.2. *[[34]] A connected projective trivalent tropical curve $T \subset \mathbb{R}^3$, of genus 1 and whose unbounded edges are of weight 1, is regular if and only if its cycle is not contained in a plane.*

Proof. We consider the natural generic parametrization of T described by example 3.5. Denote by d the degree of T, by a_0 (resp., by a_∞) the number of bounded edges (resp., of unbounded edges) of T, and by s_0 (resp., by s_∞) the number of trivalent vertices (resp., of 1-valent vertices) of T. By assumption on the unbounded edges of T, one has $a_\infty = s_\infty = 4d$. In particular, the genus of T is $1 = 1 - (s_0 + s_\infty) + (a_0 + a_\infty) = 1 - s_0 + a_0$. Finally, we denote by e_0 an arbitrary edge of the cycle, and consider the subgraph $T' = T \setminus e_0$. It is a tree containing all the vertices of T. One can enumerate the pairs (V, e), where e is an edge and V a vertex of e, in two different ways:

1. There are 3 pairs (V, e) if the vertex V is trivalent, and only one if it is 1-valent. Therefore the number of such pairs is $3s_0 + s_\infty = 3s_0 + 4d$.

2. Each edge has two vertices, thus there are $2a_0 + 2a_\infty = 2a_0 + 8d$ such pairs.

This leads to the relation $3s_0 = 2a_0 + 4d$. As the genus of T is $1 = 1 - s_0 + a_0$, the number of bounded edges of T is $a_0 = s_0 = 4d$ and the number of bounded edges of T' is $4d - 1$. As we can apply a translation and modify the lengths of these edges, the graph T' varies in a real affine space of dimension $4d + 2$. Such a graph determines a tropical curve of the given combinatorial type if the pair of vertices corresponding to the removed edge defines a line of the correct slope. If the cycle is not planar, this can be equivalently reformulated as follows: the vector connecting these vertices should be orthogonal to the normal plane of e_0. This imposes 2 independent linear conditions, and gives the expected dimension.

Reciprocally, if the cycle of T is planar, the condition of collinearity of this vector and e_0 gives only 1 linear condition. Thus the actual dimension is at least $4d + 1$ and the curve is not regular. □

Notice that the cycle of a genus 1 projective connected tropical curve in $\mathbb{R}^3$ is not planar if and only if the curve satisfied the hypothesis of theorem 3.5: the edges of the cycle span $\mathbb{R}^3$.

3.4 Real tropical curves

Definition 3.12. *A real parametrized tropical curve in $\mathbb{R}^n$ is a triple $(\overline{\Gamma}, h, c)$, where $(\overline{\Gamma}, h)$ is a parametrized tropical curve in $\mathbb{R}^n$, and $c : \Gamma \to \Gamma$ an isometric involution such that $h \circ c = h$. We denote by $\widetilde{\Gamma}$ the quotient Γ/c of Γ by c, and by $\widetilde{h}$ the map $\widetilde{\Gamma} \to \mathbb{R}^n$ induced by h. Then $(\overline{\Gamma}, h, c)$ is generic if the following conditions are satisfied:*

- *each vertex of Γ is either 3-valent or 4-valent;*
- *any neighborhood of any vertex of Γ is not mapped to a segment by h;*
- *any 4-valent vertex of Γ is invariant under c and is adjacent to exactly two edges invariant under c;*
- *if $n \geq 3$, then $\widetilde{h}$ is injective;*
- *if $n = 2$, then each point of $h(\Gamma)$ has at most two inverse images under h, and any point of $h(\Gamma)$ having two inverse images is not the image of a vertex of Γ.*

The isometry assumption implies that, for any edge e of Γ, its image $c(e)$ is bounded if and only if e is bounded. Moreover, recall that the weight of e is defined by the relation $dh_P(u_e) = w_{e,h} \cdot u_{e,h}$, with the notations of the preceding section (definition 3.8). Thus, the edges e and $c(e)$ have the same weight, and the same primitive integer vector: $w_{e,h} = w_{c(e),h}$ and $u_{e,h} = u_{c(e),h}$.

Lemma 3.3. *If $(\overline{\Gamma}, h, c)$ is generic, and if an edge of $T = h(\Gamma)$ is the common image of two different edges of Γ identified by c, then its weight is even.*

Proof. If e and $c(e)$ are two edges of Γ identified by c, their images coincide because $h \circ c = h$. Denote the resulting edge of T by $\tilde{e}$. As $(\overline{\Gamma}, h, c)$ is generic, there is no other edge of Γ whose image under h contains $\tilde{e}$. The weight of $\tilde{e}$ is then the sum of $w_{e,h}$ and $w_{c(e),h}$. As these numbers are equal, $w(\tilde{e})$ is even. $\square$

Thus, if (Γ, h, c) is generic such that each edge of $T = h(\Gamma)$ has an odd weight, the involution c is trivial. In that case, a real structure can be defined on T in a combinatorial way. The binary law defined on $\{-, +\}$ by:

$$
\begin{array}{ccc}
+ * + = + & , & - * - = + \\
- * + = - & , & + * - = -
\end{array}
$$

makes $(\{-, +\}, *)$ into an abelian group. The map $\mathbb{Z}/2\mathbb{Z} \to \{-, +\}$ defined by $0 \mapsto +$ and $1 \mapsto -$ is a group isomorphism identifying $\mathbb{Z}/2\mathbb{Z}$ with $\{-, +\}$.

If an edge e of T is of weight w, denote by v one of its primitive integer vectors (the other is $-v$). The equivalence relation $\sim_{wv}$ on $(\mathbb{Z}/2\mathbb{Z})^n$ is defined by:

$$a \sim_{wv} b \quad \Longleftrightarrow \quad a - b \text{ is equal to } (wv \bmod 2),$$

where $a-b \in (\mathbb{Z}/2\mathbb{Z})^n$ is the coordinate-by-coordinate difference and wv mod 2 is the coordinate-by-coordinate reduction of the integer vector wv in $(\mathbb{Z}/2\mathbb{Z})^n$. The equivalence classes of $\sim_{wv}$ and $\sim_{-wv}$ coincide: the choice of the primitive integer vector of the edge is unimportant.

Definition 3.13. *A phase of e is an equivalence class of the relation $\sim_{wv}$.*

As w is odd, each equivalence class is a pair $\{a,b\}$ of elements of $(\mathbb{Z}/2\mathbb{Z})^n$ such that $b = a + (wv \; mod \; 2)$. In other words, a phase of e is a pair of n-tuples of signs. If V is a trivalent vertex of T, denote by e_1, e_2, e_3 its adjacent edges. For each $i \in \{1,2,3\}$, let s_i be a phase of e_i. In the case of a tropical curve in $\mathbb{R}^n$ having only odd weights, the phases s_1, s_2, s_3 are *compatible* at V if any element of s_i is contained in exactly one s_j, $j \neq i$.

Definition 3.14. *A generic odd real tropical curve (briefly, a generic odd curve) in $\mathbb{R}^n$ is a generic tropical curve $T \subset \mathbb{R}^n$ satisfying the following conditions.*

1. *Any unbounded edge has weight* 1*;*
2. *any bounded edge has an odd weight;*
3. *the edges of T are equipped with phases compatible at each vertex.*

For every edge e of phase s, denote by $\mathbb{R}e \subset \mathbb{R}^n \times \{+,-\}^n$ the set

$$\mathbb{R}e = \left\{ \big(x, (\varepsilon_1, \dots, \varepsilon_n)\big), \ x \in e, \ (\varepsilon_1, \dots, \varepsilon_n) \in s \right\}.$$

The real part of the real tropical curve is the set $\mathbb{R}T = \bigcup_{e \subset T} \mathbb{R}e$. The degree and genus of a real tropical curve are the degree and genus of the underlying tropical curve.

The image of the real part $\mathbb{R}T$ under the “forgetful” map

$$pr_1 : \mathbb{R}^n \times \{-,+\}^n \to \mathbb{R}^n$$

coincides with the original curve T.

Remark 3.6. For generic odd plane curves, the compatibility condition ignores vertices of valency 4. This can be explained by the fact that, if (Γ, h) is a generic parametrization of T, then the pre-images of a 4-valent vertex of T are not vertices of Γ.

For any $\varepsilon \in \{-,+\}^n$, we denote by $\mathbb{R}T_\varepsilon$ the intersection of $\mathbb{R}T$ with $\mathbb{R}^n \times \{\varepsilon\}$. By misuse of language, if the phase of an edge e contains $\varepsilon \in \{+,-\}^n$, we say that e is of phase ε. In other words:

$$e \text{ is of phase } \varepsilon \quad \Longleftrightarrow \quad (e, \varepsilon) \subset \mathbb{R}T_\varepsilon \quad \Longleftrightarrow \quad \mathbb{R}e \cap (\mathbb{R}^n \times \{\varepsilon\}) \neq \varnothing.$$

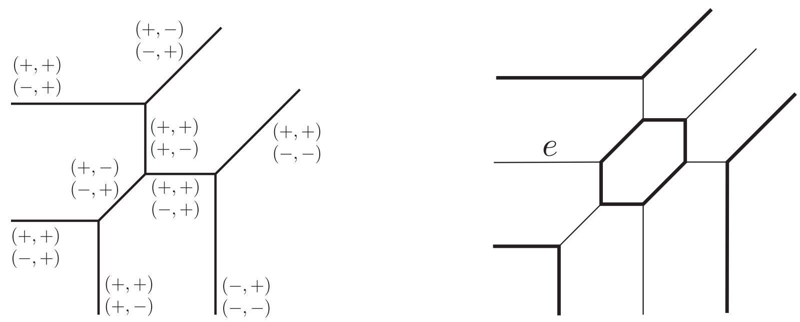

3.9 (a) A generic odd plane conic.

3.9 (b) A generic odd plane cubic.

Figure 3.9. *Representation of generic odd curves.*

A real tropical curve can be represented by marking each edge with its phase, as shown on figure 3.9 (a) in the case of a tropical real plane conic. Figure 3.9 (b) shows a tropical real plane cubic. All weights are equal to 1 and edges of phase $(+,+)$ are drawned in bold. The curve is trivalent, thus the phases of the remaining edges are determined by the compatibility rule of phases.

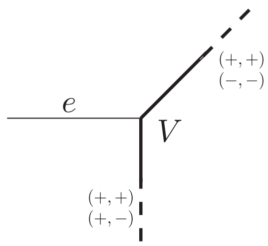

For example, denote by e the horizontal unbounded edge of the generic odd cubic which is not drawned in bold on figure 3.9 (b). This edge is adjacent to a trivalent vertex V. The two other edges adjacent to V are drawn in bold, thus their phase contains $(+,+)$. As one of them is directed by $(1,1)$ and the other by $(0,-1)$, their phases are $\{(+,+);(-,-)\}$ and $\{(+,+);(+,-)\}$ respectively. The compatibility rule of phases is satisfied at V, therefore the phase of e is necessarily $\{(-,-);(+,-)\}$.

3.5 Projectivization and star-diagram of a generic odd real tropical curve

We identify $\mathbb{R}^n$ with an affine chart of $\mathbb{R}P^n$. In particular, the closure of the union of two arcs of $\mathbb{R}^n$ going to infinity with opposite asymptotic directions is connected in $\mathbb{R}P^n$. We denote by $\mathbb{R}\mathbb{R}^n$ the set $\mathbb{R}^n \times \{-,+\}^n$, and by $\mathbb{R}^n_\varepsilon$ the open orthant of sign $\varepsilon = (\varepsilon_1, \dots, \varepsilon_n) \in \{-,+\}^n$ of $\mathbb{R}^n$:

$$\mathbb{R}^n_\varepsilon = \{(x_1, \dots, x_n) \in \mathbb{R}^n : \ \varepsilon_i x_i > 0, \ \ i = 1, \dots, n\}.$$

Finally, we define a smooth map $\mu : \mathbb{R}\mathbb{R}^n \longrightarrow (\mathbb{R}^*)^n$ by:

$$\mu(x_1, \dots, x_n, \varepsilon_1, \dots, \varepsilon_n) = (\varepsilon_1 \exp x_1, \dots, \varepsilon_n \exp x_n).$$

If $T \subset \mathbb{R}^n$ is a generic odd curve, the set $\mu(\mathbb{R}T)$ is a non-compact 1-dimensional topological submanifold of $(\mathbb{R}^*)^n$.

Lemma 3.4. *If T is projective generic odd tropical curve in $\mathbb{R}^n$, the closure of $\mu(\mathbb{R}T)$ in $\mathbb{R}P^n$ is a $1-$dimensional closed submanifold of $\mathbb{R}P^n$.*

Proof. The only possible ends of $\mu(\mathbb{R}T)$ are the images of the sets $\mathbb{R}e$ where e is an unbounded edge of T. As T is odd, an unbounded edge e has weight 1 and its phase is a pair $(\varepsilon, \varepsilon')$. In particular e has two copies in $\mathbb{R}T$:

$$\mathbb{R}e = (e \times \{\varepsilon\}) \cup (e \times \{\varepsilon'\}).$$

The curve T is projective, thus an unbounded edges is directed by $(1, \dots, 1)$ or by a vector of the standard basis of $\mathbb{R}^n$. If a primitive integer vector of e is $(1, \dots, 1)$, one has $\varepsilon = -\varepsilon'$ by definition 3.13. Thus the image of $\mathbb{R}e$ under μ is symmetric with respect to the origin:

$$\begin{aligned} \forall x \in e, \qquad \mu(x, \varepsilon) &= (\varepsilon_1 \exp x_1, \dots, \varepsilon_n \exp x_n) \\ &= (-\varepsilon'_1 \exp x_1, \dots, -\varepsilon'_n \exp x_n) \\ &= -\mu(x, -\varepsilon'). \end{aligned}$$

If a primitive integer vector of e is the i^{th} vector of the standard basis of $\mathbb{R}^n$, then $\varepsilon_i = -\varepsilon'_i$ and $\varepsilon_k = \varepsilon'_k$ if $k \neq i$. Thus the image of $\mathbb{R}e$ under μ is symmetric with respect to the coordinate hyperplane $x_i = 0$. $\square$

Definition 3.15. *The projectivization of a generic odd curve T is the $1-$dimensional closed submanifold of $\mathbb{R}P^n$ obtained by taking the closure of $\mu(\mathbb{R}T)$ in $\mathbb{R}P^n$. It is denoted by $\mathbb{P}T$.*

Example 3.8. If T is planar, its projectivization is a closed curve in $\mathbb{R}P^2$ whose only possible singular points are transversal double points. The projectivization of $T \subset \mathbb{R}^3$ is a projective link in $\mathbb{R}P^3$.

Recall that pr_1 is the projection map $(x, \varepsilon) \in \mathbb{R}^n \times \{-,+\}^n \mapsto x \in \mathbb{R}^n$. Given a phase $\varepsilon = (\varepsilon_1, \dots, \varepsilon_n) \in \{-,+\}^n$, the image of the set $\mathbb{R}T_\varepsilon$ under pr_1 coincides with the set of edges of T of phase ε.

Example 3.9. Figure 3.10 shows the set of edges of phase $(-,+)$ of the plane conic displayed on figure 3.9 (a). It is obtained by sending $\mathbb{R}C_{-,+}$ into $\mathbb{R}^2$ via the projection map $pr_1 : \mathbb{R}^2 \times \{-,+\}^2 \to \mathbb{R}^2$.

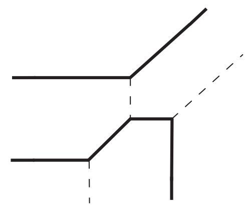

Figure 3.10. *The set of edges of phase $(-,+)$ of the real tropical plane conic C of figure 3.9 (a).*

The map μ realizes a homeomorphism between $\mathbb{R}^n \times \{\varepsilon\}$ and $\mathbb{R}^n_\varepsilon$. Therefore it induces an identification of $\mathbb{R}\mathbb{R}^n$ with $\cup\, \mathbb{R}^n_\varepsilon = (\mathbb{R}^*)^n$. In particular, $\mu(\mathbb{R}T_\varepsilon)$ is contained in the orthant $\mathbb{R}^n_\varepsilon$ and is homeomorphic to the set of edges of T of phase ε. Moreover, it is homeomorphic to the piecewise-linear set $T_\varepsilon \subset \mathbb{R}^n_\varepsilon$ defined as follows. Denote by Δ_ε the image of the set $pr_1(\mathbb{R}T_\varepsilon)$ of edges of phase ε under the symmetry:

$$S_\varepsilon : x \in \mathbb{R}^n \longmapsto \varepsilon x \in \mathbb{R}^n.$$

There exists $r > 0$ such that the image of Δ_ε under the translation t_r of vector $r\varepsilon = (r\varepsilon_1, \ldots, r\varepsilon_n)$ satisfies the following conditions:

i) every vertex of $t_r(\Delta_\varepsilon)$ is contained in $\mathbb{R}^n_\varepsilon$;

ii) every unbounded edge of $t_r(\Delta_\varepsilon)$ is either collinear to $(\pm 1, \ldots, \pm 1)$, or intersects orthogonally a coordinate hyperplane.

Definition 3.16. *For any real number $r(\varepsilon)$ satisfying the above conditions, we define the subset $T_\varepsilon(r)$ of $\mathbb{R}^n_\varepsilon$ by:*

$$T_\varepsilon(r) = t_{r(\varepsilon)}(\Delta_\varepsilon) \cap \mathbb{R}^n_\varepsilon.$$

For any $\varepsilon \in \{-,+\}^n$ and any integer $i \in \{1, \ldots, n\}$, we denote by $\mathbb{R}^n_\varepsilon(i)$ the set of points $(x_1, x_2, \ldots, x_n) \in \mathbb{R}^n_\varepsilon$ such that $x_i = 0$. This set is the intersection of the closure of $\mathbb{R}^n_\varepsilon$ in $\mathbb{R}^n$ with the coordinate hyperplane $x_i = 0$.

Lemma 3.5. *The pair $(\mathbb{R}^n_\varepsilon, T_\varepsilon(r))$ is homeomorphic to $(\mathbb{R}^n, pr_1(\mathbb{R}T_\varepsilon))$. The set $T_\varepsilon(r) \cap \mathbb{R}^n_\varepsilon(i)$ is finite of cardinality equal to the number of unbounded edges of T, of phase ε, directed by the i^{th} vector of the standard basis of $\mathbb{R}^n$.*

Proof. The first statement follows from the fact that $T_\varepsilon(r)$ is the image of $pr_1(\mathbb{R}T_\varepsilon)$ under the composition of a symmetry, a translation and the operation of intersection with $\mathbb{R}^n_\varepsilon$. The second is a consequence of definitions. □

We deduce that, in a sense, the set $T_\varepsilon(r)$ does not depend on $r(\varepsilon)$.

Corollary 3.6. *Given $\varepsilon \in \{-,+\}^n$, let r, r' be two real numbers satisfying the above conditions. Then the pairs $(\mathbb{R}^n_\varepsilon, T_\varepsilon(r))$ and $(\mathbb{R}^n_\varepsilon, T_\varepsilon(r'))$ are homeomorphic. Moreover, for any integer $i \in \{1, \ldots, n\}$, the pairs $(\mathbb{R}^n_\varepsilon(i), T_\varepsilon(r) \cap \mathbb{R}^n_\varepsilon(i))$ and $(\mathbb{R}^n_\varepsilon(i), T_\varepsilon(r') \cap \mathbb{R}^n_\varepsilon(i))$ are homeomorphic.*

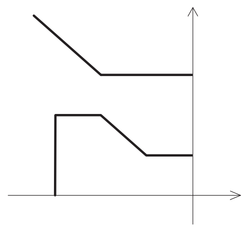

C_{-+}

Figure 3.11. *Homeomorphism class of the pair* $(\mathbb{R}^2_{-+}, C_{-+})$ *for the projective generic odd conic* C *of figure 3.9 (a).*

The real numbers $r(\varepsilon)$ can be chosen such that the closure of the union of all $T_\varepsilon(r)$ is a 1-dimensional rational polyhedral complex in $\mathbb{R}^n$, intersecting orthogonally the coordinate hyperplanes and whose only unbounded edges are directed by $(\pm 1, \ldots, \pm 1)$. The homeomorphism class of the pair $(\mathbb{R}^n, \cup_\varepsilon T_\varepsilon(r))$ does not depend on the real numbers $r(\varepsilon)$. We denote the resulting set by ΔT, and its closure in $\mathbb{R}P^n$ by $\mathrm{Clos}\,\Delta T$.

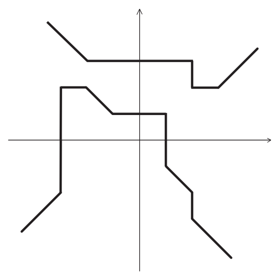

Figure 3.12. *The set* ΔC *for the projective generic odd conic* C *of figure 3.9 (a).*

Corollary 3.7. *If* T *is a projective generic odd curve, the pairs* $(\mathbb{R}P^n, \mathrm{Clos}\,\Delta T)$ *and* $(\mathbb{R}P^n, \mathbb{P}T)$ *are homeomorphic.*

Proof. It is a consequence of lemma 3.5 and the fact that $(\mathbb{R}^n, pr_1(\mathbb{R}T_\varepsilon))$ is homeomorphic to $(\mathbb{R}^n_\varepsilon, \mu(\mathbb{R}T_\varepsilon))$. $\square$

Using corollary 3.7, we dedicate the remaining part of this section to the study of a particular projective diagram of the projectivization $\mathbb{P}T$ of a generic real tropical curve T in $\mathbb{R}^2$ or $\mathbb{R}^3$. If $T \subset \mathbb{R}^3$, we denote by H_0 the hyperplane $\{z = 0\} \subset \mathbb{R}^3$, and by $pr : \mathbb{R}^3 \to H_0$ the vertical projection map. Up to a small isotopy, we can assume that the projection of T to H_0 is as most $2-$to-1, and that the inverse images of a double point are not vertices of T. If $R > 0$ is large enough, the projection of any vertex of ΔT is contained in $D(0, R)$. The set

$pr(\Delta T) \cap D(0, R)$ a 1-dimensional piecewise-linear subset of $\mathbb{R}^2$ whose singularities are at most transversal double points. At each crossing, we distinguish the projection of the lower edge.

Definition 3.17. *Given a projective generic odd curve $T \subset \mathbb{R}^3$ (resp., $T \subset \mathbb{R}^2$), the homeomorphism class of the pair $(D(0, R), pr(\Delta T) \cap D(0, R))$ (resp., of the pair $(D(0, R), \Delta T \cap D(0, R))$) is denoted by $\mathcal{D}(T)$, and called the star-diagram of T.*

Example 3.10. The projectivization of the real cubic D shown on figure 3.9 (b) has two connected components: an oval D_0 and a pseudo-line D_1, which realize the zero and the non-zero element of $H_1(\mathbb{R}P^2, \mathbb{Z}/2\mathbb{Z})$, respectively. Figure 3.13 (a) shows the piecewise-linear set ΔD and its subsets ΔD_0 and ΔD_1.

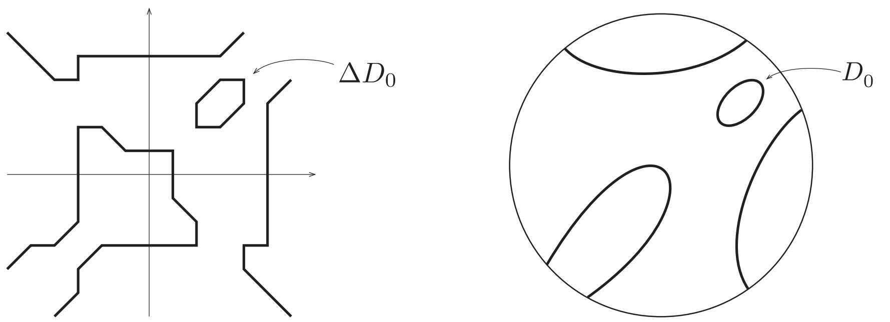

3.13 (a) The set ΔD.

3.13 (b) The star-diagram of D.

Lemma 3.8. *The set of unbounded edges of T in $\mathbb{R}^2$ or $\mathbb{R}^3$, which are not directed by a vector of the standard basis, is in bijection with the set of pairs of antipodal boundary points of $\mathcal{D}(T)$.*

Proof. Denote by e an unbounded edge of $T \subset \mathbb{R}^3$ directed by $(1, 1, 1)$. Its weight is 1, thus its phase is of the form $\{(\varepsilon_1, \varepsilon_2, \varepsilon_3), (-\varepsilon_1, -\varepsilon_2, -\varepsilon_3)\}$. The images of e in the set ΔT intersects the plane at infinity in the octants of phase $(\varepsilon_1, \varepsilon_2, \varepsilon_3)$ and $(-\varepsilon_1, -\varepsilon_2, -\varepsilon_3)$. Consequently, $pr(\Delta T)$ intersects the line at infinity in the quadrants of phase $(\varepsilon_1, \varepsilon_2)$ and $(-\varepsilon_1, -\varepsilon_2)$. If $T \subset \mathbb{R}^2$, the phase of e is of the form $\{(\varepsilon_1, \varepsilon_2), (-\varepsilon_1, -\varepsilon_2)\}$. The images of e in ΔT intersects the line at infinity in the quadrants of phase $(\varepsilon_1, \varepsilon_2)$ and $(-\varepsilon_1, -\varepsilon_2)$. In both case e corresponds to two boundary points of $\mathcal{D}(T)$ in the quadrants of phase $(\varepsilon_1, \varepsilon_2)$ and $(-\varepsilon_1, -\varepsilon_2)$. $\square$

The following result is a direct consequence of definitions 2.19 and 3.17.

Proposition 3.3. *The star-diagram of a projective generic odd curve $T \subset \mathbb{R}^3$ is a projective diagram of (the topological link corresponding to) $\mathbb{P}T$.*

The crossings of $\mathcal{D}(T)$ are in bijection with the crossings of $pr(\Delta T)$, but not with the crossings of $pr(T)$. From now until the end of the this section, we denote by P a crossing point of $pr(T)$, by e, e' the edges of T such that $P = pr(e) \cap pr(e')$, by s, s' their phases, and we assume that e and e' are not vertical.

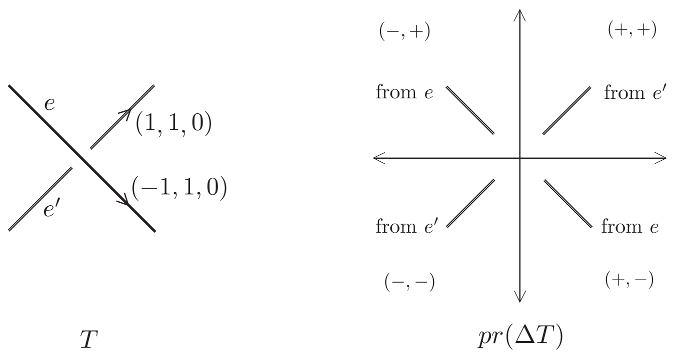

Figure 3.13. *Example of a ghost crossing.*

Example 3.11. Assume that a real tropical curve T contains an edge e of odd weight directed by $(-1, 1, 0)$ and an edge e' of odd weight directed by $(1, 1, 0)$ such that $pr(e) \cap pr(e') \neq \varnothing$. These edges are depicted on the left part of figure 3.13. If their phases are $\{(+,-,+), (-,+,+)\}$ and $\{(+,+,+), (-,-,+)\}$ respectively, then

$$\begin{aligned}\mathbb{R}e &= (e \times \{(+,-,+)\}) \cup (e \times \{(-,+,+)\})\\ \mathbb{R}e' &= (e' \times \{(+,+,+)\}) \cup (e' \times \{(-,-,+)\})\end{aligned}$$

In particular, $pr_1(\mathbb{R}e) \cup pr_1(\mathbb{R}e')$ is made of 4 non-intersecting edges, each of them contained in a different octant $\mathbb{R}^3 \times (\pm, \pm, +)$. Consequently, the image of $e \cup e'$ in $pr(\Delta T)$ consists of 4 non-intersecting edges, each of them contained in a different "quadrant" $\mathbb{R}^2 \times (\pm, \pm)$ as depicted on the right part of figure 3.13). Therefore the images of e and e' do not intersect in $D(T)$.

We define the set $S_e \subset \{-,+\}^2$ by:

$$S_e = \{(\varepsilon_1, \varepsilon_2) \,:\, \exists \varepsilon \in \{-,+\} \text{ such that } (\varepsilon_1, \varepsilon_2, \varepsilon) \text{ belongs to } s\}.$$

In particular, $(\varepsilon_1, \varepsilon_2) \in S_e$ if and only if $pr(\Delta T) \cap \mathbb{R}^2_{\varepsilon_1, \varepsilon_2}$ contains a copy of e.

Lemma 3.9. *The crossing point P induces a crossing of $D(T)$ in the quadrant of sign $(\varepsilon_1, \varepsilon_2)$ if and only if $(\varepsilon_1, \varepsilon_2) \in S_e \cap S_{e'}$.*

Proof. The crossing point P induces a crossing point of $pr(\Delta T)$ if the projections under $pr \circ pr_1 : \mathbb{R}^3 \times \{-,+\}^3 \to \mathbb{R}^2$ of the sets $\mathbb{R}e$ and $\mathbb{R}e'$ intersect in the same quadrant. This quadrant is of sign $(\varepsilon_1, \varepsilon_2)$ if and only if $(\varepsilon_1, \varepsilon_2) \in S_e \cap S_{e'}$. By definition 3.17, $D(T)$ is obtained from the vertical projection of ΔT on $\{z = 0\}$, thus the statement follows. $\square$

Even though the primitive integer vectors of e and e' are different, the cardinality of $S_e \cap S_{e'}$ can be equal to 0, 1 or 2.

Example 3.12. (i) The edges e, e' are those introduced in example 3.11 and depicted on the left part of figure 3.13, but these edges are assume to be both of phase $\{(+,-,+),(-,+,+)\}$. According to lemma 3.9, it induces 2 crossing points of $D(T)$, occuring in the quadrant of signs $(+,-)$ and $(-,+)$.

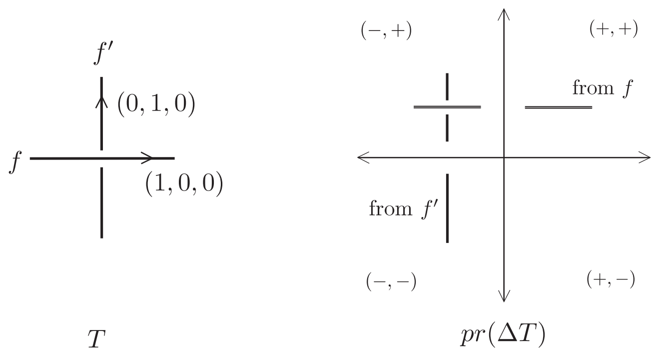

Figure 3.14. *Example of a simple crossing.*

(ii) Consider two edges f, f' with odd weights, directed by $(1,0,0)$ and $(0,1,0)$ respectively, and such that $pr(f) \cap pr(f') \neq \varnothing$. One can check that, no matter what the phases of f and f' are, this crossing induces always one crossing in $D(T)$. Figure 3.14 displays the situation when f is of phase $\{(+,+,+),(-,+,+)\}$ and f' of phase $\{(-,-,-),(-,+,-)\}$.

Definition 3.18. *The crossing point P is ghost if* $\mathrm{Card}(S_e \cap S_{e'}) = 0$*, and simple if* $\mathrm{Card}(S_e \cap S_{e'}) = 1$*. In the latter case, denote $S_e \cap S_{e'}$ by $(\varepsilon_1, \varepsilon_2)$. Then the crossing is mirror or transparent depending on if the upper edge at P is of phase $(\varepsilon_1, \varepsilon_2, -)$ or $(\varepsilon_1, \varepsilon_2, +)$.*

In other words, a simple crossing P is mirror if the image in $D(T)$ of the upper edge at P is not the upper edge of the crossing of $D(T)$ corresponding to P.

Example 3.13. The crossing point of example 3.11 is ghost. The crossing point of example 3.12 (ii) is simple and transparent. A simple crossing such that the phases of e and e' both contain $(+,+,+)$ is transparent.

The simplicity of a crossing depends only on the reduction modulo 2 of the primitive integer vectors of the edges.

Lemma 3.10. *Denote by $u_e = (a,b,c)$ and $u_{e'} = (a',b',c')$ the primitive integer vectors of e and e'. Then, P is simple if and only if $a \not\equiv a'$ [2] or $b \not\equiv b'$ [2].*

Proof. The edges e and e' are not vertical, thus the vectors $(a \bmod 2, b \bmod 2)$ and $(a' \bmod 2, b' \bmod 2)$ are different of $(0,0)$. Then $a \equiv a'$ [2] and $b \equiv b'$ [2] if and only if both vectors are equal to $(1,1)$. In this case

$$(\varepsilon_1, \varepsilon_2) \in S_e \cap S_{e'} \iff (-\varepsilon_1, -\varepsilon_2) \in S_e \cap S_{e'},$$

which precisely means that $\mathrm{Card}(S_e \cap S_{e'})$ is equal to 0 or 2. $\square$

3.6 Mikhalkin's theorem

Definition 3.19. *A real algebraic plane projective curve of degree d is a homogeneous polynomial $P \in \mathbb{R}[X_0, X_1, X_2]$ of degree d, considered up to multiplication by a non-zero real number. The curve is nonsingular if the partial derivatives $\partial_0 P$, $\partial_1 P$ and $\partial_2 P$ have no common zero in $\mathbb{C}P^2$.*

If X is a real algebraic plane projective curve of degree d, the set of complex points $\mathbb{C}X$ is the set of zeros of P in $\mathbb{C}P^2$. It is a compact Riemann surface. The complex conjugation

$$c : [x : y : z] \in \mathbb{C}P^2 \longmapsto [\overline{x} : \overline{y} : \overline{z}] \in \mathbb{C}P^2$$

acts on $\mathbb{C}X$ as an orientation-reversing involution. The *real part* of X is the set $\mathbb{R}X$ of zeros of P in $\mathbb{R}P^2$. This set coincides with $\mathrm{Fix}(c) \cap \mathbb{C}X$.

Definition 3.20. *A complex algebraic plane projective curve is nodal if the only possible singularities of the curve are non-degenerate double points (that is, locally a transversal intersection of two branches; such a double point is locally given by the equation $x^2 - y^2 = 0$ if (x, y) is a system of local coordinates).*

If a real algebraic plane projective curve X is nonsingular, the genus of $\mathbb{C}X$ is $g(d) = \frac{1}{2}(d-1)(d-2)$. In this case, $\mathbb{R}X$ is a smooth submanifold of dimension 1 of $\mathbb{R}P^2$. Therefore, it is a collection of disjoint circles, smoothly embedded in $\mathbb{R}P^2$. There are two possibilities for an embedding i of a circle S^1 in $\mathbb{R}P^2$: either $\mathbb{R}P^2 \setminus i(S^1)$ has two connected components, or it is connected. In the first case, one component is homeomorphic to an open disk and the other one to an open Möbius band. In the second case, $\mathbb{R}P^2 \setminus i(S^1)$ is homeomorphic to $\mathbb{R}^2$.

Definition 3.21. *An embedded circle in $\mathbb{R}P^2$ is an oval if its complement is not connected, and a pseudo-line otherwise.*

The two connected components of the complement of an oval are called the *interior* (homeomorphic to an open disk) and the *exterior* of the oval, respectively.

Remark 3.7. Equivalently, the type of an embedded circle in $\mathbb{R}P^2$ can be identified by its homology class in $H_1(\mathbb{R}P^2, \mathbb{Z}/2\mathbb{Z}) \simeq \mathbb{Z}/2\mathbb{Z}$: it is an oval if and only if it realizes the zero homology class.

The real part of a nonsingular real algebraic plane projective curve is homeomorphic to the disjoint union of embedded circles. Therefore, the only topological invariant of the real part of a nonsingular real algebraic plane projective curve is the number of connected components. In a given degree, the possible range for this number was given by A. Harnack in [14]. The article [14] is considered as the first publication in topology of real algebraic varieties.

Theorem 3.7 (Harnack, 1876)**.** *If d is a positive integer, the number of connected components of the real part of a nonsingular real algebraic plane projective curve of degree d is bounded from below by $d - 2\lfloor d/2 \rfloor$ and bounded from above by $g(d) + 1$. If the real part has $g(d) + 1$ components, the curve is called an M-curve.*

The upper bound $g(d) + 1$ is sharp: for every $d \geq 1$, Harnack constructed in [14] an M-curve of degree d. Moreover, he proved that, for any integer k in the admissible range given by theorem 3.7, there always exists a real curve of degree d whose real part has exactly k components. Given a nonsingular real plane projective curve X, the topological type of $(\mathbb{R}P^2, \mathbb{R}X)$ is defined by the relative position of the components of $\mathbb{R}X$.

Definition 3.22. *Consider two real algebraic plane projective curves X and X'. The pairs $(\mathbb{R}P^2, \mathbb{R}X)$ and $(\mathbb{R}P^2, \mathbb{R}X')$ have the same topological type if $(\mathbb{R}P^2, \mathbb{R}X) \simeq (\mathbb{R}P^2, \mathbb{R}X')$.*

The isotopy classification of nonsingular real algebraic plane projective curves consists to determine which topological types are realizable in a given degree. Such a classification is known for degrees ≤ 5 since the XIX$^{\text{th}}$ century. Among the famous list of twenty-three problems in mathematics which were proposed by D. Hilbert in 1900 (see [16]), the first part of the 16$^{\text{th}}$ problem raises the question of isotopy classification of real M-curves of degree 6. This classification was completed in 1969 by D. A. Gudkov in [10], using an improvement of a method of construction developed by Hilbert. At the end of the 1970's, O. Ya. Viro developed a new method of construction of nonsingular real algebraic hypersurfaces in toric varieties, called *patchworking*, and achieved the isotopy classification of real M-curves of degree 7 in [59]. The following result is a particular case of Viro's method, called *combinatorial patchworking*, in the case of plane curves.

Theorem 3.8 ([57, 60, 20])**.** *Let T be a real projective trivalent tropical curve in $\mathbb{R}^2$ of degree d. Then, there exists a nonsingular real plane projective curve X of degree d in $\mathbb{R}P^2$ such that the real part $\mathbb{R}X$ of X is isotopic to $\mathbb{P}T$.*

Theorem 3.8 had been intensively used in the past 30 years to study the topology of real plane algebraic curves. In particular, it has become one of the main tools to construct real algebraic curves whose real part have a prescribed topology. G. Mikhalkin generalized theorem 3.8 to the case of nonsingular curves in the 3-dimensional projective space.

Definition 3.23. *A nonsingular algebraic curve in $\mathbb{R}P^3$ is a nonsingular complex algebraic curve $\mathbb{C}X \subset \mathbb{C}P^3$ invariant under the involution of complex conjugation in $\mathbb{C}P^3$.*

A nonsingular real space projective algebraic curve is thus a compact connected submanifold of dimension 2 of $\mathbb{C}P^3$, that is, a compact connected Riemann surface. Its degree is the number of intersection points with a generic plane in $\mathbb{C}P^3$. It is known since [13] (see also [11]) that the genus of a real space curve of degree d is not greater than $M(d) = \frac{1}{6}d(d-3)+1$. The complex conjugation

$$c : [x : y : z : w] \in \mathbb{C}P^3 \longmapsto [\overline{x} : \overline{y} : \overline{z} : \overline{w}] \in \mathbb{C}P^3$$

acts on $\mathbb{C}X$ as an orientation-reversing involution. The real part of $\mathbb{C}X$ is the set $\mathbb{R}X = \mathrm{Fix}(c) \cap \mathbb{C}X$. It is a smooth submanifold of dimension 1 of $\mathbb{R}P^3$. Therefore, it is a collection of disjoint circles, smoothly embedded in $\mathbb{R}P^3$. Comparing with plane curves, real space curves have similar topological properties.

Theorem 3.9 ([27, 43])**.** *The number of connected components of the real part of a nonsingular real space algebraic projective curve of genus g is not greater than $g+1$. Moreover, for any integers $d \geq 1$ and $0 \leq k \leq M(d)$, there exists a real space curve of degree d, not contained in any hyperplane, whose real part has exactly $k+1$ components.*

The following generalization of the combinatorial patchworking to 3-dimensional case is a particular case of a more general theorem due to Mikhalkin [33].

Theorem 3.10. *Let T be a real regular generic tropical curve in $\mathbb{R}^3$ of degree d and genus g. There exists a nonsingular real algebraic space projective curve $\mathbb{C}X$, of degree d and genus g, whose real part is isotopic to $\mathbb{P}T$.*

In the next sections, we apply theorem 3.10 to obtain a real algebraic space curve, whose real part is contained in an affine chart of $\mathbb{R}P^3$, having a connected component isotopic to a given knot. In the case of some torus knots, such a curve can be chosen so that its real part is connected.

Chapter 4

Knots as component of real curves

4.1 RPL-realization of knots

Recallthat pr is the projection map $\mathbb{R}^3 \to \mathbb{R}^2$ onto the plane $\{z = 0\}$. For any integer $i \in \{1, 2, 3\}$, denote by u_i the integer vector whose i^{th} coordinate is 1 and the other coordinates are zero. Given $i \neq j \in \{1, 2, 3\}$, put $u_{ij} = u_i + u_j$. Finally, we set $u_{123} = u_1 + u_2 + u_3 = (1, 1, 1)$.

Lemma 4.1. *Let $K \subset \mathbb{R}^3$ be a knot, and σ any (geometric) braid presentation of K. There exists a RPL-knot G_σ isotopic to K, such that $pr(G_\sigma)$ is homeomorphic to $pr(\sigma)$, and satisfying the following conditions.*

1. *Any edge of G_σ is directed by u_1, u_2, u_3, u_{13} or u_{23}.*
2. *The sum of the primitive integer vectors of two adjacent edges (pointing away from their vertex) is equal to $\pm u_{12}$, $\pm u_{23}$, $\pm u_{13}$, u_{123} or $-u_3$.*

Proof. Up to an isotopy not modifying the homeomorphism class of $pr(\sigma)$, one can assume that σ is generic in the following sense: if $P = (a, b)$ is a crossing point of $pr(\sigma)$, then there exists $\varepsilon > 0$ such that the stripe $B_{P,\varepsilon} = [a-\varepsilon, a+\varepsilon] \times \mathbb{R}$ does not contain any other crossing point of $pr(\sigma)$. Therefore $pr(\sigma) \cap B_{P,\varepsilon}$ is isotopic to the union k straight lines, where $k - 2$ are disjoint and parallel and 2 intersect transversally as shown on figure 4.1.

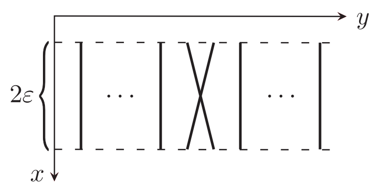

Figure 4.1. *The stripe $pr(\sigma) \cap B_{P,\varepsilon}$.*

The set $\sigma \cap (B_{P,\varepsilon} \times \mathbb{R})$ is isotopic to the RPL-graph G_P^- depicted on figure 4.2 (a) or to the RPL-graph G_P^+ depicted on figure 4.2 (b) according to the nature of the crossing point. Any edge of these graphs is directed by u_1 or u_2, except one which is emphasized with an arrow on figure 4.2. The latter is directed by u_{13} in the case of G_P^-, and by u_{23} in the other case.

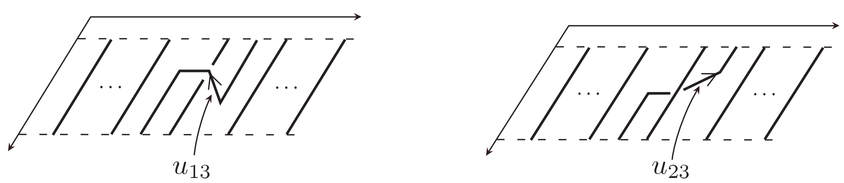

4.2 (a) The RPL-graph G_P^-.

4.2 (b) The RPL-graph G_P^+.

Figure 4.2.

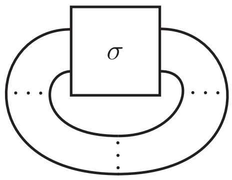

Figure 4.3. *Canonical closure of the braid σ.*

The length of the edges of the graphs $G_P^{\pm}$ which are not directed by u_1 can be chosen such that the set

$$G_\sigma^0 = \bigcup_P G_P^{\pm}$$

is a RPL-braid isotopic to σ, where the union is taken over all crossing points of $pr(\sigma)$. Recall that σ is the disjoint union of k strings. Each string is an interval embedded in $\mathbb{R}^3$ (see definition 2.1 of chapter 1). The canonical closure $l(\sigma)$ is obtained by gluing k smooth intervals to σ such that the projection of the resulting link is a diagram of K, see figure 4.3. In particular, the projection of the closing arcs do not intersect.

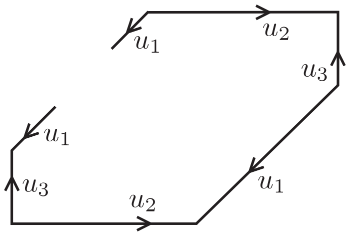

Figure 4.4. *The RPL-graph G_c.*

The rational graph G_c depicted on figure 4.4 has 7 bounded edges directed either by u_1, u_2 or u_3. Roughly speaking, it is a rational PL-graph imitating the closing arcs used in the canonical closure of a braid. The length of the edges of k copies $G_c^1, G_c^2, \ldots, G_c^k$ can be chosen such that the set

$$G_\sigma^0 \ \cup \ \bigcup_{i=1}^{k} G_c^i$$

is a RPL-realization of $l(\sigma)$. In particular it is a RPL-knot isotopic to K. It satisfies the required conditions, and is denoted by G_σ. □

Every vertex of G_σ is bivalent. Moreover, there are 10 different types of vertices, labeled from A_1 to A_{10} as described on figure 4.5. For each type, the primitive integer vectors of the two adjacent edges (pointing away from the vertex) are shown.

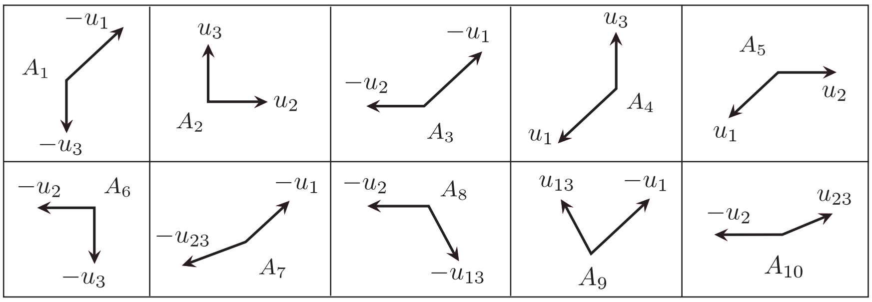

Figure 4.5. *The possible types of the vertices of G_σ.*

4.2 Real algebraic realizations of knots

The RPL-knot G_σ can be completed into a projective tropical curve of genus 1 with all weights equal to 1. First of all, every edge of G_σ can be equipped with the weight 1, making G_σ into a weighted RPL-knot. Then, at each vertex of G_σ one can attach some additional edges of weight 1. As in the proof of the above lemma, denote by k the number of strings of σ and by N the number of crossing points $pr(\sigma)$.

Lemma 4.2. *The weighted RPL-knot G_σ can be completed into an elliptic projective trivalent tropical curve T_σ of degree $N+3k$, whose edges are of weight 1 and such that every connected component of $T_\sigma \setminus G_\sigma$ is either a single unbounded edge or three adjacent edges, two of them being unbounded.*

Proof. To any (bivalent) vertex V of G_σ, we glue an edge e of weight 1. The primitive integer vector v of e is determined by the balancing condition. For example, if V is of type A_7, the balancing condition is $-u_1 - u_{23} + v = 0$ and gives $v = u_1 + u_{23} = u_{123}$, see figure 4.6.

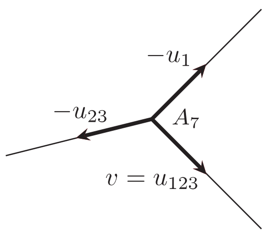

Figure 4.6. *The balancing condition for a vertex of type A_7.*

If v is equal to u_{123} or $-u_i$, $i \in \{1,2,3\}$, then e is an unbounded edge of T_σ and thus a connected component of $T_\sigma \setminus G_\sigma$. It is the case if V is of type A_7, A_8, A_9 and A_{10}. Otherwise, e is not an unbounded edge of T_σ and has a second vertex V_e. One can check that, for every type of vertex of G_σ, two unbounded edges of weight 1 can be glued to V_e such that their primitive integer vectors are equal to $-u_i$, $i \in \{1,2,3\}$, or u_{123}. In that case e is contained in a connected component of $T_\sigma \setminus G_\sigma$ made of three adjacent edges. It is the case if V is of type A_1 to A_6. For example, if V is of type A_1, then e is directed by $v = u_{13}$ and the unbounded edges adjacent to V_e are directed by $-u_2$ and u_{123}, see figure 4.7.

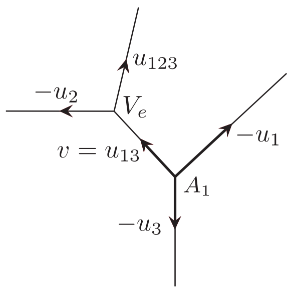

Figure 4.7. *The balancing condition for a vertex of type A_1.*

By the balancing condition, T_σ has the same number of unbounded edges in each of the directions u_{123}, $-u_1$, $-u_2$ and $-u_3$, as required for a projective tropical curve. It remains to determine $\deg T_\sigma$. The RPL-graph G_P^- contains a vertex of each types A_5, A_8, A_9. On the other hand, G_P^+ contains a vertex of each types A_5, A_7, A_{10}. A connected component of $T_\sigma \setminus G_\sigma$ adjacent to a vertex of type A_7 or A_8 (respectively, of type A_9 or A_{10}) is made of a single unbounded edge directed by u_{123} (respectively, by $-u_3$). A connected component adjacent to a vertex of type A_5 is made of 3 adjacent edges. The two unbounded ones are directed by $-u_1$ and $-u_2$. Therefore, the union of the connected components of $T_\sigma \setminus G_\sigma$ adjacent to the vertices of G_P^- (or G_P^+) contain one unbounded edge directed respectively by $-u_1$, $-u_2$, $-u_3$ and u_{123}. Thus, the contribution of $G_P^\pm$ to the degree of T_σ is 1. Similarly, one can check that the contribution of G_c to the degree of T_σ is 3. As T_σ contains N graphs $G_P^\pm$ and k copies of G_c, it is a projective tropical curve of degree $1 \times N + 3 \times k$. $\square$

The map $\iota : \mathbb{R}^3 \hookrightarrow \mathbb{R}P^3$ defined by $\iota(x,y,z) = [x:y:z:1]$ is an embedding. Its image is the affine chart $U \simeq \mathbb{R}^3$ defined by

$$U = \{[x:y:z:t] \in \mathbb{R}P^3 \ : \ t \neq 0\}.$$

Theorem 4.1. *Given a (geometric) braid presentation σ of K with k strings and N crossings, there exists a real algebraic nonsingular curve $X_\sigma \subset \mathbb{R}P^3$ of genus 1 and degree $N+3k$, which has two unlinked components. One of these is isotopic to ιK.*

Proof. Every edge e of T_σ is of weight 1, thus the equivalence classes of $\mathbb{Z}_2^3$ under the relation $\simeq_e$ are pairs of 3−tuples of signs. Then the phase of an edge of G_σ is defined to be the only equivalence class containing $(+,+,+)$. If e_0 is an edge of $T_\sigma \setminus G_\sigma$, denote by e, e' the edges of G_σ adjacent to e_0. They are not collinear, thus the phases $s_e, s_{e'}$ of e, e' satisfy $\mathrm{Card}(s_e \cap s_{e'}) = 1$. As

Card $((s_e \cup s_{e'}) \setminus (s_e \cap s_{e'})) = 2$, the compatibility rule of phases determines the phase $s_0 = \{\varepsilon_1, \varepsilon_2\}$ of e_0. Furthermore, s_0 does not contain $(+,+,+)$.

The phase of every edge adjacent to G_σ is determined, thus it remains to provide phases to the edges of T_σ which are not adjacent to G_σ. The latters are unbounded according to lemma 4.2. Assume that the edges f, f' are unbounded and adjacent to e_0, and denote by V their common vertex. The compatibility rule of phases implies that the phases $s_f, s_{f'}$ of f, f' have to contain ε_1 or ε_2. For example, assume that $\varepsilon_1 \in s_f$. Then $\varepsilon_2 \in s_{f'}$, and

$$(+,+,+) \in s_f \qquad \Longleftrightarrow \qquad (+,+,+) \in s_{f'}$$

by the compatibility rule of phases. In that case, s_f (resp., $s_{f'}$) is defined to be the equivalence class containing ε_2 (resp., containing ε_1). In any case, neither s_f nor $s_{f'}$ does contain $(+,+,+)$.

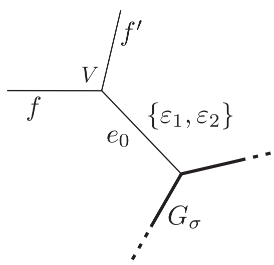

Figure 4.8. *A connected component of* $T_\sigma \setminus G_\sigma$ *made of* 3 *adjacent edges.*

The curve T_σ is regular by lemma 3.2. Thus theorem 3.10 produces a real algebraic nonsingular curve $X_\sigma \subset \mathbb{R}P^3$, of the same genus and degree as T_σ, and whose real part is isotopic to $\mathbb{P}T_\sigma$. The edges of T_σ whose phase contains $(+,+,+)$ are exactly the edges of G_σ. In other words, the positive real part of T_σ coincides with $G_\sigma \times \{(+,+,+)\}$. Consequently, the projectivization of T_σ has a connected component X_0 isotopic to $\mathbb{P}G_\sigma$. The graph G_σ is affine and homeomorphic to K, thus $\mathbb{P}G_\sigma$ is isotopic to ιK. Furthermore, the real part of X_σ can not have more than 2 connected components (theorem 3.9). Thus the projectivization of $T_\sigma \setminus G_\sigma$ is isotopic to a second component X_1 of $\mathbb{R}X_\sigma$. In particular $\mathbb{P}(T_\sigma \setminus G_\sigma)$ is connected in $\mathbb{R}P^3$. □

This general result can be applied to classical knots, for which braid presentations are well known.

Corollary 4.2. *Given positive integers p, q, there exists a nonsingular real algebraic curve $X_{p,q} \subset \mathbb{R}P^3$ of genus* 1 *and degree $q(p-1)+3p$ which has two unlinked components. One of them is isotopic to $\iota K(p,q)$.*

Proof. The torus braid $B(p,q)$ introduced in section 2.6 is a braid presentation of the torus knot $K(p,q)$ with p strings. The number of crossing points of $pr(B(p,q))$ is $q(p-1)$, thus the statement follows from theorem 4.1. □

It is interesting to look for improvements of corollary 4.2 in several directions. One can try to get a curve of smaller degree. Another option is to try to get a curve with a single connected component. This is the content of the next chapter. The following result is an analog of theorem 4.1 in the case of 2-bridge knots. The tropical curve T_σ used in the proof leads to a real curve of a smaller degree than theorem 4.1.

Theorem 4.3. *Given an odd integer m and positive integers $a_1, \ldots, a_m$, there exists a real algebraic nonsingular curve $X_{a_1,\ldots,a_m} \subset \mathbb{R}P^3$ of genus 1 and degree $\sum a_i + 6$ which has two unlinked components. One of them is isotopic to $\iota K(a_1, \ldots, a_m)$.*

Proof. The plat closure of the 4-braid $b(a_1, \ldots, a_m)$ is isotopic to $K(a_1, \ldots, a_m)$ (proposition 2.1). During the proof of theorem 4.1, we imitate the canonical closing procedure (described in section 2.4) with the braid σ to get a RPL-braid isotopic to σ. We proceed in a similar way with the braid $b(a_1, \ldots, a_m)$ and imitate the plat closing procedure described at the end of section 2.4. Until the end of the proof, we denote $b(a_1, \ldots, a_m)$ by σ. Notice that this braid is made of several "boxes", each of them being of the form $\sigma_2^{a_i}$ if i is odd, or $\sigma_1^{-a_i}$ if i is even.

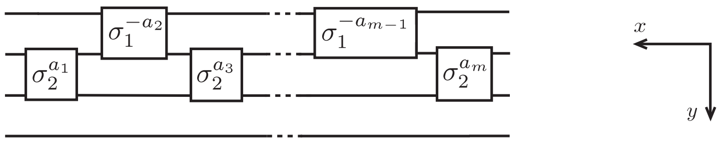

Figure 4.9. *The braid $\sigma = b(a_1, \ldots, a_m)$.*

Up to isotopy, one can assume that, given any crossing $P = (a, b)$ of $pr(\sigma)$, there exists $\varepsilon > 0$ such that $B_{P,\varepsilon} = [a - \varepsilon, a + \varepsilon] \times \mathbb{R}$ does not contain any other crossing of $pr(\sigma)$. Therefore $pr(\sigma) \cap B_{P,\varepsilon}$ is isotopic to the union of 4 straight lines as shown on figure 4.10.

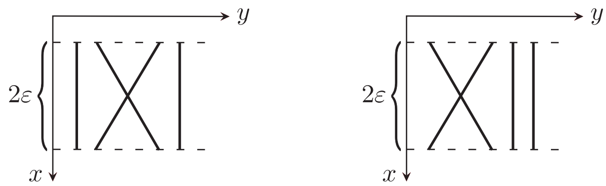

4.10 (a) If P is a crossing of some $\sigma_2^{a_i}$.

4.10 (b) If P is a crossing of some $\sigma_1^{-a_i}$.

Figure 4.10. *The stripe $pr(\sigma) \cap B_{P,\varepsilon}$.*

The set $\sigma \cap (B_{P,\varepsilon} \times \mathbb{R})$ is isotopic to the RPL-graph G_P^- or G_P^+ according to the nature of the crossing point. Any edge of these graphs is directed by u_1 or u_2, except one which is emphasized by an arrow onf figure 4.11. The latter is directed by u_{13} in G_P^- and by u_{23} in G_P^+. Figure 4.11 shows the RPL-graphs $G_P^{\pm}$ if the crossing point P belongs to a box of the form $\sigma_2^{a_i}$.

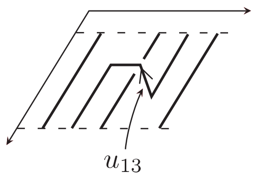

4.11 (a) The RPL-graph G_P^-.

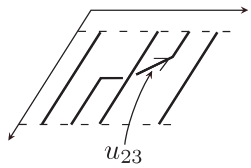

4.11 (b) The RPL-graph G_P^+.

Figure 4.11. *The RPL-graph $G_P^{\pm}$ if P is a crossing of some $\sigma_2^{a_i}$.*

The lengths of the edges of $G_P^{\pm}$ which are not directed by u_1 can be chosen such that the set

$$G_\sigma^0 = \bigcup_P G_P^{\pm},$$

is a RPL-braid isotopic to σ, where the union is taken over all crossing points of $pr(\sigma)$. It is the disjoint union of 4 strings. The "boxes" $\sigma_2^{a_1}$ and $\sigma_1^{-a_2}$ can be connected with a RPL-graph shown on figure 4.12 (a). The "boxes" $\sigma_2^{a_m}$ and $\sigma_1^{-a_{m-1}}$ can be connected with a RPL-graph shown on figure 4.12 (b). Finally, the "boxes" $\sigma_2^{a_1}$ and $\sigma_2^{a_m}$ can be connected with a RPL-closing arc shown on figure 4.12 (c).

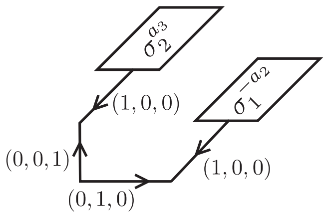

4.12 (a) Between $\sigma_2^{a_1}$ and $\sigma_1^{-a_2}$.

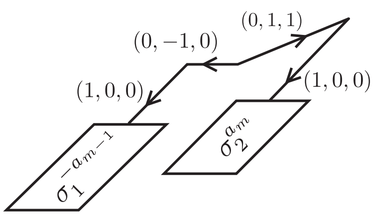

4.12 (b) Between $\sigma_2^{a_m}$ and $\sigma_1^{-a_{m-1}}$.

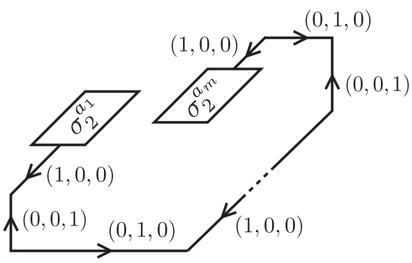

4.12 (c) Between $\sigma_2^{a_1}$ and $\sigma_2^{a_m}$.

Figure 4.12. *Rational closing arcs.*

The result is a RPL-knot isotopic to $K(a_1, \dots, a_m)$. The number of crossing points of $pr(\sigma)$ is $\Sigma_i a_i$, and the contribution to the degree of the four RPL-closing arcs is 6. Therefore, this RPL-knot can be completed into an elliptic real trivalent tropical curve T_σ of degree $\Sigma_i a_i + 6$ satisfying the properties of lemma 4.2. As T_σ is regular by lemma 3.2, the end of the proof is similar to the one of theorem 4.1 and the result follows. $\square$

Chapter 5

Torus knots as connected real curves

Notations : the following pages contain several figures representing (parts of) real tropical curves in $\mathbb{R}^3$. An edge whose phase contains $(+,+,+)$ is drawn in bold. A primitive integer vector of an edge is sometimes indicated by its Euclidean coordinates (a,b,c), or by the label $ax+by+cz$. An arrow shows the direction of the chosen primitive integer vector. Finally, an unbounded edge directed by $(-1,0,0)$ (respectively, by $(0,-1,0)$, by $(0,0,-1)$, by $(1,1,1)$) is called a x-edge (respectively, a y-edge, a z-edge, a t-edge).

5.1 RPL-realizations of torus knots

Fix $0 < p < q$ coprime integers. The torus braid $B(p, q)$ introduced in section 2.6 is the q^{th} power of the braid $b_p = \sigma_1 \cdots \sigma_{p-1}$ displayed on figure 5.1 (a). Figure 5.1 (b) shows a RPL-realization of b_p, denoted by Γ_p.

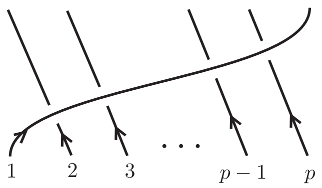

5.1 (a) A diagram of b_p.

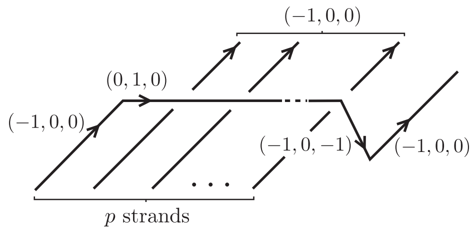

5.1 (b) The RPL-realization Γ_p of b_p.

Figure 5.1.

As shown on figure 5.2, we glue q copies of Γ_p to obtain a rational PL realization of $B(p, q)$. We could apply a PL canonical closure as in the proof of lemma 4.1, and obtain a RPL-realization of $K(p, q)$.

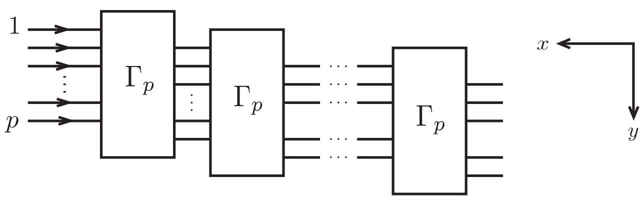

Figure 5.2. *RPL-realization of the braid $B(p, q)$.*

We proceed differently. The RPL-braid is partially closed with $p-1$ copies of the rational PL graph shown on figure 5.3, by connecting endpoints of the braid as shown on figure 5.4. The endpoints of two edges in the directions $(1, 0, 0)$ and $(-1, 0, 0)$ are left free.

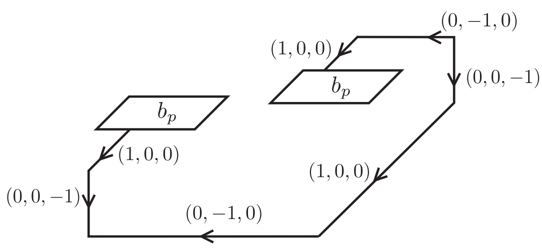

Figure 5.3. *RPL-"closing" graph.*

We extend these edges into unbounded edges. The result is a RPL-long knot Σ (see section 2.3), with two unbounded edges in the directions $(1,0,0)$ and $(-1,0,0)$, isotopic to the long torus knot $K^0(p,q)$.

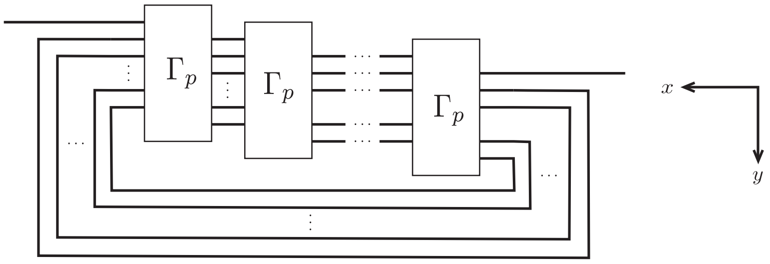

Figure 5.4. *The RPL-long knot* Σ.

We modify Σ as shown on figure 5.5: the first and the last $p-1$ copies of Γ_p are modified. Roughly speaking, the last $p-1$ copies of Γ_p are deleted, and somehow included in the RPL-"closing" graphs. The length of the edges of these arcs are modified in order to obtain a RPL-long knot which is still isotopic to $K^0(p,q)$. This resulting graph is denoted by $\Sigma^0_{p,q}$. It contains:

- $q-p$ copies of the RPL-braid Γ_p;
- $p-1$ RPL-closing arcs isotopic to the one of figure 5.3;
- one modified copy of Γ_p containing an unbounded edge directed by $(0,-1,0)$.

The remaining unbounded edge is directed by $(-1,0,0)$.

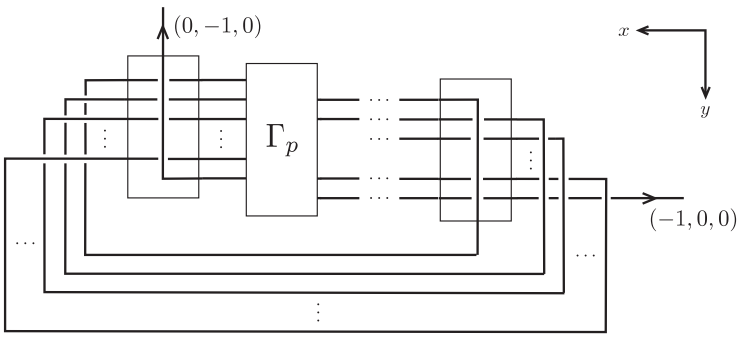

Figure 5.5. *TheRPL-long knot* $\Sigma^0_{p,q}$.

We assign the weight 1 to every edge, making $\Sigma^0_{p,q}$ into a weighted RPL-long knot. All vertices are of valency 2, and their 8 possible types, labeled from A_1 to A_8, are described in figure 5.6. For each type, primitive integer vectors of the two edges adjacent to the vertex are indicated following the convention introduced at the beginning of the current chapter. More precisely:

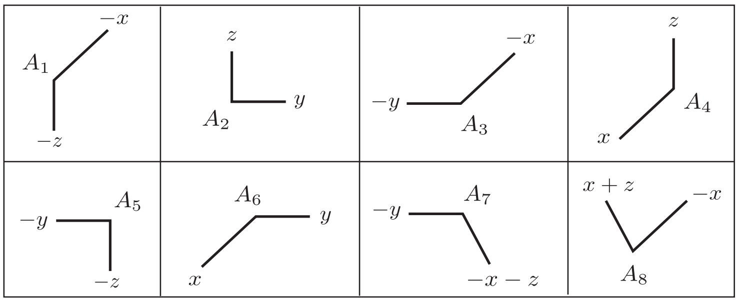

Figure 5.6. *Different types of vertices of* $\Sigma^0_{p,q}$.

– the first modified copy of Γ_p contains a vertex of each type A_7 and A_8;
– each copy of the RPL-braid Γ_p contains a vertex of each type A_6, A_7 and A_8;
– each RPL-closing arc contains a vertex of each type $A_1, A_2, \ldots, A_6$.

Consequently, the RPL-long knot $\Sigma^0_{p,q}$ contains:

– $q-p+1$ vertices of each type A_7 and A_8;
– $p-1$ vertices of each type $A_1, A_2, \ldots, A_5$;
– $q-1$ vertices of type A_6.

By attaching some additional edges to each vertex, we complete $\Sigma^0_{p,q}$ into a projective trivalent tropical curve in $\mathbb{R}^3$ with respect to the following condition.

$\mathcal{C}_0$ | *Each additional edge is of weight* 1 *and the balacing condition is satisfied at each vertex, and and the degree of the resulting tropical curve is minimal among tropical curves containing* $\Sigma^0_{p,q}$ *and having only edges of weight* 1.

Figure 5.7 shows the added edges adjacent to each vertex according to the type of the vertex. The additional edges are drawn in bold, and primitive integer vectors of the unbounded ones are indicated. As every edge has the weight 1, a primitive integer vector of an additional bounded edge can be determined following the balancing condition. The resulting tropical curve is denoted by $T_{p,q}$.

Lemma 5.1. *The tropical curve* $T_{p,q}$ *is trivalent, projective, of genus* 0 *and of degree* $2p+q-2$. *Moreover, the subgraph* $\Sigma^0_{p,q}$ *of* $T_{p,q}$ *is isotopic to the long torus knot* $K^0(p,q)$ *(with respect to the vocabulary of section 2.3).*

Proof. By construction $\Sigma^0_{p,q}$ is isotopic to $K^0(p,q)$. As it has no cycle, the genus of $T_{p,q}$ is equal to 0. Recall that $\Sigma^0_{p,q}$ has $q-p+1$ vertices of each type A_7 and A_8, $p-1$ vertices of each type $A_1, A_2, \ldots, A_5$, and $q-1$ vertices of type A_6. The degree of $T_{p,q}$ is the result of a simple computation based on figure 5.6. □

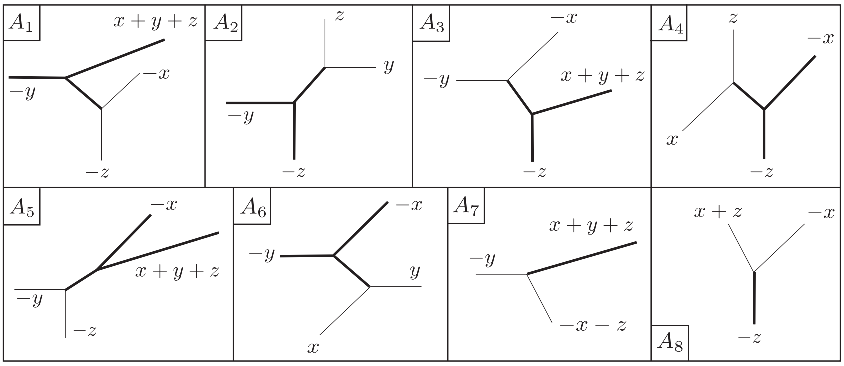

Figure 5.7. *Additional edges attached to each vertex of* $\Sigma^0_{p,q}$.

Example 5.1. Figure 5.8 shows the projection of the tropical curve $T_{4,7}$ on the plane $\{z = 0\}$. This curve has genus 0 and degree 13. The projection of the subgraph $\Sigma^0_{4,7}$ is drawn in bold on the picture. A vertical edge of $T_{4,7}$ (directed by $(-1, 0, 0)$ or $(1, 0, 0)$) is mapped to a point under the projection map. Such an edge is indicated by an empty circle if it is unbounded, and by a bold circle, otherwise. Finally, at every crossing point, the image of the lower edge is represented by a broken line.

We provide compatible phases to the edges of $T_{p,q}$ according to the following condition.

$\mathcal{C}_\varepsilon$ | *The phase of an edge of* $\Sigma^0_{p,q}$ *contains* $(+, +, +)$.

In order to provide phases to the edges of $T'_{p,q} = T_{p,q} \setminus \Sigma^0_{p,q}$, we introduce the map "distance to Σ"

$$d_\Sigma : E(T_{p,q}) \longrightarrow \{0, 1, 2\},$$

defined on the set of edges of $T_{p,q}$. The image of an edge e is:

- 0 if e belongs to $\Sigma^0_{p,q}$;
- 1 if e belongs to $T'_{p,q}$ and is adjacent to $\Sigma^0_{p,q}$;
- 2 if e belongs to $T'_{p,q}$ and is adjacent to an edge e' such that $d_\Sigma(e') = 1$.

If e is adjacent to $\Sigma^0_{p,q}$ (resp., to an edge e' such that $d_\Sigma(e') = 1$), the vertex $e \cap \Sigma^0_{p,q}$ (resp., $e' \cap \Sigma^0_{p,q}$) is called the *nearest* Σ*-vertex* of e. The nearest Σ-vertex of an edge of $\Sigma^0_{p,q}$ is not defined. The set $T'_{p,q}$ is a disconnected graph whose number of components is the number of vertices of $\Sigma^0_{p,q}$. According to the construction of $T_{p,q}$ (figure 5.7), a connected component of $T'_{p,q}$ is a single unbounded edge if its nearest Σ-vertex is of type A_7 or A_8, or a tree with one vertex and three edges, only one of which being bounded. More precisely, the distance to $\Sigma^0_{p,q}$ of an edge of $T'_{p,q}$ is 1 if the edge is bounded or unbounded and

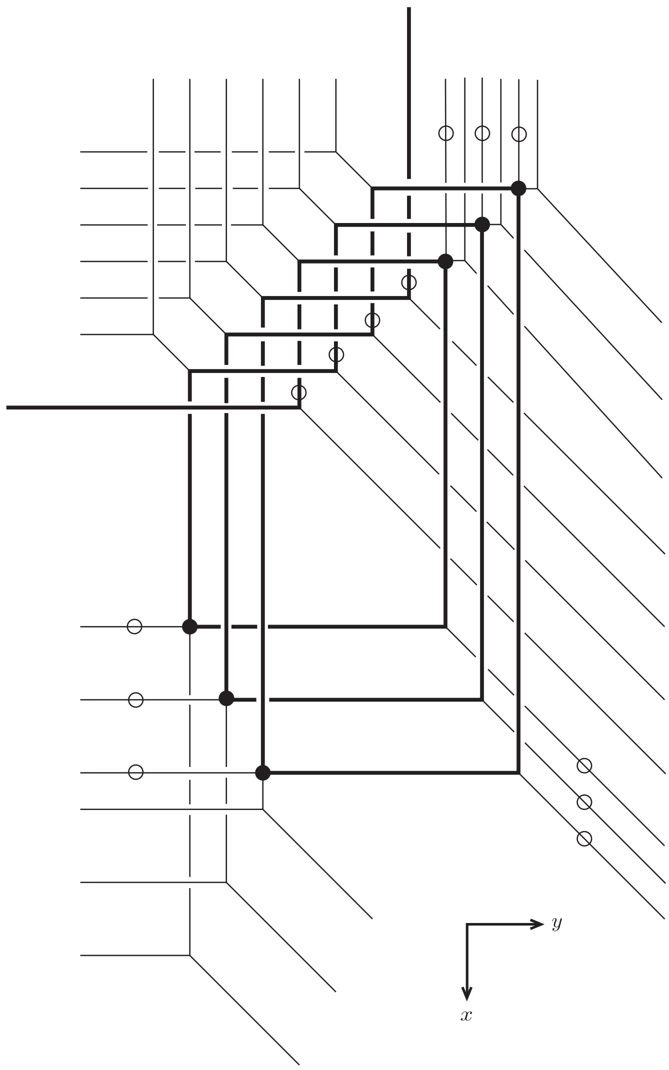

Figure 5.8. *The projective trivalent tropical curve $T_{4,7}$.*

adjacent to an A_7 or A_8 vertex, or 2 if it is unbounded and not adjacent to an A_7 or A_8 vertex. Consider the following condition:

$\mathcal{C}'_\varepsilon$ | *The phase of an unbounded edge of $T'_{p,q}$ contains $(+,+,+)$ if and only if its nearest Σ-vertex is of type A_6. The phase of a t-edge whose nearest Σ-vertex is of type A_1 contains $(+,-,-)$, otherwise it contains $(+,-,+)$.*

Remark 5.1. According to lemma 3.8, the second part of condition $\mathcal{C}'_\varepsilon$ means that the boundary points of the star-diagram of $T_{p,q}$ occur in the quadrants of signs $(+,-)$ and $(-,+)$.

Recall the compatibility rule of phases in the case of 3 adjacent edges e_1, e_2, e_3 of weight 1. The phase of e_i is an element s_i of the quotient set $(\mathbb{Z}/2\mathbb{Z})^3/\sim_e$ (see section 3.4 for a description of the equivalence relation $\sim_e$). As the weight of e_i is 1, the quotient set is in 1-to-1 correspondence with $(\mathbb{Z}/2\mathbb{Z})^2$. Therefore s_i is a pair of 3-tuples which are equivalent with respect to the $\sim_e$. The compatibility rule requires that each element of s_i is contained is exactly one s_j with $j \neq i$.

Lemma 5.2. *Conditions $\mathcal{C}_0$, $\mathcal{C}_\varepsilon$ and $\mathcal{C}'_\varepsilon$ determine a compatible system of phases on the edges of the tropical curve $T_{p,q}$.*

Proof. Each edge is of weight 1, thus the equivalence classes of $\sim_e$ form a partition of $(\mathbb{Z}/2\mathbb{Z})^3$ into 4 pairs. In particular, only one of them contains $(+,+,+)$. Therefore $\mathcal{C}_0$ completely determines the phases of the edges of $\Sigma^0_{p,q}$. As $\Sigma^0_{p,q}$ is bivalent, this collection of phases is consistent with the compatibility rule of phases.

Consider an edge e of $T'_{p,q}$ such that $d_\Sigma(e) = 1$. The nearest Σ-vertex V of e belongs to e. The two other edges adjacent to V belong to $\Sigma^0_{p,q}$. In particular, their phases are already determined. The phase of e is then determined by the compatibility rule of phases.

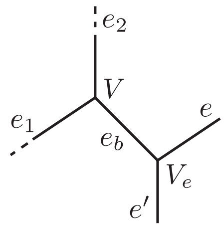

Figure 5.9.

If $d_\Sigma(e) = 2$, then e is unbounded and the nearest Σ-vertex V of e is of type A_1, A_2, A_3, A_4, A_5 or A_6. We introduce the following notations:

- e_1, e_2 are the two edges of $\Sigma^0_{p,q}$ adjacent to V,
- V_e is the vertex of e,
- e_b is the bounded edge adjacent to V_e,
- e' is the second unbounded edge adjacent to V_e,

as shown on figure 5.9. As $d_\Sigma(e_b) = 1$, the phase of e_b is already determined. Moreover e_1 and e_2 belong to $\Sigma^0_{p,q}$, thus their phases both contain $(+,+,+)$. Hence, the phase s_b of e_b does not contain $(+,+,+)$.

Assume that V is of type A_2, A_4 or A_6. Then e_1, e_2 and e, e' are pairwise parallel and neither e nor e' is directed by $(1,1,1)$ (figure 5.7). For example, assume that e and e_1 are parallel as depicted on figure 5.9. The quotient sets of $\sim_e$ and $\sim_{e_1}$ are equal: the 4 possible phases of e and e_1 coincide. The phase s_b of e_b is already determined. According to the compatibility rule of phases, the two elements of $(\mathbb{Z}/2\mathbb{Z})^3/\sim_e$ whose intersection with s_b is empty cannot be a phase of e. Though s_b does not contains $(+,+,+)$, one of the two remaining elements of $(\mathbb{Z}/2\mathbb{Z})^3/\sim_e$ contains $(+,+,+)$. If V is of type A_6 (resp., of type A_2 or A_4), the latter should be (resp., should not be) the phase of e by condition $\mathcal{C}'_\varepsilon$.

If V is of type A_1, A_3 or A_5, one of the unbounded edges, say e, is directed by $(1,1,1)$ (figure 5.7). Its phase is then determined by condition $\mathcal{C}'_\varepsilon$. As the phase of e_b is already known, the one of e' is determined by the compatibility rule of phases at V_e. One has to check that the latter is an equivalence class of the relation $\sim_{e'}$.

type of the vertex	A_1	A_3	A_5
phase of e	$\{(+,-,-),(-,+,+)\}$	$\{(+,-,+),(-,+,-)\}$	$\{(+,-,+),(-,+,-)\}$
phase of e_b	$\{(-,+,+),(+,+,-)\}$	$\{(+,-,+),(-,+,+)\}$	$\{(+,-,+),(+,+,-)\}$
$(\mathbb{Z}/2\mathbb{Z})^3/\sim_{e'}$	$\{(+,+,+),(+,-,+)\}$ $\{(+,+,-),(+,-,-)\}$ $\{(-,+,+),(-,-,+)\}$ $\{(-,-,-),(-,+,-)\}$	$\{(+,+,+),(+,+,-)\}$ $\{(+,-,+),(+,-,-)\}$ $\{(-,+,+),(-,+,-)\}$ $\{(-,-,-),(-,-,+)\}$	$\{(+,+,+),(-,+,+)\}$ $\{(+,+,-),(-,+,-)\}$ $\{(+,-,+),(+,+,-)\}$ $\{(-,-,-),(+,-,-)\}$
phase of e'	$\{(+,+,-),(+,-,-)\}$	$\{(-,+,-),(-,+,+)\}$	$\{(-,+,-),(+,+,-)\}$

For each of the 3 possile types of the vertex V, the above table contains: the phase of e determined by condition $\mathcal{C}'_\varepsilon$, the phase of e_b imposed by the compatibility rule of phases at V_e and the possible phases of e' according to the definition of $\sim_{e'}$. □

5.2 Morse modification of a real tropical curve

We introduce the notion of a "Morse" modification of a real tropical curve. The purpose of such a modification is to modify the star-diagram of the curve in a neighbourhood of a crossing as described on figure 5.10. We assume that there exists a closed ball $B \subset \mathbb{R}^3$ whose intersection with the given real tropical curve T has the same combinatorial type as the graph G depicted on figure 5.11. It

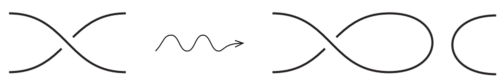

Figure 5.10. *Diagram of a Morse modification.*

contains two A_6-vertices, denoted by V and V'. The vertical projection of G is shown on the right part of figure 5.11.

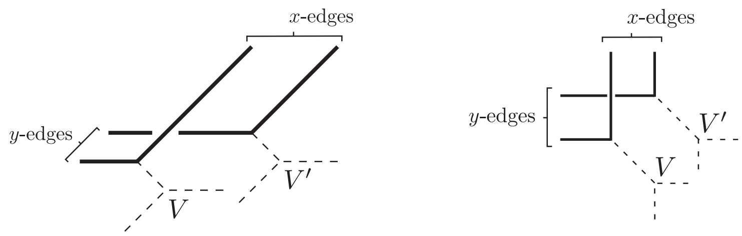

Figure 5.11. *The graph G and its vertical projection.*

Consider the graph G' obtained in the following way. Without modifying their phases, the two x-edges of G are replaced by two bounded edges directed by $(1,0,0)$. These edges are connected by a path consisting of a bounded edge directed by $(0,1,0)$ and a bounded edge directed by $(0,0,1)$, shown on the left part of figure 5.12. The modified graph contains three new vertices of types A_4, A_5 and A_6. As in the construction of the curve $T_{p,q}$ described in section 5.1, we attach some edges at these vertices according to figure 5.7. The resulting graph is denoted by G', and its vertical projection is shown on figure 5.12. The following lemma is also a definition.

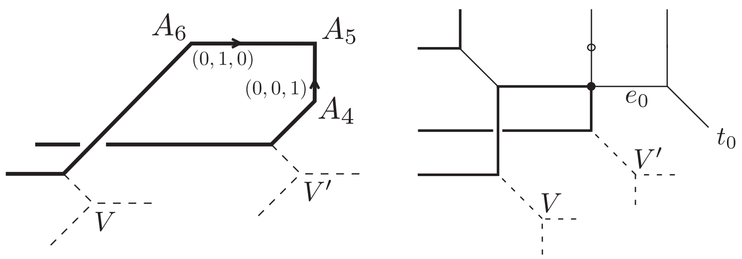

Figure 5.12. *The graph G' and its vertical projection.*

Lemma 5.3. *The length of the bounded edges of G' can be adjusted such that the result of replacing G by G' is a generic projective tropical curve. If their weights are equal to* 1*, the phases of these edges can be determined by conditions $\mathcal{C}_0$, $\mathcal{C}_\varepsilon$ and $\mathcal{C}'_\varepsilon$. The result is called a Morse modification of the original real tropical curve.*

Proof. The first part follows from the fact that generic curves form a dense subset of the set of projective tropical curves in $\mathbb{R}^3$. The second part can be proven as lemma 5.2 above. □

5.3 Nature of the crossings of $pr(T_{p,q})$

Proposition 3.3 asserts the star-diagram $D(T_{p,q})$ of $T_{p,q}$ is a projective link diagram of $\mathbb{P}T_{p,q}$. It is determined by the lower arc at each crossing and the endpoints of each arc of the diagram. By definition 3.17, $D(T_{p,q})$ is obtained from the projection of $\Delta T_{p,q}$ on the coordinate hyperplane $\{z = 0\}$. Therefore, in order to determine of a projective diagram of $\mathbb{P}T_{p,q}$, one should

i) specify the nature of the crossing points of $pr(T_{p,q})$: according to definition 3.18, it can be simple or ghost on one hand, and mirror or transparent on the other;

ii) determine the pairs of t-edges of $T_{p,q}$ whose images in $D(T_{p,q})$ are the endpoints of the same arc: it follows from lemma 3.8 that the set of t-edges is in bijective correspondence with pairs of antipodal boundary points of the star-diagram.

Denote by $V_1, \ldots, V_{q-1}$ the A_6-vertices of $T_{p,q}$, with the convention that the x-coordinate of V_{i+1} is smaller than the x-coordinate of V_i. Figure 5.3 shows the projection of $\Sigma^0_{p,q}$ on the plane $\{z = 0\}$ with the A_6-vertices labeled from V_1 to V_{q-1}.

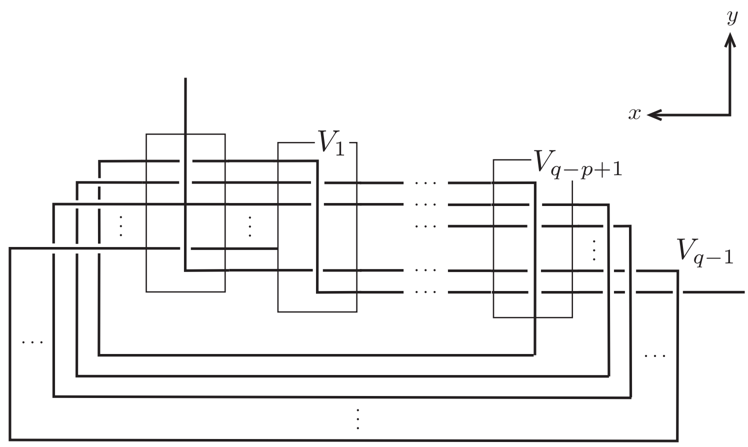

Figure 5.13.

The set of crossings of $pr(T_{p,q})$ can be divided into 2 subsets with respect to the following decomposition of $T_{p,q}$:

$$T_{p,q} = \{\text{edges of phase } (+,+,+)\} \bigcup \{\text{other edges}\}$$

Denote by $T^+_{p,q}$ the set of edges of phase $(+,+,+)$. According to condition $\mathcal{C}_\varepsilon$, it contains $\Sigma^0_{p,q}$ and other edges. The latters are exactly the unbounded edges whose nearest Σ-vertex is of type A_6. The next statement follows directly from lemma 3.10 and the fact that a crossing of $pr(T_{p,q})$ involving two edges of phase $(+,+,+)$ is transparent.

Lemma 5.4. *A crossing obtained by projecting two edges of $T^+_{p,q}$ is simple and transparent. Moreover, the image of such a crossing in $D(T_{p,q})$ is contained in the positive quadrant.*

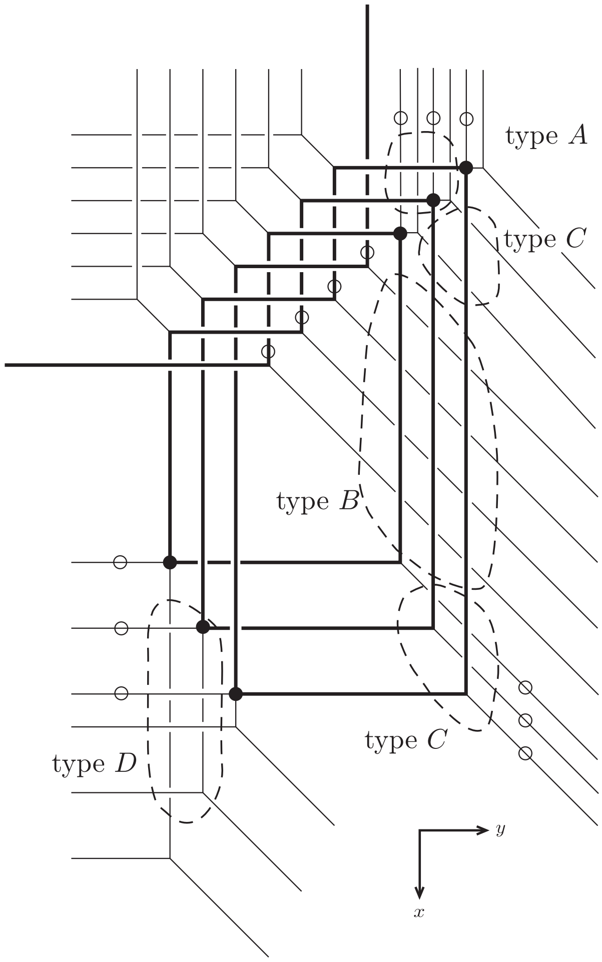

Figure 5.14. *Crossing points of $pr(T_{4,7})$.*

The remaining crossings of $pr(T_{p,q})$ are the projection of 2 edges, such that at least one of them does not belong to $T_{p,q} \setminus T^+_{p,q}$. One divides these crossings into several subsets (as shown on figure 5.3 in the case of $T_{4,7}$):

– a crossing of type A is the projection of a bounded edge of $\Sigma^0_{p,q}$, directed by $(0,1,0)$ and adjacent to a vertex V_k, and of an edge of $T_{p,q} \setminus T^+_{p,q}$;

– a crossing of type B is the projection of a t-edge adjacent to a A_7-vertex of $\Sigma^0_{p,q}$, and of a bounded edge of $\Sigma^0_{p,q}$ directed by $(1,0,0)$;

– a crossing of type C is the projection of a bounded edge of $T_{p,q} \setminus T^+_{p,q}$ directed by $(1,1,0)$, and of a bounded edge of $\Sigma^0_{p,q}$ directed by $(1,0,0)$;

– a crossing of type D is the projection of a bounded edge of $T_{p,q} \setminus T^+_{p,q}$ directed by $(1,0,1)$, and of a bounded edge of $T_{p,q} \setminus T^+_{p,q}$ directed by $(0,1,0)$, both of them having distance to Σ equal to zero.

Lemma 5.5. *A crossing of type A is simple, transparent and the corresponding crossing of $D(T_{p,q})$ is contained in the $(+,+)$-quadrant.*

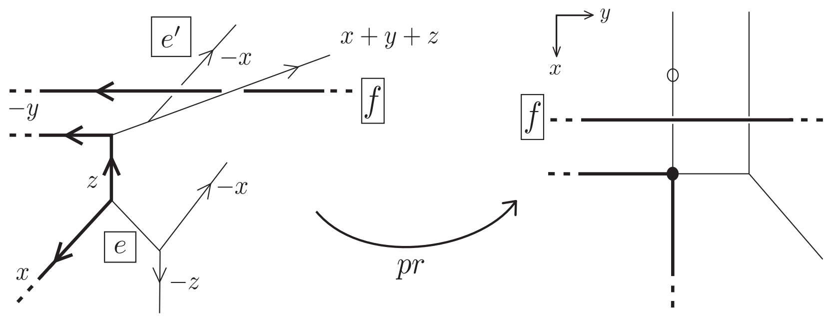

Figure 5.15. *Crossings of type A of $pr(T_{p,q})$.*

Proof. There are two different types of A-crossings: either it is the projection of a bounded edge f of $\Sigma^0_{p,q}$ directed by $(0,1,0)$ and a bounded edge e of $T_{p,q} \setminus T^+_{p,q}$ directed by $(-1,0,-1)$, or it is the projection of f and a x-edge e' of $T_{p,q} \setminus T^+_{p,q}$. Figure 5.15 shows a subset of $T_{p,q}$ whose projection onto the plane $\{z=0\}$ contains the two kinds of A-crossings. Lemma 3.10 implies that both are simple. In order to prove that they are transparents, lets take care of the phases of the edges. By condition $\mathcal{C}_\varepsilon$, the phase of f is $\{(+,+,+),(+,-,+)\}$.

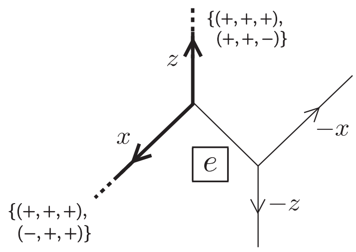

Figure 5.16. *First kind of crossing of type A.*

Phase of e : the edge e has a distance to Σ equal to 1. The edges of $\Sigma^0_{p,q}$ adjacent to e are directed by $(1,0,0)$ and $(0,0,1)$. According to condition $\mathcal{C}_\varepsilon$, their phases are $\{(+,+,+),(-,+,+)\}$ and $\{(+,+,+),(+,+,-)\}$ respectively. The compatibility rule of phases implies that the phase of e is necessarily $\{(-,+,+),(+,+,-)\}$.

Phase of e' : the edge e' has a distance to Σ equal to 2. The edges of $\Sigma^0_{p,q}$ adjacent to the nearest Σ-vertex of e are directed by $(0,1,0)$ and $(0,0,1)$. According to condition $\mathcal{C}_\varepsilon$, their phases are $\{(+,+,+),(+,-,+)\}$ and $\{(+,+,+),(+,+,-)\}$ respectively. The compatibility rule implies that the phase of the bounded edge connecting e' to $\Sigma^0_{p,q}$ is necessarily $\{(+,-,+),(+,+,-)\}$. As e' is an $x-$edge of weight 1, its phase has to be $\{(+,-,+),(-,-,+)\}$ or $\{(+,+,-),(-,+,-)\}$. Only the second possibility is compatible with the fact that the t-edge adjacent to e' should be of phase $\{(+,-,+),(-,+,-)\}$ by condition $\mathcal{C}'_\varepsilon$.

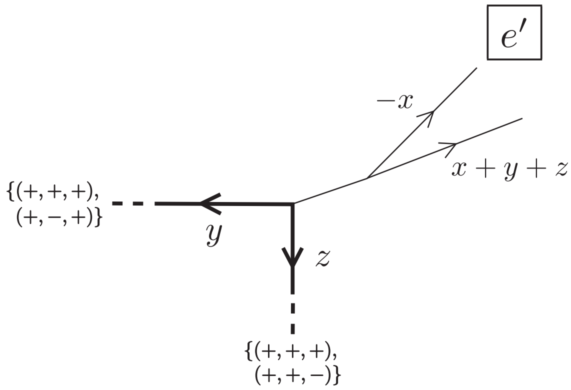

Figure 5.17. *Second kind of crossing of type A.*

The first kind of A-crossing is the projection of the edge f of phase $\{(+,+,+),(+,-,+)\}$, and the edge e of phase $\{(+,+,-),(-,+,+)\}$. Therefore it is transparent. As $S_f \cap S_e = \{(+,+)\}$, it induces a crossing point of $D(T_{p,q})$ in the quadrant $(+,+)$ by lemma 3.9. Similarly, the second kind of A crossing is the projection of f and of the edge e' of phase $\{(+,+,-),(-,+,-)\}$. Therefore it is transparent and induces a crossing point of $D(T_{p,q})$ in the quadrant $(+,-)$. $\square$

Lemma 5.6. *A crossing of type B is simple, transparent, and the corresponding crossing of $D(T_{p,q})$ is contained in the $(-,+)$-quadrant .*

Proof. As the crossing point P is the projection of a t-edge and a bounded edge directed by $(1,0,0)$, a crossing of type B is simple by lemma 3.10. According to condition $\mathcal{C}'_\varepsilon$, the phase of the t-edge is $\{(+,-,+),(-,+,-)\}$. The bounded edge is the upper edge at P, and is of phase $\{(+,+,+),(-,+,+)\}$ since it belongs to $\Sigma^0_{p,q}$. According to definition 3.18, it is a transparent crossing and induces a crossing point of $D(T_{p,q})$ in the quadrant $(-,+)$ by lemma 3.9. $\square$

Lemma 5.7. *A crossing of type C is simple, transparent, and the corresponding crossing of $D(T_{p,q})$ is contained in the $(-,+)$-quadrant.*

Proof. Denote by P a crossing of type C. It is the projection of a t-edge and a bounded edge directed by $(1,0,0)$. Thus it is simple by lemma 3.10. The bounded edge is the upper edge at P, and is of phase $\{(+,+,+),(-,+,+)\}$ since it belongs to $\Sigma^0_{p,q}$. The t-edge is of phase $\{(+,-,+),(-,+,-)\}$ by condition $\mathcal{C}'_\varepsilon$. According to definition 3.18, it is transparent and induces a crossing point of $D(T_{p,q})$ in the quadrant $(-,+)$ by lemma 3.9. □

Lemma 5.8. *A crossing of type D is simple, mirror and the corresponding crossing of $D(T_{p,q})$ is contained in the quadrant of phase $(+,+)$.*

Proof. There are 2 kinds of crossing of type D. Either such a crossing is the projection of two bounded edges e,f of $T_{p,q}\setminus T^+_{p,q}$ directed by $(0,-1,-1)$ and $(1,0,1)$ respectively, or it is the projection of f and an y-edge e' of $T_{p,q}\setminus T^+_{p,q}$, see figure 5.18. These crossings are simple by lemma 3.10. In order to prove that these crossings are transparent, one has to take care of the phases of the edges. As f is adjacent to two edges of $\Sigma^0_{p,q}$ directed by $(1,0,0)$ and $(0,0,1)$, the phase of f is necessarily $\{(+,+,-),(-,+,+)\}$. Similarly, the edge e is adjacent to two edges of $\Sigma^0_{p,q}$ directed by $(0,0,1)$ and $(0,1,0)$. Thus its phase is $\{(+,+,-),(+,-,+)\}$.

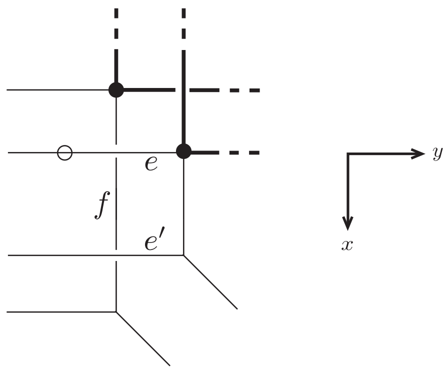

Figure 5.18. *Crossings of type D.*

Phase of e': its distance to Σ is equal to 2. It is adjacent to a bounded edge, directed by $(1,0,1)$. As this bounded edge is adjacent to two edges of $\Sigma^0_{p,q}$ directed by $(1,0,0)$ and $(0,0,1)$, the condition $\mathcal{C}_0$ and the compatibility rule imply that the phase of this bounded edge is $\{(-,+,+),(+,+,-)\}$. The edge e' is an y-edge of weight 1, thus the phase of e' has to be $\{(-,+,+),(-,-,+)\}$ or $\{(+,+,-),(+,-,-)\}$. The t-edge adjacent to e' has a nearest Σ-vertex of type A_1, thus its phase is $\{(+,-,-),(-,+,+)\}$ by condition $\mathcal{C}'_\varepsilon$. According to the compatibility rule, the phase of e' is therefore necessarily $\{(+,+,-),(+,-,-)\}$.

The statement then follows from definition 3.18 and lemma 3.9 as in the proof of the preceeding lemma. □

5.4 Determination of the star-diagram of $T_{p,q}$

Recall that the star-diagram $D(T_{p,q})$ is obtained by intersecting the projection of $\Delta T_{p,q}$ on $\{z = 0\}$ with a closed disk containing the projection of every vertex of $\Delta T_{p,q}$. The intersection points of the boundary of the disk with $\Delta T_{p,q}$ correspond to unbounded edges of $\Delta T_{p,q}$. By definition, the only unbounded edges of $\Delta T_{p,q}$ are the images of the t-edges of $T_{p,q}$. Therefore an arc of $D(T_{p,q})$ corresponds to a pair of $t-$edges which are connected by a particular type of subgraph of $T_{p,q}$, defined as follows.

Definition 5.1. *Consider two $t-$edges e, e' of a generic real tropical curve T contained in $\mathbb{R}^2$ or $\mathbb{R}^3$. A $t-$arc of length n connecting e and e' is a sequence $e_1 = e, e_2, \dots, e_{n-1}, e_n = e'$ of edges of T such that, if s_i denotes the phase of e_i, the following conditions are satisfied.*

1. *None of $e_2, \dots, e_{n-1}$ is a $t-$edge.*
2. *For every unbounded edge $f \notin \{e, e'\}$ occurring in the sequence, there exists a unique $i \in \{2, \dots, n-2\}$ such that $f = e_i$ and $e_{i+1} = e_i$.*
3. *If e_i is an unbounded edge, different from e and e', such that $e_i = e_{i+1}$ (see 2.), then the cardinality of $s_i \cap s_{i+1}$ is equal to 2. Otherwise, $\mathrm{Card}(s_i \cap s_{i+1}) = 1$.*
4. *For $i \in \{1, \dots, n-1\}$, either $e_i = e_{i+1}$ or $e_i \cap e_{i+1}$ is a common vertex of e_i and e_{i+1}. The first case occurs if and only if e_i is unbounded.*

A $t-$arc connecting e and e' is denoted by ee' or sometimes $\{e_1, \dots, e_n\}$.

With the notations of the above definition, consider the subset of $\mathbb{R}T$ defined by

$$\bigcup_{i=1}^{n-1} e_i \times (s_i \cap s_{i+1}) \bigcup e_n \times (s_{n-1} \cap s_n).$$

The image of this set in ΔT is a piecewise-linear path connecting the image of e contained in the orthant of phase $s_1 \cap s_2$ and the image of e' contained in the orthant of phase $s_{n-1} \cap s_n$. This piecewise-linear path induces an arc of the star-diagram $D(T)$ connecting the boundary points corresponding to $e \times (s_1 \cap s_2)$ and $e' \times (s_{n-1} \cap s_n)$. We denote it by $[ee']$.

Example 5.2. Consider the real tropical line $T \subset \mathbb{R}^2$ shown on figure 5.19 (a) (all edges are of weight 1). The set ΔT is depicted on figure 5.19 (b). The curve T has only one $t-$edge, denoted by e on figure 5.19 (a). This edge is connected to itself by a $t-$arc of length 6 made of the following edges:

- $e_1 = e$ is of phase $\{(+,+), (-,-)\}$;
- e_2 is a $x-$edge of T, whose phase is $\{(+,+), (-,+)\}$;
- $e_3 = e_2$ according to condition 2 of definition 5.1;
- e_4 is a $y-$edge of T, whose phase is $\{(-,+), (-,-)\}$;
- $e_5 = e_4$ according to condition 2 of definition 5.1;

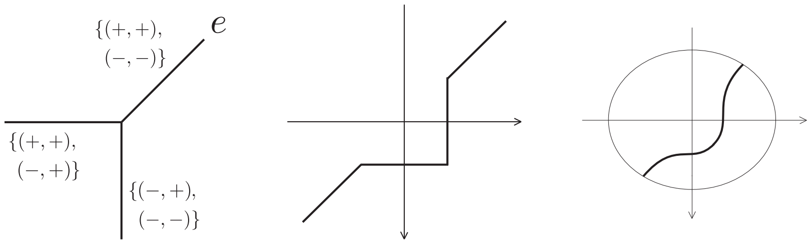

5.19 (a) A real tropical line T in $\mathbb{R}^2$.

5.19 (b) The set ΔT.

5.19 (c) The star diagram of T.

Figure 5.19.

- $e_6 = e$.

By definition (see section 3.5), the union of images of the edges e_i in ΔT is a piecewise-linear subset of ΔT (which actually coincides with ΔT is the case of our real tropical line). This subset connects the two images of e in ΔT which are contained in the quadrants of phase $(+, +)$ and $(-, -)$ respectively. According to lemma 3.8, the subsets $e \times \{(+, +)\}$ and $e \times \{(-, -)\}$ of $\mathbb{R}T$ correspond to two boundary points of $D(T)$, contained in the quadrants of phase $(+, +)$ and $(-, -)$ respectively. These boundary points are connected by an arc, shown on figure 5.19 (c), which is the image in $D(T)$ of the above piecewise-linear subset of ΔT.

The notation ee' is ambiguous: in general, two $t-$edges can be connected by two $t-$arcs.

Lemma 5.9. *There exists at most one $t-$arc connecting any pair of $t-$egdes of $T_{p,q}$. Moreover, no $t-$edge of $T_{p,q}$ is connected to itself by a $t-$arc.*

Proof. If e, e' are $t-$edges of $T_{p,q}$ connected by two $t-$arcs, the antipodal boundary points m, n and m', n' of $D(T_{p,q})$ corresponding to e, e' by lemma 3.8 are connected by two arcs as shown on figure 5.20. As $D(T_{p,q})$ is a projective diagram of $\mathbb{P}T_{p,q}$, the projectivization of $T_{p,q}$ has a connected component C whose diagram is made of the two arcs of figure 5.20.

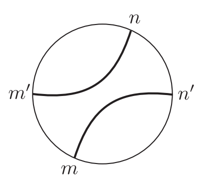

Figure 5.20. *Diagram of the component C.*

By theorem 3.10, the projective link $\mathbb{P}T_{p,q}$ is isotopic to the real point set of a real space algebraic curve of genus 0. Such curve is connected, thus C is the only connected component of $\mathbb{P}T_{p,q}$. Similarly, if a $t-$edge is connected to itself by a $t-$arc, the star diagram of $T_{p,q}$ contains an arc connecting two antipodal boundary points corresponding to the given $t-$edge. For the reason explained above, this arc would be the diagram of the only connected component of $\mathbb{P}T_{p,q}$. However $T_{p,q}$ has more than two $t-$edges, thus its star-diagram has more than 4 boundary points, contradicting the situations described above. $\square$

The following result is a consequence of lemma 5.9.

Lemma 5.10. *The map $ee' \longmapsto [ee']$ is well defined, and realizes a bijection between the set of $t-$arcs of $T_{p,q}$ and the set of arcs of $D(T_{p,q})$.*

Recall that $\Sigma^0_{p,q}$ is obtained from a polygonal realization of the torus braid $B(p,q)$ and $p-1$ polygonal closing arcs as described in section 5.1. Each polygonal arc contains a vertex of type A_1, A_3 and A_5, to which a $t-$edge is attached when $\Sigma^0_{p,q}$ is completed into $T_{p,q}$, see figure 5.7. We denote by t_i, t'_i and t''_i the three $t-$edges attached to the i^{th} polygonal arc as shown on figure 5.21.

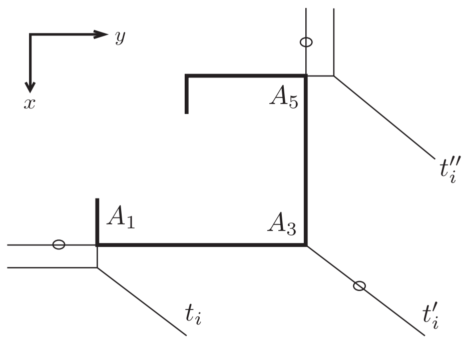

Figure 5.21.

Lemma 5.11. *For any distinct integers $i,j \in \{1,\dots,p-1\}$, the edges t_i, t'_i and t_j, t'_j are connected by $t-$arcs of length 13. The arcs $[t_it'_i]$ and $[t_jt'_j]$ of $D(T_{p,q})$ intersects twice, as shown on figure 5.22.*

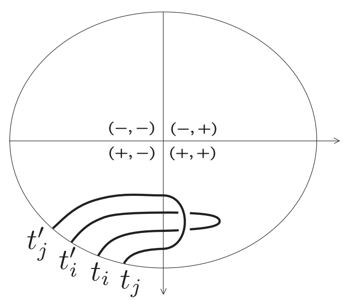

Figure 5.22. *The arcs $[t_it'_i]$ and $[t_jt'_j]$ in $D(T_{p,q})$.*

Proof. The $t-$arc $t_i t_i'$ is made of the following edges (see figure 5.23):

- $e_1 = t_i$ is of phase $\{(+,-,-),(-,+,+)\}$;
- $e_2 = e_3$ is an y-edge of phase $\{(+,+,-),(+,-,-)\}$;
- e_4 is a bounded edge directed by $(1,0,1)$ of phase $\{(-,+,+),(+,+,-)\}$;
- e_5 is a bounded edge directed by $(0,0,1)$ of phase $\{(+,+,+),(+,+,-)\}$;
- e_6 is a bounded edge directed by $(0,1,1)$ of phase $\{(+,+,-),(+,-,+)\}$;
- e_7 is a z-edge of phase $\{(+,-,-),(+,-,+)\}$;
- $e_8 = e_9$ is an y-edge of phase $\{(+,+,-),(+,-,-)\}$;
- $e_{10} = e_6$;
- e_{11} is a bounded edge directed by $(0,1,0)$ of phase $\{(+,+,+),(+,-,+)\}$;
- e_{12} is a bounded edge directed by $(1,1,0)$ of phase $\{(+,-,+),(-,+,+)\}$;
- $e_{13} = t_i'$ is of phase $\{(+,-,+),(-,+,-)\}$.

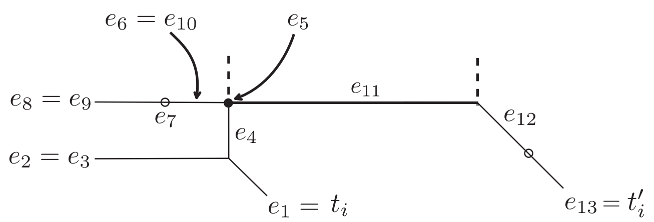

Figure 5.23. *The $t-$arc $t_i t_i'$ in $T_{p,q}$.*

As shown on figure 5.24 (b), the projection of $t_i t_i'$ and $t_j t_j'$ has two crossing points. Both are of type D, thus are simple, mirror and the corresponding crossings of $D(T_{p,q})$ occur in the $(+,+)$-quadrant by lemma 5.8. $\square$

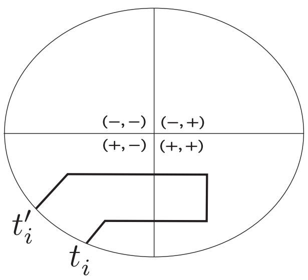

5.24 (a) Image of a $t-$arc $t_i t_i'$ in $\Delta T_{p,q}$.

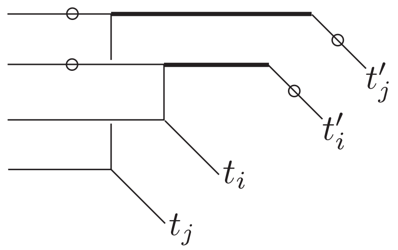

5.24 (b) The $t-$arcs $t_i t_i'$ and $t_j t_j'$.

Figure 5.24.

Lemma 5.12. *For any distinct integers $i, j \in \{1, \dots, p-1\}$, the edges t'_i, t''_i and t'_j, t''_j are connected by $t-$arcs of length 16. The arcs $[t'_i t''_i]$ and $[t'_j t''_j]$ of $D(T_{p,q})$ intersects twice, as shown on figure 5.25.*

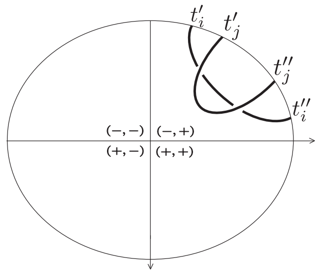

Figure 5.25. *The arcs $[t'_i t''_i]$ and $[t'_j t''_j]$ in $D(T_{p,q})$.*

Proof. The $t-$arc $t'_i t''_i$ is made of the following edges, as shown on figure 5.26 (a)):

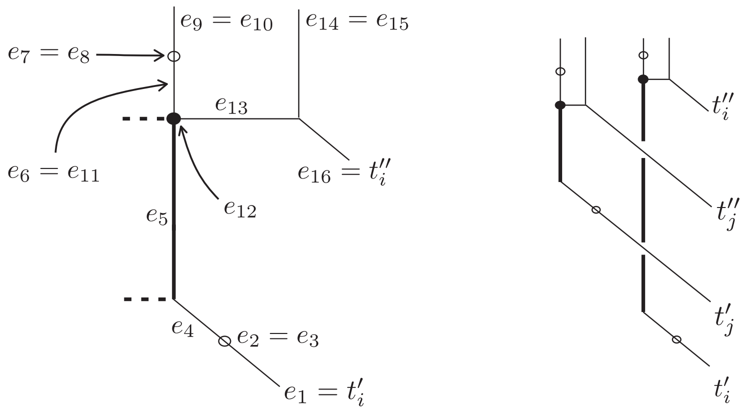

5.26 (a) The t-arc $t'_i t''_i$.

5.26 (b) The $t-$arcs $t'_i t''_i$ and $t'_j t''_j$.

Figure 5.26.

- $e_1 = t'_i$ and $e_{16} = t''_i$ are of phase $\{(+, -, +), (-, +, -)\}$;
- $e_2 = e_3$ is a z-edge of phase $\{(-, +, +), (-, +, -)\}$;
- e_4 is a bounded edge directed by $(1, 1, 0)$ of phase $\{(-, +, +), (+, -, +)\}$;
- e_5 is a bounded edge directed by $(1, 0, 0)$ of phase $\{(+, +, +), (-, +, +)\}$;
- e_6 is a bounded edge directed by $(1, 0, 1)$ of phase $\{(+, +, -), (-, +, +)\}$;
- $e_7 = e_8$ is a z-edge of phase $\{(-, +, +), (-, +, -)\}$;

- $e_9 = e_{10}$ is an x-edge of phase $\{(+,+,-),(-,+,-)\}$;
- $e_{11} = e_6$;
- e_{12} is a bounded edge directed by $(0,0,1)$ of phase $\{(+,+,+),(+,+,-)\}$;
- e_{13} is a bounded edge directed by $(0,1,1)$ of phase $\{(+,-,+),(+,+,-)\}$;
- $e_{14} = e_{15}$ is an x-edge of phase $\{(+,+,-),(-,+,-)\}$.

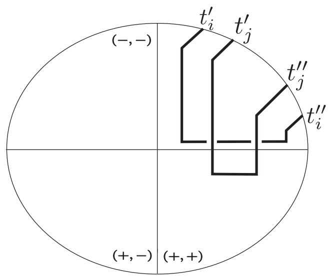

Figure 5.27. *The images of $t'_it''_i$ and $t'_jt''_j$ in $\Delta T_{p,q}$.*

As shown on figure 5.26 (b), the projection of the $t'_it''_i$ and $t'_jt''_j$ has two crossing points. Both are of type C, thus are simple, transparent and the corresponding crossings of $D(T_{p,q})$ occur in the $(-,+)$-quadrant by lemma 5.7. Figure 5.27 shows the image of $t'_it''_i$ and $t'_jt''_j$ in $\Delta T_{p,q}$. $\square$

The degree of $T_{p,q}$ is $2p+q-2$. As the weight of each edge is equal to 1, this curve has $2p+q-2$ t-edges. Among them, $3(p-1)$ are of type t_i, t'_i, t''_i. The $q-p+1$ remaining ones are adjacent to a vertex of $\Sigma^0_{p,q}$. They can be labeled from t_p to t_q, and we assume that the first coordinate of the vertex of t_k is larger than the one of t_{k+1}, as shown on figure 5.29 in the case of $T_{4,7}$.

Lemma 5.13. *The edges t_p and t_q are connected by a t-arc containing any edge of $\Sigma^0_{p,q}$. The corresponding arc $[t_pt_q]$ of $D(T_{p,q})$ intersects any arc of the from $[t'_it''_i]$ as shown on figure 5.28.*

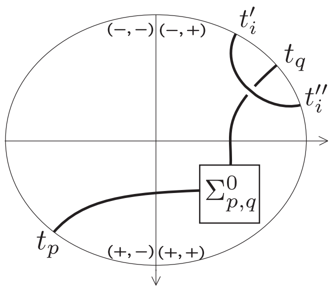

Figure 5.28. *Intersection of the arcs $[t_pt_q]$ and $[t'_it''_i]$.*

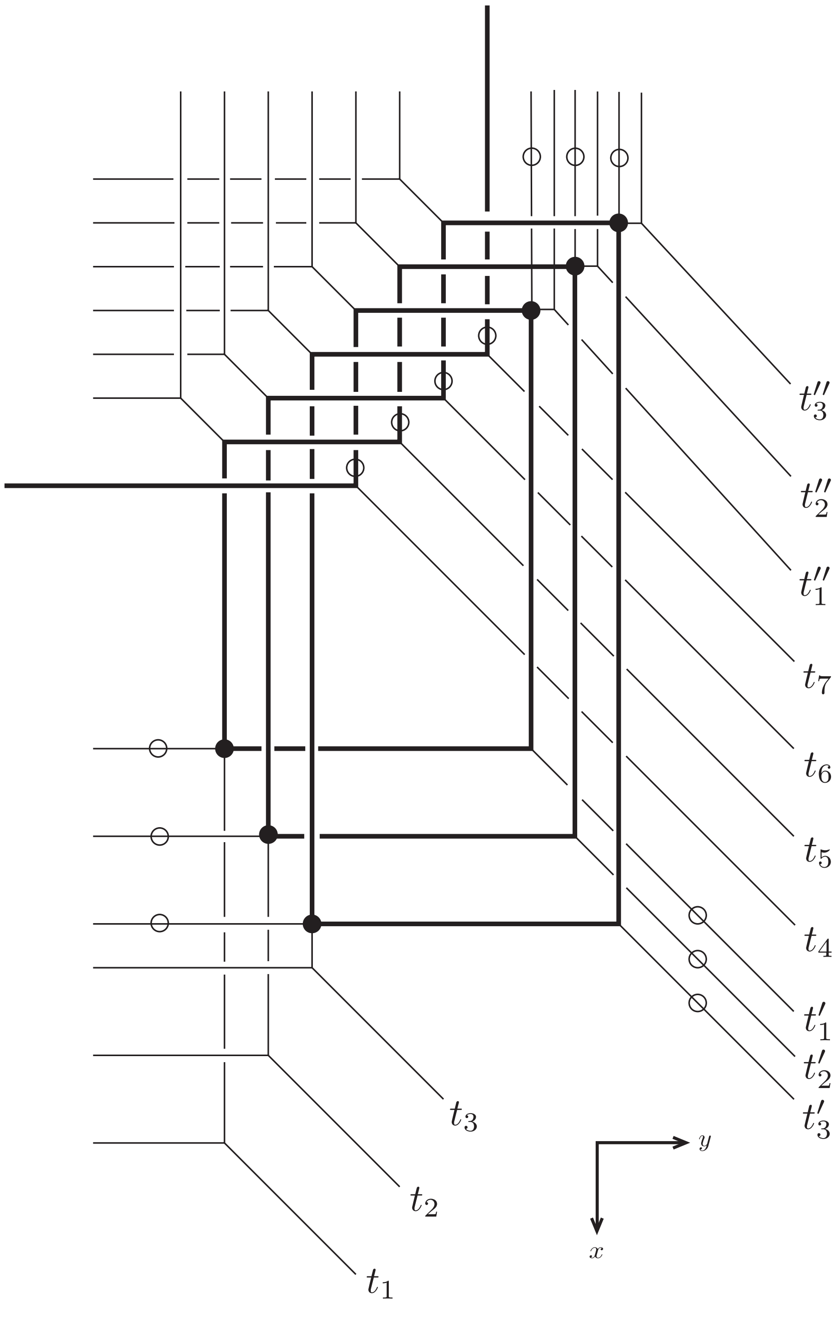

Figure 5.29. *The $t-$edges of the tropical curve $T_{4,7}$.*

Proof. Denote by n the number of edges of t_pt_q. The latter is sketched on figure 5.30 (a) in the case $p = 4$ and $q = 7$. The edges $e_1 = t_p$ and $e_n = t_q$ are of phase $\{(+,-,+),(-,+,-)\}$ by condition $\mathcal{C}'_\varepsilon$. The union of $e_2,\ldots,e_{n-1}$ coincides with the set of edges of $\Sigma^0_{p,q}$. In particular:

- the phase of each of them contains $(+,+,+)$;
- e_2 is the y-edge adjacent to t_p. Its phase is $\{(+,+,+),(+,-,+)\}$, so the phases of e_1 and e_2 both contain $(+,-,+)$;
- e_{n-1} is the bounded edge adjacent to t_q directed by $(-1,0,-1)$. Its phase is $\{(+,+,+),(-,+,-)\}$, so the phases of e_{n-1} and e_n both contain $(-,+,-)$;

Consequently, the boundary point of $[t_pt_q]$ corresponding to $e_1 = t_p$ is contained in the $(+,-)$−quadrant of $D(T_{p,q})$, and the one corresponding to $e_n = t_q$ is contained in the $(-,+)$−quadrant.

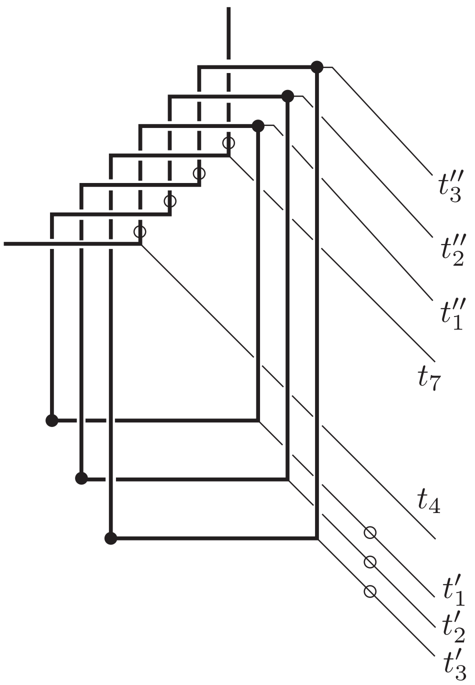

5.30 (a) The t-arc t_4t_7 in $T_{4,7}$.

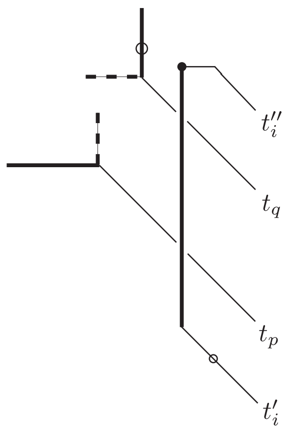

5.30 (b) Intersection of the projections of t_pt_q and $t'_it''_i$.

Figure 5.30.

As shown on figure 5.30 (b), the projections of t_pt_q and $t'_it''_i$ on the plane $\{z = 0\}$ intersect twice. As these two crossings are of type B as shown on figure 5.3, both are simple and transparent by lemma 5.6. One of these involves t_p and a bounded edge e of $t'_it''_i$ directed by $(1,0,0)$, and the second involves t_q and the same edge e. The latter belongs to $\Sigma^0_{p,q}$, thus its phase is $\{(+,+,+),(-,+,+)\}$ according to condition $\mathcal{C}_\varepsilon$. As $S_e \cap S_{t_p} = S_e \cap S_{t_q} = \{(-,+)\}$, the two above crossings induce two crossings of $D(T_{p,q})$ in the $(-,+)-$quadrant. Nevertheless, only the boundary point of $[t_p t_q]$ corresponding to t_q is contained in the $(-,+)-$quadrant. Therefore $[t'_i t''_i]$ intersects $[t_p t_q]$ only in the $(-,+)-$quadrant. $\square$

Lemma 5.14. *1. For any integer $k \in \{1, \ldots, q-p\}$, the edges t_k and t_{k+p} are connected by a $t-$arc. The corresponding arc $[t_k t_{k+p}]$ is shown on figure 5.31 (a).*

2. For any integer $l \in \{1, \ldots, p-1\}$, the edges t_{q-p+l} and t''_l are connected by a $t-$arc. The corresponding arc $[t_{q-p+l} t''_l]$ is shown on figure 5.31 (b).

3. The arcs of $D(T_{p,q})$ (respectively, the $t-$arcs of $T_{p,q}$) described in 1. and 2. are called diagonal arcs *(respectively,* diagonal $t-$arcs*). Any pair of diagonal arcs intersects as shown on figure 5.31 (c).*

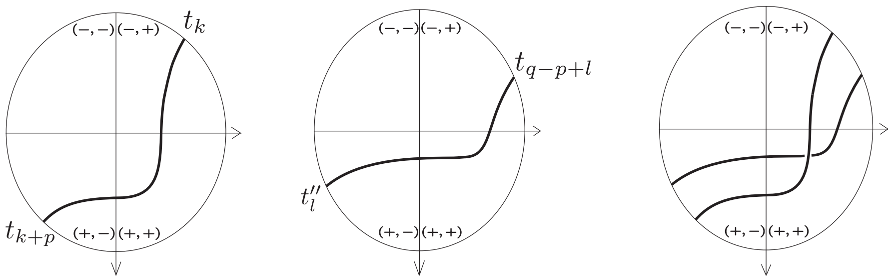

5.31 (a) 5.31 (b) 5.31 (c) Intersection of two diagonal arcs.

Figure 5.31. *Diagonal arcs of $D(T_{p,q})$.*

Proof. If $k \leq p-1$, the $t-$arc $t_k t_{k+p}$ is shown on 5.32 (a). It is made of the following edges:

- $e_1 = t_k$ is of phase $\{(+,-,-),(-,+,+)\}$;
- e_2 is a bounded edge directed by $(1,0,1)$ of phase $\{(-,+,+),(+,+,-))\}$;
- e_3 is a bounded edge directed by $(1,0,0)$ of phase $\{(+,+,+),(-,+,+)\}$;
- e_4 is a bounded edge directed by $(1,0,1)$ of phase $\{(-,+,+),(+,-,+)\}$;
- $e_5 = e_6$ is a $x-$edge of phase $\{(-,+,+),(+,+,+)\}$;
- $e_7 = e_8$ is a $y-$edge of phase $\{(+,+,+),(+,-,+)\}$;
- $e_9 = e_4$;
- e_{10} is a bounded edge directed by $(0,1,0)$ of phase $\{(+,+,+),(+,-,+)\}$;
- $e_{11} = t_{k+p}$ is of phase $\{(+,-,+),(-,+,-)\}$.

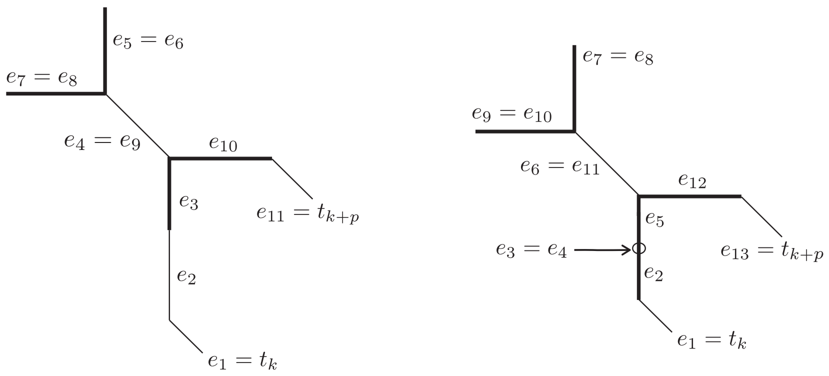

5.32 (a) If $k \leq p - 1$.

5.32 (b) If $k \geq p$.

Figure 5.32. *The $t-$arc $t_k t_{k+p}$.*

If $k \geq p$, the $t-$arc $t_k t_{k+p}$ is shown on figure 5.32 (b). It is made of the following edges:

- $e_1 = t_k$ is of phase $\{(+,-,+),(-,+,-)\}$;
- e_2 is a bounded edge directed by $(1,0,1)$ of phase $\{(+,+,+),(-,+,-)\}$;
- $e_3 = e_4$ is a z-edge of phase $\{(-,+,-),(-,+,+)\}$;
- e_5 is a bounded edge directed by $(1,0,0)$ of phase $\{(+,+,+),(-,+,+)\}$;
- $e_6 = e_{11}$ is a bounded edge directed by $(1,1,0)$ of phase $\{(-,+,+),(+,-,+)\}$;
- $e_7 = e_8$ is an x-edge of phase $\{(+,+,+),(-,+,+)\}$;
- $e_9 = e_{10}$ is an y-edge of phase $\{(+,+,+),(+,-,+)\}$;
- e_{12} is a bounded edge directed by $(0,1,0)$ of phase $\{(+,+,+),(+,-,+)\}$;
- $e_{13} = t_{k+p}$ is of phase $\{(+,-,+),(-,+,-)\}$.

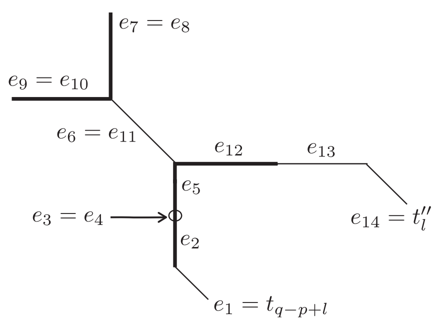

Figure 5.33. *The $t-$arc $t_{q-p+l}t''_l$.*

If $l \in \{1, \ldots, p-1\}$, the $t-$arc $t_{q-p+l}t''_l$ is shown on figure 5.33. It is made of the following edges:

- $e_1 = t_{q-p+l}$ is of phase $\{(+,-,+),(-,+,-)\}$;
- e_2 is a bounded edge directed by $(1,0,1)$ of phase $\{(+,+,+),(-,+,-)\}$;
- $e_3 = e_4$ is a z-edge of phase $\{(-,+,-),(-,+,+)\}$;
- e_5 is a bounded edge directed by $(1,0,0)$ of phase $\{(+,+,+),(-,+,+)\}$;
- e_6 is a bounded edge directed by $(1,1,0)$ of phase $\{(-,+,+),(+,-,+)\}$;
- $e_7 = e_8$ is an x-edge of phase $\{(+,+,+),(-,+,+)\}$;
- $e_9 = e_{10}$ is an y-edge of phase $\{(+,+,+),(+,-,+)\}$;
- $e_{11} = e_6$;
- e_{12} is a bounded edge directed by $(0,1,0)$ of phase $\{(+,+,+),(+,-,+)\}$;
- e_{13} is a bounded edge directed by $(0,1,1)$ of phase $\{(+,+,-),(+,-,+)\}$;
- $e_{14} = t''_l$ is of phase $\{(+,-,+),(-,+,-)\}$.

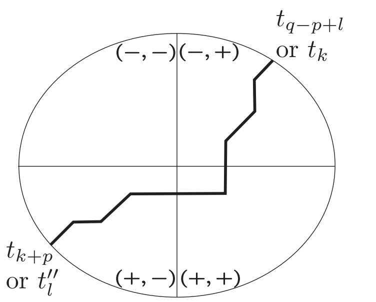

5.34 (a) The image of a diagonal arc in $\Delta T_{p,q}$.

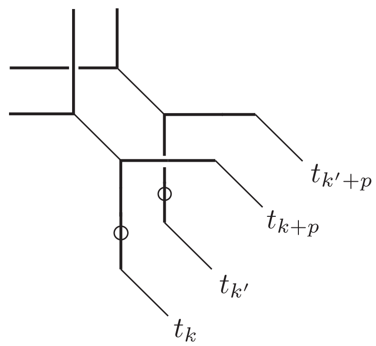

5.34 (b) The projection of the diagonal $t-$arcs t_kt_{k+p} and $t_{k'}t_{k'+p}$.

Figure 5.34.

The image of a diagonal arc in $D(T_{p,q})$ is shown on figure 5.34 (a). As shown on figure 5.34 (b) in the case of $t-$arcs t_kt_{k+p} and $t_{k'}t_{k'+p}$ with $k, k' \geq p$, the projection of two diagonal arcs has two crossing points. One is the projection of two edges of $\Sigma^0_{p,q}$. As these edges belong to the $t-$arc t_pt_q (see lemma 5.13), the corresponding crossing of $D(T_{p,q})$ is contained in $[t_pt_q]$. The second crossing is simple and transparent, as it is the projection of two unbounded edges whose phases contain $(+,+,+)$. Moreover, the corresponding crossing of $D(T_{p,q})$ is contained in the quadrant of phase $(+,+)$. $\square$

The star diagram of $T_{p,q}$ is the result of the superposition of the arcs determined in lemma 5.11, 5.12, 5.13 and 5.14. However, some of its crossing points can be easily eliminated by applying $\Omega-$moves: for any $i, j \in \{1, \ldots, p-1\}$, the crossing points of $[t_i t_i']$ and $[t_j t_j']$ (resp., of $[t_i' t_i'']$ and $[t_j' t_j'']$) are eliminated by an $\Omega-$move Ω_2 as shown on figure 5.35 (a) (resp., as shown on figure 5.35 (b)).

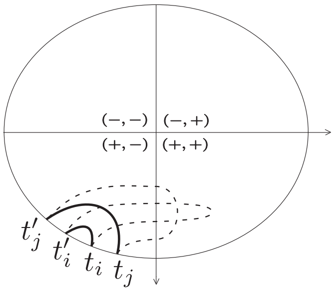

5.35 (a) Isotopy of the arcs $[t_i t_i']$ and $[t_j t_j']$.

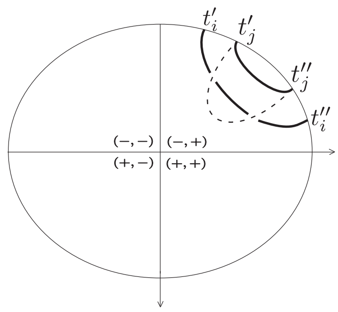

5.35 (b) Isotopy of the arcs $[t_i' t_i'']$ and $[t_j' t_j'']$.

Figure 5.35.

Thus $D(T_{p,q})$ is equivalent to the projective diagram depicted on figure 5.36.

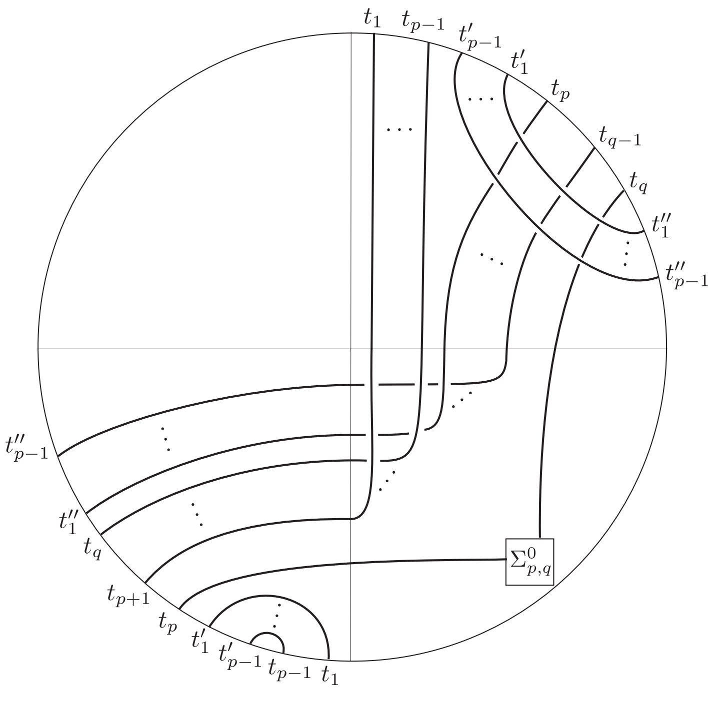

Figure 5.36. *The star diagram of* $T_{p,q}$.

5.5 Algebraic affine torus knots in $\mathbb{R}P^3$

Proposition 5.1. *If $0 < p < q$ are coprime integers, there exists a Morse modification of $T_{p,q}$ of degree $2p + q - 1$ and genus 1, denoted by $T^m_{p,q}$, whose star diagram is shown on figure 5.37.*

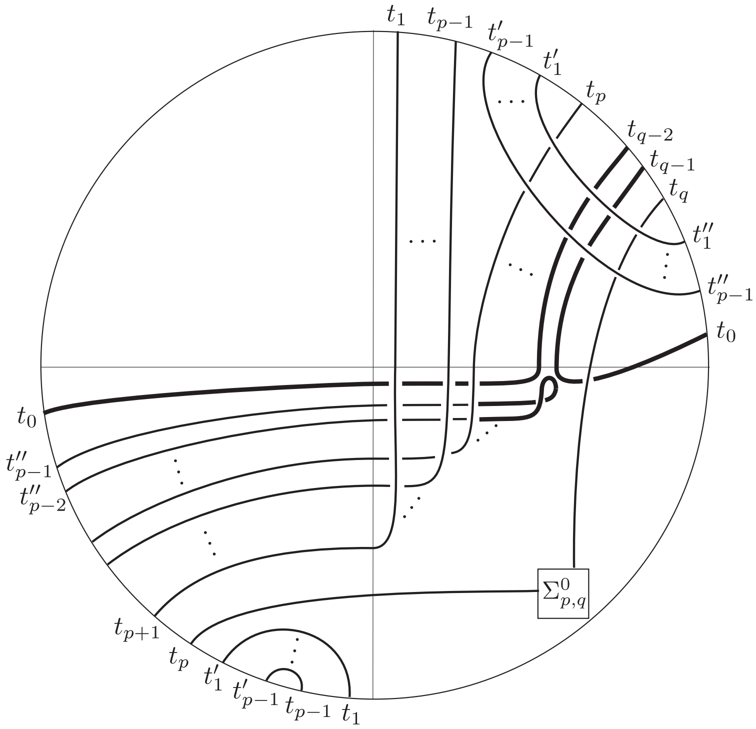

Figure 5.37. *The star diagram of $T^m_{p,q}$.*

Proof. The projections of $t_{q-2}t''_{p-2}$ and $t_{q-1}t''_{p-1}$ are shown on figure 5.38.

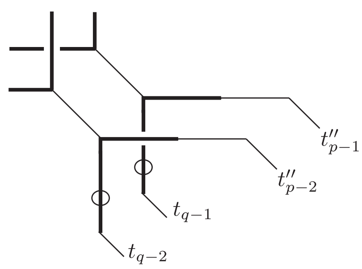

Figure 5.38. *The $t-$arcs $t_{q-2}t''_{p-2}$ and $t_{q-1}t''_{p-1}$.*

Figure 5.39 (a) shows the subgraph $G \subset T_{p,q}$ made of the two x-edges and the two y-edges of the above t-arcs. We perform a Morse modification by replacing G by the graph G' shown on figure 5.39 (b) in such a way that the vertex of t_0 has the largest $y-$coordinate among vertices of $t-$edges of $T^m_{p,q}$. This can be achieved by setting the length of the bounded edge adjacent to t_0 large enough. The weight of any additional edge is set to 1, and the phase of any edge is uniquely determined by conditions $\mathcal{C}_0, \mathcal{C}_\varepsilon, \mathcal{C}'_\varepsilon$ and the compatibility rule. The resulting real tropical curve $T^m_{p,q}$ has genus 1 and its degree exceeds the degree of $T_{p,q}$ by 1.

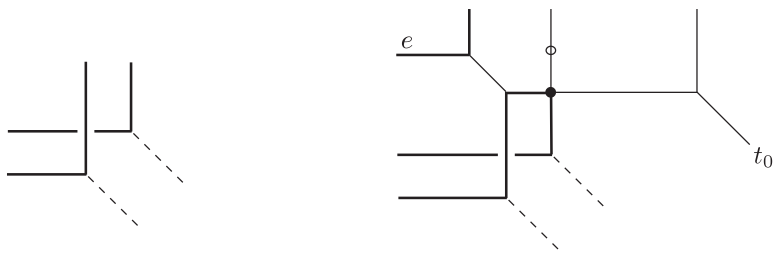

5.39 (a) The graph G.

5.39 (b) The graph G'.

Figure 5.39. *Morse modification of $T_{p,q}$.*

As shown on figure 5.39 (b), we denote by e the $y-$edge of G' which is not contained in G and by t_0 the additional $t-$edge. The projection of e intersects the projection of every $x-$edge of $T^m_{p,q}$ whose vertex has a smaller $y-$coordinate than the vertex of e. Except the two $x-$edges contained in G (which are no longer $x-$edges of G'), every $x-$edge of $T_{p,q}$ whose nearest Σ-vertex is of type A_6 is also an $x-$edge of $T^m_{p,q}$ and its vertex has a smaller $y-$coordinate than the vertex of e. There are $q-3$ such edges, thus $pr(T^m_{p,q})$ has $q-3$ additional crossing points. Each of these is the projection of e and an $x-$edge whose phases both contain $(+,+,+)$ and therefore is simple and transparent. In particular, the lower edge at the corresponding crossings of $D(T^m_{p,q})$ is the image of e.

Otherwise, t_0 is connected to t_{q-1} and t_{q-2} by $t-$arcs shown on figure 5.40. Additional edges (contained in $T^m_{p,q}$ but not in $T_{p,q}$) are drawn in bold. The phase of each edge is indicated, with respect to conditions $\mathcal{C}_0$, $\mathcal{C}_\varepsilon$ and $\mathcal{C}'_\varepsilon$, except for some of them. Considering the phases of two adjacent edges, the phases of the latters can easily be determined by the compatibility rule. With the notations of definition 5.1, one can check that t_0 is connected to t_{q-1} by a $t-$arc $\{e_i\}$ of lentgh 13 such that:

- $e_1 = t_0$ and $e_{13} = t_{q-1}$,
- $s_1 \cap s_2 = \{(-,+,-)\}$ and $s_{12} \cap s_{13} = \{(-,+,-)\}$.

In particular, the boundary points of $[t_0 t_{q-1}]$ occurs in the $(-,+)-$quadrant of $D(T^m_{p,q})$. Moreover, $pr(T^m_{p,q})$ has an additional crossing point involving the bounded edge adjacent to t_0 and the only $x-$edge of $\Sigma^0_{p,q}$, as shown on figure

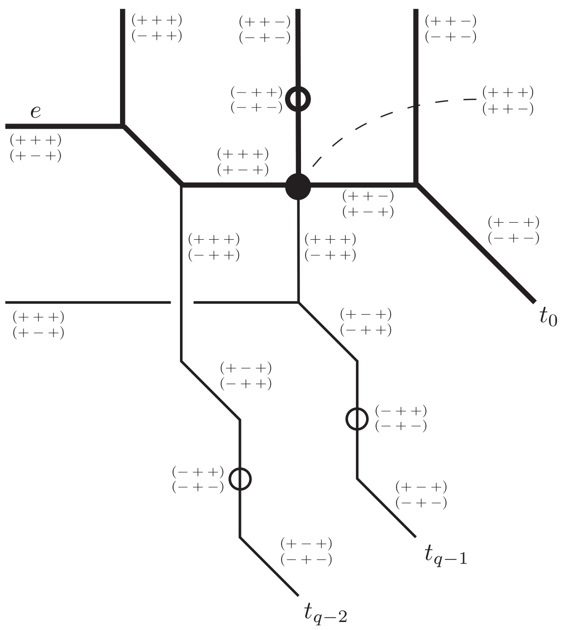

Figure 5.40. *The t-arcs containing t_0.*

5.41. The phases of those edges are $\{(+,-,+),(-,+,-)\}$ and $\{(+,+,+),(-,+,+)\}$ respectively, therefore this crossing is simple and transparent. The corresponding crossing of $D(T^m_{p,q})$ occurs in the $(-,+)-$quadrant and its lower arc is the image of the bounded edge.

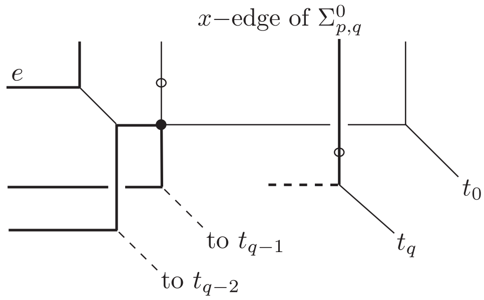

Figure 5.41. *Additional crossing point of $pr(T^m_{p,q})$ involving t_0t_{q-1}.*

On the other hand, t_0 is connected to t_{q-2} by a $t-$arc $\{e_i\}$ of lentgh 16 such that:

- $e_1 = t_0$ and $e_{16} = t_{q-2}$,
- $s_1 \cap s_2 = \{(+,-,+)\}$ and $s_{15} \cap s_{16} = \{(-,+,-)\}$.

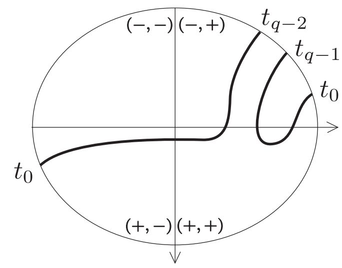

Figure 5.42. *The arcs of $D(T^m_{p,q})$ involving the additional edge t_0.*

In particular, the boundary points of $[t_0t_{q-2}]$ occurs in the $(-,+)$ and $(+,-)-$ quadrants. The additional crossing points of $pr(T^m_{p,q})$ involving t_0t_{q-2} are the projection of e and the $x-$edges of $T^m_{p,q}$ whose vertex has a smaller $y-$coordinate than the vertex of e, thus are already be described in this proof. Both arcs $[t_0t_{q-1}]$ and $[t_0t_{q-2}]$ are shown on figure 5.42. We deduce the star diagram of $T^m_{p,q}$ as shown on figure 5.37, on which the part of the diagram affected by the Morse modification is drawn in bold. □

We say that an arc of a projective diagram can be *killed* if it can be eliminated by a finite sequence of $\Omega-$moves.

Proposition 5.2. *If $q>0$ is odd, then $\mathbb{P}T^m_{2,q}$ is isotopic to $\iota K(2,q)$.*

Proof. We show that the star diagram of $T^m_{2,q}$ is connected to a projective diagram of $\iota K(2,q)$ by a finite sequence of $\Omega-$moves.

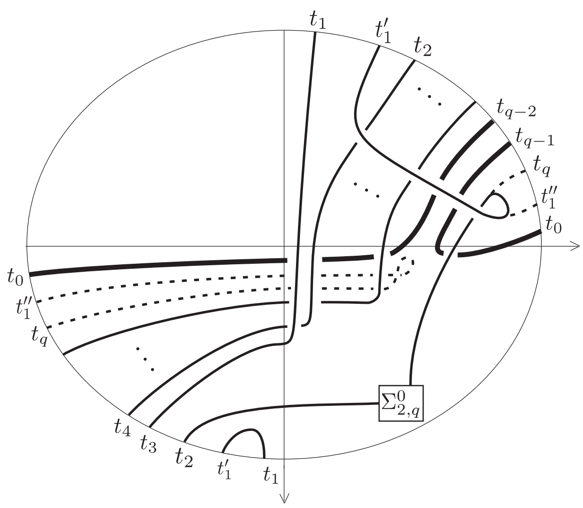

Figure 5.43. *Elimination of the arc $[t_1''t_q]$ of $D(T^m_{2,q})$.*

First of all, the arc $[t_1''t_q]$ can be killed by a sequence of $\Omega-$moves described on figure 5.43. This arc is no longer contained in the resulting diagram, as the new arc $[t_1' t_2]$ somehow "includes" the former arc $[t_1'' t_q]$. In the same way, the following arcs can be successively killed:

$$[t_1 t_1'], [t_0 t_{q-1}], [t_{q-3} t_{q-2}], [t_{q-5} t_{q-4}], \ldots, [t_4 t_5], [t_2 t_3].$$

The resulting projective diagram does not intersect the boundary, and is isotopic to the closure of $\Sigma^0_{2,q}$, see figure 5.44. As the latter is a diagram of $\iota K(2,q)$, the statement follows. □

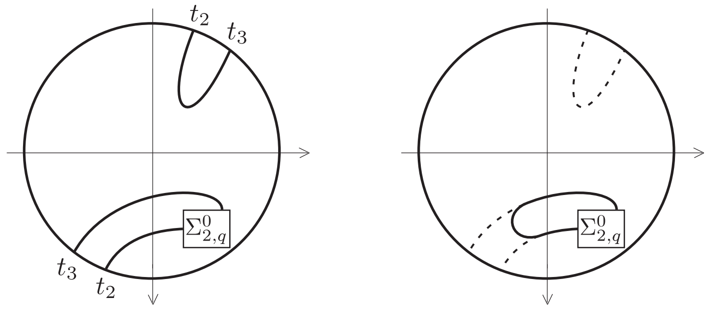

Figure 5.44. *Elimination of the last arc of $D(T^m_{2,q})$.*

Theorem 5.1. *If $q > 0$ is odd, there exists a real algebraic nonsingular curve $X_{2,q} \subset \mathbb{R}P^3$, of genus 1 and degree $q+3$, whose real part is isotopic to $\iota K(2,q)$.*

Proof. The regularity of the real tropical curve $T^m_{2,q}$ is a consequence of lemma 3.2. The statement then follows from theorem 3.10 and proposition 5.2. □

Proposition 5.3. *If $p > 2$ is odd, then $\mathbb{P}T^m_{p,p+2}$ is isotopic to $\iota K(p, p+2)$.*

Proof. As p is odd, it is prime with $p+2$ and $K(p, p+2)$ is a knot. The proof is quite similar to that of proposition 5.2. The star diagram of $T^m_{p,p+2}$ is connected to a projective diagram of $\iota K(p, p+2)$ via a finite sequence of $\Omega-$moves. The arc $[t''_{p-2} t''_{p-1}]$ can be killed by a sequence of $\Omega-$moves described on figure 5.45. This arc is no longer contained in the resulting projective diagram, as it is somehow "included" in the new arc $[t'_{p-1} t'_{p-2}]$. In the same way, the following arcs can be successively killed:

$$[t'_{p-1} t'_{p-2}], [t_{p-1} t_{p-2}], [t''_{p-3} t''_{p-4}], [t'_{p-3} t'_{p-4}], \ldots$$

As p is odd, this process ends when the arc $[t_2' t_1']$ is killed. The latter is no longer contained in the resulting projective diagram, as it is somehow "included" in the new arc $[t_2 t_1]$. The projective diagram obtained after this step is shown on figure 5.46 (a). Finally, a sequence of $\Omega-$moves successively kills the arcs $[t_2 t_1]$, $[t_{p+2} t_{p+1}]$ and $[t_p t_0]$, as shown on figure 5.46 (b). As the resulting projective diagram is a diagram of $\iota K(p, p+2)$, the statement follows.

□

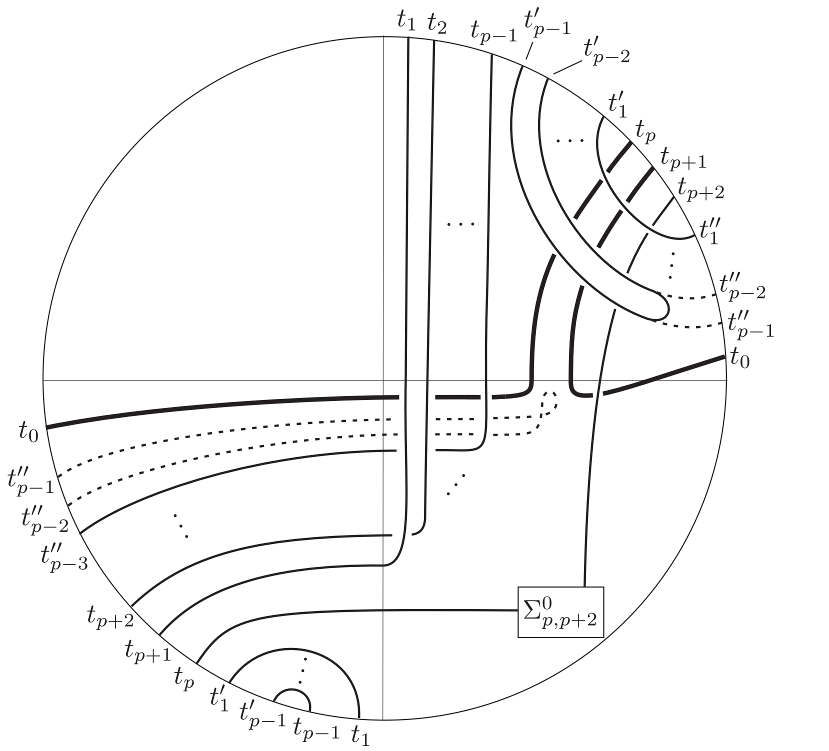

Figure 5.45. *Elimination of the arc $[t''_{p-1}t''_{p-2}]$ of $D(T^m_{p,p+2})$.*

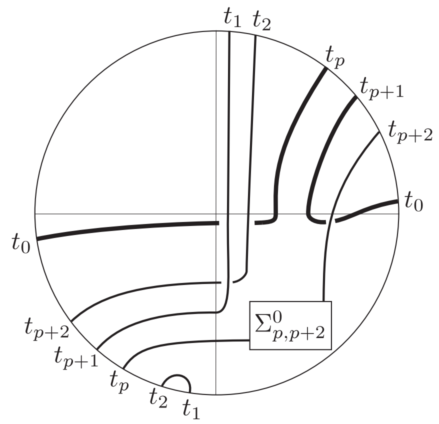

5.46 (a) A projective diagram equivalent to $D(T^m_{p,p+2})$.

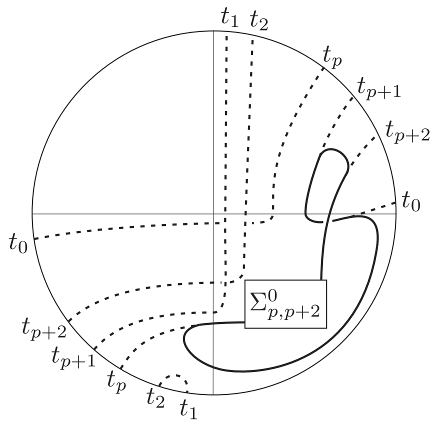

5.46 (b) Final $\Omega-$moves.

Theorem 5.2. *If $p > 2$ is odd, there exists a nonsingular real algebraic curve $X_{p,p+2} \subset \mathbb{R}P^3$, of genus 1 and degree $3p+1$, whose real part is isotopic to $\iota K(p, p+2)$.*

Proof. The regularity of the real tropical curve $T^m_{p,p+2}$ is a consequence of lemma 3.2. The statement then follows from theorem 3.10 and proposition 5.3.
□

Bibliography

[1] Birman, J.S. — *Braid, links and mapping class groups*, Ann. of Math. Studies **82**, Princeton Univ. Press, 1974.

[2] Bergman, G.M. — *The logarithmic limit set of an algebraic variety*, Trans. AMS, **157** (1971), 459–469.

[3] Bieri, R. and Groves, J.R.J. — *The geometry of the set of characters induced by valuations*, J. Reine Angew. Math., **347** (1984), 168–195.

[4] Birman, J. and Menasco, W. — *Studying links via closed braids III: Classifying links which are closed 3-braids*, Pacific J. Math. **161** (1993), 25–113.

[5] Bjorklund, J. — *Real algebraic knots of low degree*, preprint arXiv:0905:4186v1.

[6] Brugallé, E. — *Courbes algébriques réelles et courbes pseudoholomorphes réelles dans les surfaces réglées*, thèse de doctorat, Université de Rennes I, 2004.

[7] Brusotti, L. — *Sulla generazzione di curve piane algebriche reali mediante "piccola variazione" di une curve spezzata*, Annali di Mat. **22** (1913), no.3, 117 – 169.

[8] Burde, G. and Zieschang, R. — *Knots*, de Gruyter Studies in Mathematics, **5**, Berlin, 2003.

[9] Cohn, P.M. — *Puiseux's theorem revisited*, J. Pure Appl. Algebra **31** (1984), 1–4; correction, **52** (1988), 197–198.

[10] Gudkov, D. A. — *Complete topological classification of the disposition of ovals of a sixth order curve in the projective plane*, Gor'kov. Gox. Univ. Ucen. Zap. Vyp. **87** (1969), 118 – 153.

[11] Gruson, L. and Peskine, C. — *Genre des courbes de l'espace projectif*, *in* Algebraic geometry (Tromso, 1977), Lecture Notes in Math., **687**, Springer, Berlin (1978), 31–59.

[12] Haas, B. — *Les multilucarnes: nouveaux contre-exemples à la conjecture de Ragsdale*, C. R. Acad. Sci Paris Série I Math. **320** (12) (1995), 1507 – 1512.

[13] Halphen, G. — *Mémoire sur la classification des courbes gauches algébriques*, J. Ec. Polyt. **52** (1882), 1–200.

[14] Harnack, A. — *Über vieltheiligkeit der ebenen algebraischen curven.*, Math. Ann. **10** (1876), 189–199.

[15] Harris, J. — *Curves in projective spaces*, Séminaire de Mathématiques Supérieures, **85**, Montréal (1982).

[16] Hilbert, D. — *Mathematische probleme*, Arch. Math. Phys. **1** (1901), 43 – 64.

[17] Hilbert, D. — *Ęber die reellen Züge algebraischen Curven*, Mathematische Annalen **38** (1891), 115–138.

[18] Itenberg, I. — *Contre-exemples à la conjecture de Ragsdale*, C. R. Acad. Sci. Paris Série I Math. **317** (1993) no. 3, 277 – 282.

[19] Itenberg, I. — *On the number of even ovals of a nonsingular curve of even degree in* $\mathbb{R}P^2$, *in* Topology, ergodic theory, real algebraic geometry, volume 202 of Amer. Math. Soc. Transl. Serie 2, 2001, 121 – 129.

[20] Itenberg, I. and Viro, O. — *Patchworking real algebraic curves disproves the Ragsdale conjecture*, Math. Intelligencer 18 (1996), 19–28.

[21] Kapranov, M. — *Amoebas over non-archimedean fields*, preprint (2000).

[22] Kapranov, M., Einsiedler, M. and Lind, D. — *Non-archimedean amoebas and tropical varieties*, preprint arXiv:math.AG/0408311.

[23] Kassel, C. and Turaev, V. — *Braid groups*, Springer, 2008.

[24] Kedlaya, K. — *Power series and p-adic algebraic closures*, J. Number Theory **89** (2001) no. 2, 324–339.

[25] Kenyon, R. and Okounkov, A. — *Planar dimers and Harnack curves*, preprint arXiv:math.AG/0311062.

[26] Kenyon, R., Okounkov, A. and Sheffield, S. — *Dimers and amoebae*, preprint arXiv:math.AG/0311005.

[27] Klein, F. — *Ueber eine neue Art der Riemann'schen Flächen*, Math. Ann. **7** (1873), 558–566.

[28] Koseleff, P.-V. and Pecker, D. — *Chebyshev diagrams for rational knots*, preprint arXiv:0906.4083v1.

[29] Koseleff, P.-V. and Pecker, D. — *Chebyshev knots*, J. Knot Theory Ramifications **20** (2011), no.4, 575–593.

[30] Koseleff, P.-V. and Pecker, D. — *Chebyshev diagrams for two-bridge knots*, Geometriae Dedicata **150** (2011), no.1, 405–430.

[31] Koseleff, P.-V. and Pecker, D. — *Harmonic knots*, preprint arXiv:1203.4376v1.

[32] Markwig, H., Markwig, T. and Jensen, A.N. — *An algorithm for lifting points in a tropical variety*, preprint arXiv:0705.2441.

[33] Mathematisches Forschungsinstitut Oberwolfach, report no. 57/2007, *Tropical Geometry.*

[34] Mikhalkin, G. — *Enumerative tropical algebraic geometry in* $\mathbb{R}^2$, J. Amer. Math. Soc. **18** (2005), 313–377.

[35] Mikhalkin, G. — *Amoebas of algebraic varieties and tropical geometry*, preprint arXiv:0403015v1.

[36] Mikhalkin, G. — *Tropical geometry*, preprint (2009), available at www.mpim-bonn.mpg.de/webfm_send/13.

[37] Mikhalkin, G. — *Decomposition into pair-of-pants for complex algebraic hypersurfaces*, Topology **43**, issue 5 (2004), 1035–1065.

[38] Mikhalkin, G. — *Tropical geometry and its applications*, preprint arXiv:0601041.

[39] Mikhalkin, G. and Orevkov, S. — *Topology of algebraic curves of degree* 5 *in* $\mathbb{R}P^3$, to appear.

[40] Murasugi, K. — *Knot theory and its applications*, Birkhauser (1996).

[41] Murasugi, K. — *On the braid index of alternating links*, Trans. Amer. Math. Soc. **326**, no. **1** (1991), 237–260.

[42] Payne, S. — *Fibers of tropicalization*, preprint arXiv:0705.1732.

[43] Pecker, D. — *Un théorème de Harncak dans l'espace*, Bull. Sci. Math. **118** (1994), 475–484.

[44] Petrovsky, I. G. — *On the topology of real plane algebraic curves*, Ann. Math. **39** (1938), no.1, 189 – 209.

[45] Ragsdale, V. — *On the arrangement of the real branches of plane algebraic curves*, Amer. J. Math. **28** (1906), 377–404.

[46] Ribenboim, P. — *Fields: algebraically closed and others*, Manuscripta Math. **75** (1992), 115–150.

[47] Rullgard, H. — *Polynomial amoebas and convexity*, preprint, Stockholm University (2001).

[48] Speyer, D. — *Uniformizing tropical curves I: genus zero and one*, preprint arXiv:0711.2677.

[49] Sturmfels, B. — *Viro's theorem for complete intersections*, Annali della Scuola Normale Superiore di Pisa (4) **21** (1994), no.3, 377 – 386.

[50] Sturmfels, B. and Speyer, D. — *Tropical mathematics*, preprint arXiv:math.CO/0408099.

[51] Sturmfels, B., Theobald, T. and Richert-Gebert, J. — *First steps in tropical geometry*, preprint arXiv:math.AG/0306366.

[52] Tabera, L. — *Tropical plane geometric constructions*, preprint arXiv:math.AG/0511713.

[53] V. Drobothukina, Yu. — *An analogue of the Jones polynomial for links in $P^3_{\mathbb{R}}$ and a generalization of the Kauffman-Murasugi theorem*, Leningrad Math. J. **2** (1991), no. 3, 613–630.

[54] V. Drobothukina, Yu. — *Classification of projective Montesinos links*, St. Petersburg Math. J. **3** (1992), no. 1, 97–107.

[55] V. Drobothukina, Yu. — *Classification of links in $P^3_{\mathbb{R}}$ with at most six crossings*, Topology of manifolds and varieties, 87–121, Adv. Soviet Math., 18, Amer. Math. Soc., Providence, RI, 1994.

[56] Vassiliev, V. A. — *Cohomology of knot spaces*, Theory of singularities and its applications, Advances Soviet Math. **1** (1990).

[57] Viro, O. Ya. — *Patchworking real algebraic varieties*, preprint, Uppsala University (1994).

[58] Viro, O. Ya. — *Real algebraic plane curves: constructions with controlled topology*, Leningrad Math. J. **1** (1990), 1059–1134.

[59] Viro, O. Ya. — *Curves of degree* 7*, curves of degree* 8 *and the Ragsdale conjecture*, Soviet Math. Dokl. **22** (1980), 566–570.

[60] Viro, O. Ya. — *Gluing of plane real algebraic curves and construction of curves of degree* 6 *and* 7, Lect. Notes Math. **1060**, Springer, Berlin, 1984, 187 – 200.

[61] Wyman, A. — *Über die reellen Züge der ebenen algebrauschen Kurven*, Math. Ann. **90** (1923), 222–228.